

Recent Progress on Cellulose-Based Ionic Compounds for Biomaterials

Yang Yang, Yi-Tung Lu, Kui Zeng, Thomas Heinze, Thomas Groth, and Kai Zhang*

Glycans play important roles in all major kingdoms of organisms, such as archaea, bacteria, fungi, plants, and animals. Cellulose, the most abundant polysaccharide on the Earth, plays a predominant role for mechanical stability in plants, and finds a plethora of applications by humans. Beyond traditional use, biomedical application of cellulose becomes feasible with advances of soluble cellulose derivatives with diverse functional moieties along the backbone and modified nanocellulose with versatile functional groups on the surface due to the native features of cellulose as both cellulose chains and supramolecular ordered domains as extractable nanocellulose. With the focus on ionic cellulose-based compounds involving both these groups primarily for biomedical applications, a brief introduction about glycoscience and especially native biologically active glycosaminoglycans with specific biomedical application areas on humans is given, which inspires further development of bioactive compounds from glycans. Then, both polymeric cellulose derivatives and nanocellulose-based compounds synthesized as versatile biomaterials for a large variety of biomedical applications, such as for wound dressings, controlled release, encapsulation of cells and enzymes, and tissue engineering, are separately described, regarding the diverse routes of synthesis and the established and suggested applications for these highly interesting materials.

1. Introduction

Cellulose and hemicelluloses represent the most abundant biomaterials on the Earth and represent major structural components in cell walls of plant that provide them with sufficient mechanical


strength to withstand extreme mechanical forces.^[1] Cellulose is also a polymeric material that has been used by humans for long time to produce diverse products, such as fibers for clothes and paper, but also as the first material that has been modified to generate synthetic fibers for textile industry, films for kinemato and photography, food industry, and many others applications.^[2] Modified cellulose was also used as the first polymer membrane materials for successful hemodialysis of patients with acute kidney failure,^[3] is still used in some cases for making filters for hemodialysis, and is also a useful material in biotechnology for adsorbent materials, blotting membranes and filters.^[4]

Cellulose as polymeric chains of anhydroglucose units (AGUs) connected via β -1,4-glycosidic bonds can also form fibrillar domains of high crystallinity which is very difficult to dissolve in common solvents. It does not possess any desired bioactivity toward mammalian proteins and cells except for some undesired activation of the complement system due to the presence of hydroxyl

groups.^[5] On the other hand, oligo- and polysaccharides that exist in mammals including humans have a plethora of functions that are closely linked to the types of monosaccharides, glycosidic bonds, sequences of and functional moieties existing on monosaccharides.^[6] Because of the important functions of

Dr. Y. Yang, K. Zeng, Prof. K. Zhang
Wood Technology and Wood Chemistry
University of Goettingen
Büsgenweg 4, Göttingen 37077, Germany
E-mail: kai.zhang@uni-goettingen.de

Dr. Y. Yang
State Key Laboratory of Pulp and Paper Engineering
South China University of Technology
Wushan Road 381, Guangzhou 510640, P. R. China

 The ORCID identification number(s) for the author(s) of this article can be found under <https://doi.org/10.1002/adma.202000717>.

© 2020 The Authors. Published by WILEY-VCH Verlag GmbH & Co. KGaA, Weinheim. This is an open access article under the terms of the Creative Commons Attribution-NonCommercial License, which permits use, distribution and reproduction in any medium, provided the original work is properly cited and is not used for commercial purposes.

DOI: 10.1002/adma.202000717

Y.-T. Lu, Prof. T. Groth
Department Biomedical Materials
Institute of Pharmacy
Martin Luther University Halle-Wittenberg
Heinrich-Damerow-Strasse 4, Halle (Saale) 06120, Germany

Prof. T. Heinze
Institute of Organic Chemistry and Macromolecular Chemistry
Friedrich Schiller University of Jena
Centre of Excellence for Polysaccharide Research
Humboldt Straße 10, Jena D-07743, Germany

Prof. T. Groth
Interdisciplinary Center of Materials Science
Martin Luther University Halle-Wittenberg
Halle (Saale) 06120, Germany

Prof. T. Groth
Laboratory of Biomedical Nanotechnologies
Institute of Bionic Technologies and Engineering
I. M. Sechenov First Moscow State University
Trubetskaya Street 8, 119991 Moscow, Russian Federation

glycans, e.g., their involvement in controlling the blood coagulation as by heparin, their therapeutic application is highly desirable. However, quantities of glycans that can be obtained from animal sources are often limited, related to time and labor consuming processes of purification and carry often also a certain risk to transmit diseases.^[7]

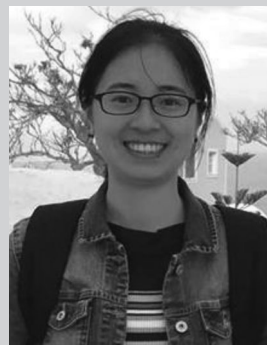
Hence, the development of synthetic and semisynthetic glycans mimicking those that are found in humans is an important task. However, synthesis of oligosaccharides from scratch with solid phase approaches may provide identical glycans to their natural blueprint,^[8] but is still quite expensive and may only provide smaller quantities of high activity that are suitable to make diagnostic devices, but not for large scale clinical applications as required for anticoagulation of blood or as material for making wound dressing, biomedical implants, hydrogels and tissue engineering scaffolds. On the other hand, regioselective derivatization of polysaccharides that endow them with the desired derivatizing patterns and functional groups that resemble the composition of glycans found in humans may provide another possibility to deliver biomaterials of high purity, functionality and abundance for biomedical applications without the risk of potential infections and other undesired side effects of natural compounds obtained from animal sources. Thus, abundant polysaccharides, such as cellulose, represent a highly attractive platform for the development of bioactive compounds.

Here, we provide first a brief survey on the structure and function of animal glycans and in particular the ionic features of glycosaminoglycans (GAGs) as model for the functionalization of cellulose granted improved biological properties that mimic nature roles as GAGs. We describe the synthesis of diverse ionic cellulose derivatives as anionic and cationic cellulose derivatives with subsequent description of their applications as biomaterials followed by a section of synthesis and application of surface-modified nanocellulose. As we show in more detail, these products obtained from cellulose provide a versatile platform to address a larger variety of biomedical applications, which makes cellulose-based materials highly interesting for further development in biomedical and biotechnological fields.

2. Glycoscience and Glycosaminoglycans

2.1. Proteoglycans, Glypicans, and Glycolipids as Cell and Extracellular Matrix Components

Natural, negatively charged and branched oligo- and polysaccharides play important roles for functionality of proteins. N- and O-glycosylation has versatile effects on the functions and also stability of proteins, such as enzymes, cell surface receptors, coagulation and complement factors, immunoglobulins and transport proteins in blood plasma.^[6] In addition, such glycosylation patterns may also be involved in the recognition of self and foreign objects, which include blood group factor recognition, heterophilic cell–cell adhesions by interaction of selectin glycoprotein ligands with corresponding selectins on blood platelets, endothelial cells, leukocytes, and also tumor cells.^[9] A common feature of these glycosylated proteins is the presence of terminal sialic acid of monosaccharides that contribute to the surface charge of cells due to the presence of



Yang Yang received her Ph.D. degree in biomass science and engineering from South China University of Technology. Now she is a postdoctoral research associate with Prof. Kai Zhang at Georg-August-University of Goettingen and South China University of Technology. She mainly focused on biomass, especially cellulose-based functional materials for biomaterials, flexible electronics, and photonic materials.



Kai Zhang is Professor and Principal Investigator of the group Wood Technology and Wood Chemistry, department head of the Department for Wood Technology and Wood-Based Composites, Georg-August-University of Goettingen. He studied in Hefei University of Technology (B.Eng.), China, and Dresden University of Technology (M.S. and Ph.D. 2011), Germany. After research stations in Dresden University of Technology, the Pennsylvania State University, and Darmstadt University of Technology, he joined University of Goettingen in 2015. One of the major research fields in his group is the preparation of functional materials derived from biobased polymers, such as biomaterials from polysaccharides, via diverse chemical and physical approaches.

carboxyl groups, while other monosaccharides possess *N*-acetyl groups.^[6] Moreover, glycolipids are integral components of the cell surface membrane containing extracellular glycan chains that are also characterized by the presence of negatively charged monomeric glycan groups, such as sialic acids and sulfatides in acidic glycosphingolipids.^[10]

Other glycosylated components on cell surface are proteoglycans (PG) that are highly glycosylated but being also part of the extracellular matrix (ECM).^[11] A major family of cell surface proteoglycans are syndecan 2 and 4, while typical PG of ECM are aggrecan and small leucine-rich repeat proteoglycans (SLRP). PG can also be stored in intracellular vesicles and released upon demand by cells, like serglycin in mast cells that are found in tissues like mucosa, which can release GAGs, such as heparin.^[11] PGs are generally characterized by a protein core with specific protein sequences containing serines that serve as links to longer linear chains of GAGs through a bridge of trisaccharide Xyl–Gal–Gal. A proteoglycan can contain several of such GAG side chains.

A classic feature of GAGs is the occurrence of specific disaccharide units that are composed of an *N*-acetylglucosamine

Table 1. Overview of GAGs with natural roles, physiological functions, and affinity to proteins.

GAG	Location	Natural role	Physiological function	Affinity to ECM/cytokines/ chemokines/growth factor	Ref.
Heparin	Intracellular/ Extracellular	Storage of proteases in mast cell granules, growth factor binding, direct signal transducer, activation or inhibition of cytokines, involved in assembly of focal adhesions	Cell proliferation and differentiation, cell–cell adhesion, cell–matrix adhesion, antitumor, anticoagulant, anti-inflammatory	FN, VN, laminin, FGF-1, FGF-2, FGF-10, PDGF, BMP-2, IL-10, CXCL12, MCP-1, CCR2	[13,14,15–17]
HS	Cell surface/ pericellular/extracellular	Growth factor binding, direct signal transducer, activation or inhibition of cytokines, involved in assembly of focal adhesions	Cell proliferation and differentiation, cell–cell adhesion, cell–matrix adhesion, antitumor, anticoagulant, anti-inflammatory	FN, VN, laminin, FGF-1, FGF-2, VEGF, PDGF, HB-EGF, BMP-2, SHH, IL-10, CXCL12, MCP-1, CCR5	[14,15,17–19]
DS	Extracellular	Interaction with collagen in regulation of fibrillogenesis, growth factor interaction	Cellular proliferation, extracellular matrix stability, tensile strength of skin, anticoagulant, wound healing	FGF-2, FGF-7, HB-EGF, MCP-1	[20]
CS	Cell surface/ pericellular/extracellular	Interaction with neurons and neural cell adhesion molecules, interaction with collagen in regulation of fibrillogenesis, binding to HA as PG affecting tissue mechanics, growth factor interaction	Inhibitor of cellular processes including axonal growth, cell migration and plasticity, modulator of neural stem cells (brain-CS), cartilage repair, anti-inflammatory, wound healing, antitumor	Collagen V, FGF-1, FGF-2, FGF-7, FGF-10, PDGF, BMP-4, NGF, SHH, BDNF, IL-10, CXCL12	[15,16,18,21]
KS	Extracellular	Affects the fibrillization of collagen, growth factor binding	Maintains hydration level and transparency of cornea, neural regeneration and plasticity, decelerate cartilage damage, anti-inflammatory	IGFBP-2, SHH	[22,23]
HA	Extracellular	Integrity, adjustment of viscosity and compression resistance of tissues (including binding of PG like aggrecan) crosslinking with hyaladherins (CD44 and TSG-6), interactions with specific cell surface receptors (CD44 and RHAMM)	Cell proliferation, migration, differentiation, angiogenesis, HMW HA: antiangiogenic, immunosuppressive, anti-inflammatory LMW HA: angiogenic, immunostimulatory, proinflammatory	TGF- β 1, BMP-2, NGF, IL-2, IL-10, CXCL12, TSG-6	[11,17,24]

FGF: fibroblast growth factor; VEGF: vascular endothelial growth factor; PDGF: platelet-derived growth factor; HB-EGF: heparin binding-epidermal growth factor; NGF: neural growth factor; BDNF: brain-derived neurotrophic factor; TSG: tumor necrosis factor-inducible gene; RHAMM: receptor for hyaluronan mediated motility; BMP: bone morphogenetic protein; SHH: sonic hedgehog; IL: interleukins; TGF- β 1: transforming growth factor β 1; CXCL: C–X–C motif chemokine; CCR: C–C chemokine receptor; MCP-1: monocyte chemoattractant protein-1; IGFBP: insulin-like growth factor binding protein; FN: fibronectin; VN: vitronectin.

(GlcNAc) or *N*-acetylgalactosamine (GalNAc) unit and a uronic ring as either glucuronic (GlcA) or iduronic acid (IdoA) that carry a negative charge due to the presence of a carboxylic acid at C6 position of the hexuronic acid. Another feature of GAGs except for hyaluronan is the presence of sulfate groups as *N*-sulfation at C2 position of the GlcNAc or GalNAc subunit of dimers and/or *O*-sulfation at hydroxyl groups of both groups of building blocks, which generate strong negative charges of GAGs chains and thus the proteoglycans. The presence of these charged functional carboxylic and sulfate groups together with the presence of hydroxyl groups plays important roles not only in binding of ions and water that are critical for mechanical properties of tissues, such as the compression stability, and contribution to homeostasis of electrolytes, but also for the binding of a plethora of proteins that functionally regulate behavior of cells and tissues, including cell adhesion, migration, proliferation, differentiation, and survival.^[12]

According to the distinct GAGs as side chains linked to core proteins, three types of PGs can be categorized: HSPGs containing heparin/heparan sulfate (HS), CS/DSPGs containing chondroitin/dermatan sulfate (CS/DS) and KSPGs containing keratan sulfate (KS). While the sulfated GAGs are modified by specific enzymes in the Golgi apparatus of eukaryotic cells, the large hyaluronan (HA) molecule is synthesized by a transmembrane

protein, namely HA synthases. Hence, HA is not attached to a core protein. Instead, it attracts in the extracellular space PGs that form large complexes with the HA molecule like aggrecan.^[11,12] Depending on the location, sulfated GAGs and nonsulfated HA are distinctly responsible for regulating intracellular, cell surface and extracellular functions that are either related to the interaction with proteins inside the cell or involved in organization and function of extracellular soluble (e.g., cytokines) or fixed proteins (ECM). A survey of roles and functions of GAGs and their interactions with proteins are shown in **Table 1**.

2.2. Relationship between Compositions of Glycosaminoglycans and Their Biological Activity

The biological roles of GAGs are often related to their high affinity to GAG-binding proteins. For this recognition, the presence of basic amino acids lysine, arginine and glutamine is found to be essential in GAG-binding domains of proteins for the interaction with negatively charged sulfate and carboxyl groups of GAGs via ionic interaction.^[25,26] However, not the entire binding ability comes from electrostatic forces, because hydrogen bonding also occurs between these and other amino acids in proteins and hydroxyl, *N*/*O*-sulfate groups, and

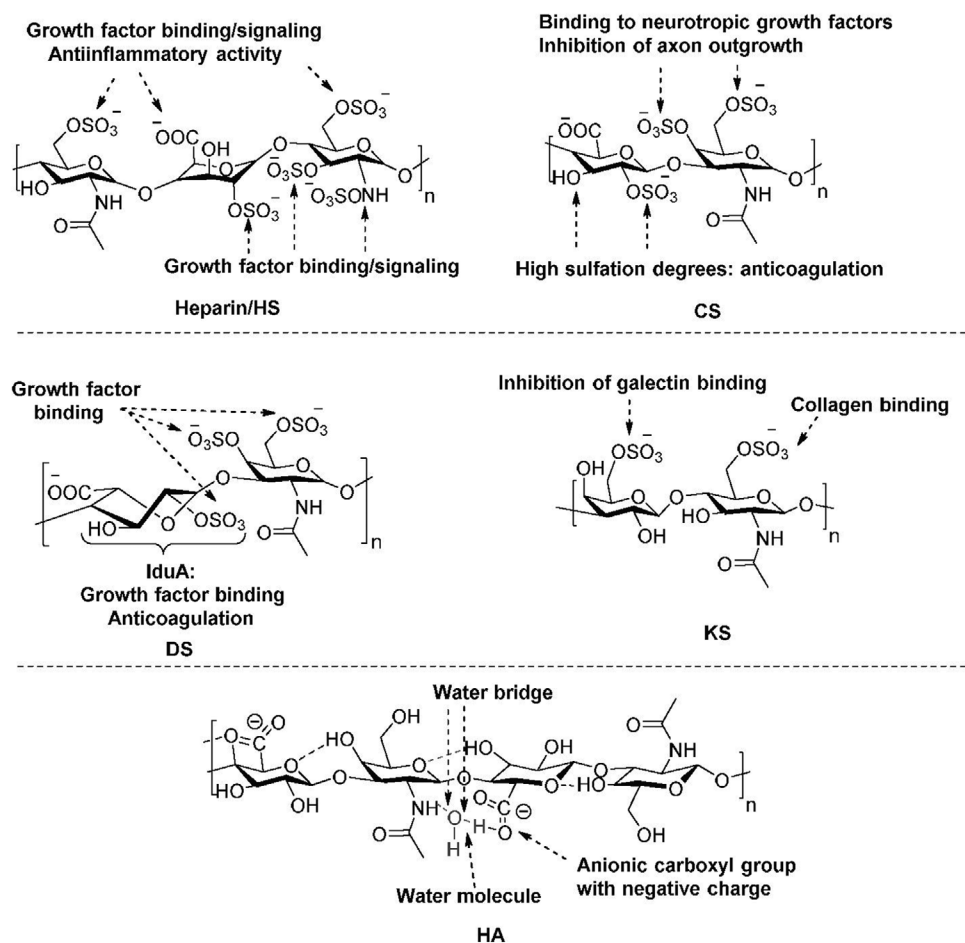


Figure 1. Illustration of the interactions between ionic patterns of GAGs and proteins. HS: heparin sulfate; CS: chondroitin sulfate; DS: dermatan sulfate; KS: keratan sulfate; HA: hyaluronan. Reproduced with permission.^[37] Copyright 2013, Elsevier.

N-acetyl groups in GAGs. Cardin and Weintraub examined the distributions and distances of amino acid sequences XBBXB or XBBBXXB, where B stands for basic amino acids like lysine or arginine and X for another amino acid that are typical for heparin-binding sites of proteins including ECM proteins (e.g., vitronectin and fibronectin), growth factors (e.g., fibroblast growth factor-2, FGF-2) and a multitude of cytokines and chemokines.^[26,27] GAGs act also as coreceptors to endow formation of complexes to change the conformation of proteins (ECM proteins and growth factors) to increase the affinity to their respective cellular ligands (e.g., growth factors receptors and integrins), and therefore strengthen the binding to promote cell adhesion and signal transduction.^[28] Another, well studied example is the role of heparin as anticoagulant. Binding of heparin alters the conformation of antithrombin III (AT III), which increases the affinity of AT III to activated clotting factors, such as thrombin and factor Xa tremendously.^[26] In comparison, DS works in another way to inhibit thrombin by binding to heparin cofactor II (HCII) via electrostatic interaction (Figure 2a).^[29]

It is worth to mention that the distribution and content of ionic groups on GAGs predominately determine GAG-protein interactions. A single GAG with sufficient content of 2-O-, 6-O-, and N-sulfate groups and molecular weight can act as

coreceptor, which binds more than one protein in certain situations. For example, FGF-2 and FGF receptor (FGFR) on cell surfaces are bound simultaneously by HS cell surface PG, such as syndecan-4, resulting in the formation of a ternary complex toward FGF signal pathway that promotes mitogenic activity of cells.^[26,30] Other sulfated GAGs in their corresponding PGs possess similar scenarios of sulfation pattern to bind proteins.^[31–33] In addition, carboxyl and sulfate groups in GlcA and IdoA are the keys to induce the conformational change of GAGs, which provides them with sufficient flexibility to interact with proteins.^[32,34,35] Among the sulfated GAGs, KS has the least feasibility to bind proteins via sulfate groups, but OH groups at C6 position of the galactosamine are found to interact with galectins through hydrogen bonding.^[36] HA, the solely nonsulfated GAG, acts as excellent lubricator in synovial fluid of joints and retains water in tissues, which makes them compression resistant. It is the only GAG that can directly bind to cell surface receptors CD-44, RHAMM and others that regulate several cellular functions (Figure 1).^[37]

Binding of GAGs to growth factors and corresponding cell receptors not only induces signal transduction that governs cell growth and differentiation, but also acts as a storage depot protecting growth factors from proteolytic degradation to prolong

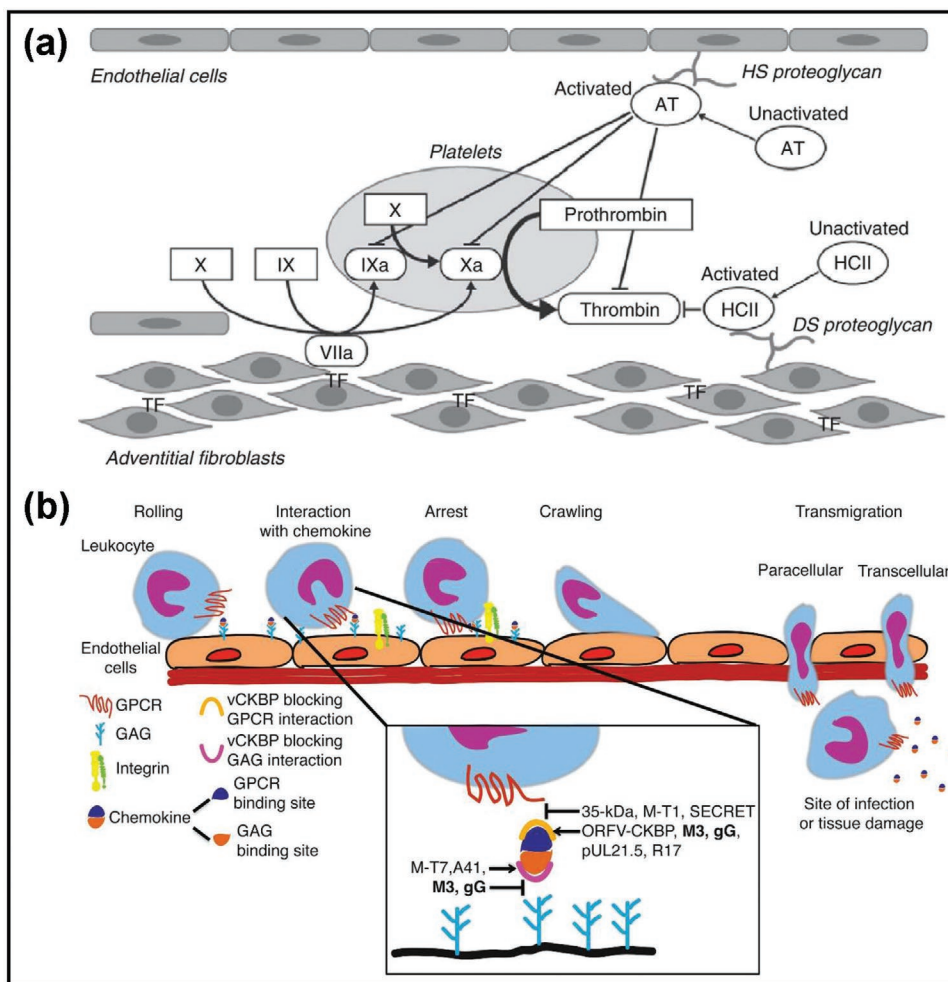


Figure 2. GAG-binding proteins promote anticoagulation and anti-inflammation. a) HS binds antithrombin, while DS binds HCII to inhibit thrombin and factor Xa. Reproduced with permission.^[29] Copyright 2010, Elsevier. b) GAGs-capturing chemokines facilitate leukocyte rolling and extravasation to inflamed tissue. Reproduced with permission.^[38] Copyright 2016, Elsevier.

their half-life as it is found for PG of the ECM.^[33] Likewise, cytokines and chemokines that play an essential role in inflammation and immune response involve interactions with GAGs. GAGs assist chemokines (e.g., monocyte chemoattractant protein-1 (MCP-1), C-X-C motif chemokine (CXCL)12, C-C chemokine receptor (CCR) type 5) to specifically interact with G-protein coupled receptors (GPCRs) and control cell migration and localization that enable leukocytes rolling and extravasation to the inflamed tissue (**Figure 2b**).^[17,26,38] In particular, HA was extensively studied regarding the effect of its molecular weight on inflammation. The binding of high molecular weight HA to CD-44 promotes the production of anti-inflammatory cytokines and inhibits toll-like receptors (TLR) signaling toward nuclear factor- κ B (NF- κ B) translocation that activates macrophages and other leukocytes. In comparison, low molecular weight HA acts conversely and activates TLR signaling associated with release of pro-inflammatory cytokines.^[39] HA may also support tumor development by promoting release of anti-inflammatory factors from macrophages and preventing extravasation of leukocytes that might defeat tumor cells.^[11] Hyaladherins including tumor necrosis α -stimulated gene 6 (TSG-6) are groups of HA-binding

molecules crosslinked to CD-44, which contribute to the development of provisional wound matrix for tissue healing and may have also dampening effects in autoimmune diseases.^[23]

Regarding the specific physiological properties and high binding affinity to ECM proteins, growth factors, cytokines and chemokines to interact with their corresponding cell receptors that activate signal transduction pathways, bioactive GAGs possess a huge therapeutic potential in: a) tissue regeneration and wound dressing, b) encapsulation of cells and biopharmaceuticals, c) anticoagulation, and d) treatment of autoimmune disorders. For example, native or modified GAGs are widely employed in tissue engineering, such as cartilage, skin, vocal cord/fold, bone regeneration, and repair.^[11,26,35,40] Recently, GAGs have been used to generate anti-inflammatory coatings on materials that suppress activation of macrophages,^[41] which may pave the way to generate better compatibility of implanted medical devices like pace makers or biosensors. However, the purification of GAGs from animal sources requires several critical processes that limit their availability, and heterogeneous GAGs from batch to batch are usually obtained, sometimes even with the risk of contamination.^[25] Therefore, the

exploration of other glycans including cellulose and chitosan as more abundant naturally occurring polysaccharides bears a fascinating potential to serve as bioactive components of biomedical devices and therapeutics.^[42,43]

Particularly cellulose draws plenty of attention due to the presence of hydroxyl groups that permit versatile chemical modifications to mimic anionic GAGs or other glycans, which can provide superior tunable functionality of such GAGs-mimicking biopolymers. In recent years, cellulose derivatives containing diverse ionic groups, such as acidic carboxylic, phosphate and sulfate groups as well as positively charged amino groups, were broadly studied and applied as potential biomaterials. Beside the polymeric, soluble derivatives obtained from cellulose, also its native crystalline structure can provide another platform for the preparation of diverse ionic, biologically active nanomaterials. We will describe in more detail later in this work how both classes of these materials can be synthesized. Moreover, biomaterials derived from polymeric cellulose derivatives and nanocellulose-based compounds show promising biological properties and application areas that will be also described in more detail below.

Before a material or technology can generally be practically used as biomaterials, their impacts on the environment and human health need to be thoroughly assessed. Therefore, some critical biological properties, i.e., biocompatibility, cytotoxicity and biodegradability, must be evaluated before they are applied in practice. Biocompatibility is the ability of a foreign material implanted in the body to exist in harmony with tissues without causing deleterious changes, which is an essential requirement for biomedical materials.^[44] Hemocompatibility is another significant property of biocompatibility, especially for blood-contacting biomaterials and artificial organs, such as artificial blood vessels, pumps, and artificial hearts. Cytotoxicity refers to adverse effects of a substrate on cell viability. Generally, evaluation methods of cytotoxicity include four categories: 1) methods that assess cell damage on the basis of cell morphology, 2) methods that measure cell damage, 3) methods that measure cell growth, and 4) methods that measure specific

metabolic activities.^[45] Biodegradability and bio-absorbability are the ability of the materials and their products to degrade and/or be absorbed or safely eliminated from the body. The degradation of cellulose occurs via hydrolysis by cellulases that hydrolyze the β -1,4-glucosidic linkages. Native cellulose exhibits limited *in vivo* degradation due to the lack of cellulases in human body. Thus, cellulose may be considered as nonbiodegradable *in vivo* or really slowly degradable, resulting in both durability and long-term chemical stability, which proved to be beneficial for a wide range of biomedical applications, such as surgical repair and engineered cartilage.^[46] But for some other biomedical applications, the biodegradable ability of cellulose based materials should be improved.^[47] Oxidized cellulose has shown to be more susceptible to hydrolysis and therefore potentially degradable by human body.^[48]

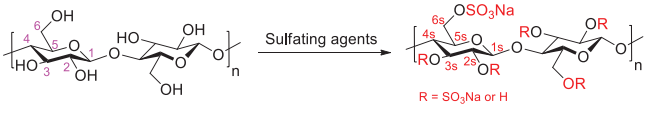
3. Ionic Compounds Based on Cellulose Derivatives and Their Applications as Biomaterials

3.1. Synthesis of Ionic Cellulose Derivatives

3.1.1. Negatively Charged Ionic Cellulose Derivatives

Cellulose Sulfate: Cellulose, as the most abundant polysaccharide in nature, is a linear-chain polysaccharide composed of β -1,4-linked D-anhydroglucopyranose units (AGUs). Each AGU contains hydroxyl groups at C2, C3, and C6 position, which can undergo the typical sulfation reactions of primary and secondary alcohols to synthesize cellulose sulfate (CS). CS with GAGs-analogue sulfation patterns can be synthesized using diverse sulfating reagents, e.g., ClSO₃H, H₂SO₄, SO₂, SO₃, SO₄, SO₂Cl₂, and SO₂-pyridine complex.^[49–55] Distinct sulfation routes are suitable for diverse starting materials, such as microcrystalline cellulose, α -cellulose, bacterial cellulose and cellulose derivatives including cellulose trifluoroacetates. These sulfation methods are generally carried out in heterogeneous, quasi-homogeneous and homogeneous state, as summarized in **Table 2**.

Table 2. Schematic illustration and general methods for the synthesis of CS.



	Cellulose		Cellulose Sulfate		
Synthesis	Starting material	Sulfating agent	Position	DS _s	Ref.
Quasihomogeneous	MCC ^{a)} or AC ^{b)}	ClSO ₃ H/acetic anhydride	6- and 2-O-	Broad DS range	[54,55]
Heterogeneous	Bacterial cellulose ^{c)}	ClSO ₃ H-DMF complex	Preferentially 6- > 2- > 3-O-	0.04–0.86	[53]
Heterogeneous	AC ^{d)}	H ₂ SO ₄	–	Uncontrollable	[52]
Homogeneous	Cellulose powder ^{e)}	SO ₂ or SO ₃ /N ₂ O ₄	Preferentially 6-O-	Low DS	[51]
Quasihomogeneous	Linters cellulose ^{f)}	SO ₂ Cl ₂ or NH ₂ SO ₃	Preferentially 6-O-	0.15–2.95	[49]
Quasihomogeneous	Cellulose trifluoroacetates ^{g)}	SO ₃ -pyridine complex	3-O-	0.98	[50]

^{a)}MCC: microcrystalline cellulose, degree of polymerization (DP): 275–277; ^{b)}AC: α -cellulose (97.0%, with a DP of averagely 1180); ^{c)}Prepared by incubation of *Acetobacter x.* in a culture media containing coconut juice; ^{d)}Isolated from tree *Lantana camara*; ^{e)}A hydrolytically degraded and subsequently disintegrated cellulose powder from spruce sulfite pulp with DP_{Cu} of 160 was used for most of those experiments; ^{f)}Linters cellulose (DP of averagely 1090); ^{g)}The DS ascribed to trifluoroacetyl group was 1.5, and the DP of starting cellulose was 460.

A particular sulfating route could affect the intrinsic characteristics of obtained CS, which include the molecular weight, total degree of substitution (DS) ascribed to sulfate groups (DS_S), the distribution and the position of sulfate groups. Correspondingly, these structural properties can be determined using various analytical methods, for instance, low angle light scattering and gel permeation chromatography (GPC) for molecular weights, elemental analysis for total DS, nuclear magnetic resonance (NMR) analysis for partial DS and distribution of sulfate groups, FT-IR and FT Raman spectroscopy for qualitative and empirically quantitative analysis of sulfate groups. These details were also partially reviewed by the groups of Edgar,^[56] Heinze^[57] and Zhang.^[58]

The total DS_S of CS can be calculated based on the contents of sulfur and carbon, which are determined with elemental analysis as follows

$$\text{Total DS}_S = (S\%/32)/(C\%/72) \quad (1)$$

where S% is the content of sulfur in wt% and C% is the content of carbon in wt%.

NMR spectroscopy is an important analytical tool for the determination of the content and purity of a sample as well as its molecular structure. Thanks to the excellent solubility of CS with a broad range of DS in water, the partial DS ascribed to sulfate groups and thus their distribution within the AGUs can be determined based on the integration of the corresponding carbon signals within ¹³C NMR spectrum after measuring D₂O solutions of CS (Figure 3). In comparison, ¹H NMR spectra of polysaccharides often show overlapping signals of diverse protons. Because the proton decoupling (nuclear Overhauser effect) influences the signal intensity of diverse carbon atoms on the cellulose backbone to distinct extents, the partial DS can be then calculated by determining the ratios of integrals of signals derived from the “substituted” and “nonsubstituted” carbon atoms to the sum of both.^[55] For example, before and after the modification of hydroxyl groups at C6 position by sulfate groups, the chemical shift of C6 is changed from 60 ppm

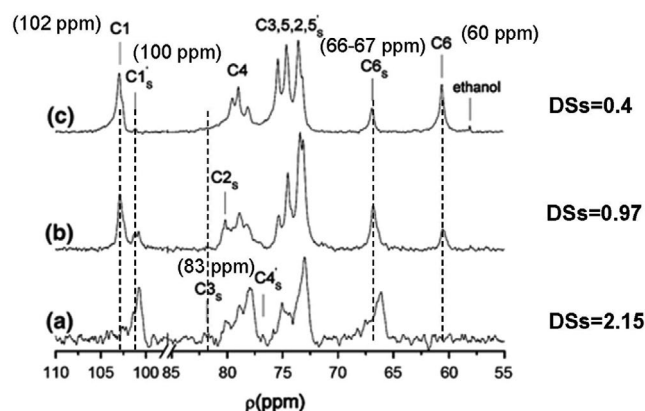


Figure 3. Characteristic ¹³C-NMR spectra (110–55 ppm) of: a) CS with DS of 2.15, b) CS with DS of 0.97, and c) CS with DS of 0.4 in D₂O at RT showing the chemical shifts of corresponding carbon atoms for the determination of partial DS ascribed to sulfate groups at a particular position at cellulose backbone. Reproduced with permission.^[55] Copyright 2010, Springer Nature.

(nonsubstituted) to 66–67 ppm (substituted) within ¹³C-NMR spectrum, and the integrals of their corresponding signals can be used for the calculation of the partial DS attributed to the sulfation at 6-O-position.^[59]

CS has advantageous physicochemical properties, such as excellent biocompatibility, water solubility, pronounced hydrophilicity, biodegradability and nontoxicity. In addition to these physicochemical properties, CS also exhibited excellent biological activities, e.g., anticoagulation, antiviral activity and promoting effect on cell growth and differentiation. Moreover, CS can be applied into drug carrier and tissue engineering scaffolds. These increasingly interests for scientists to use CS in diverse biomedical and bioengineering fields will be further described later.

Cellulose Phosphate: Phosphorus compounds present in a large group of natural materials demonstrate diverse biological activities. These compounds are diversified in their chemical structures ranging from phospholipids to nucleic acids,^[60] and are widely used in diverse fields, such as analytical^[61] and medicinal chemistry.^[62] In order to artificially introduce phosphorus into organic small molecules, a few general methods have been developed to form covalent bonds such as P–C^[63] and P–O bonds.^[64] In addition to the low molecular weight organophosphorus compounds, the introduction of phosphate groups into polysaccharides backbone is an important route to prepare diverse phosphated derivatives of polysaccharides.^[65,66]

Esterification of hydroxyl groups on cellulose backbone is the general process to prepare cellulose phosphate (CP). There are various routes to synthesize CP (Table 3). In 1949, Reid et al. investigated diverse methods to introduce phosphate groups into cotton cloth to synthesize flame- and glow-proof cloth. The method using POCl₃ as the phosphorylating agent was adopted.^[67] This method suffers from great loss in tensile strength after the modification and low contents of phosphate groups.

The approaches for the synthesis of CP was then further developed by using (NH₄)₂HPO₄/urea,^[68] phosphorous acid in molten urea^[69] or H₃PO₄/P₂O₅/Et₃PO₄^[71] as phosphating agent with various reaction times and temperatures, in order to prepare CP with alterable total DS ascribed to phosphate groups (DS_P) and water-solubility. In 2002, Gospodinova et al. for the first time reported a method to do phosphorylation of microcrystalline cellulose via solvent-free microwave treatment.^[73] This method achieved CP with a broad range of DS_P without further purification. In 2003, Petreus et al. found that the aqueous NaOH system for dissolving cellulose should have considerable potential for the synthesis of CP.^[70] They scoped various phosphating agents, such as phosphoric and phosphorous acids, phenyl- and phenoxy phosphonic dichlorides and an amido phosphite oligomer. In 2006, water-soluble CP with alterable DS_P were prepared after the reaction of microcrystalline cellulose with phosphorous acid in molten urea.^[72] At the same time, they reported a new efficient method to determine the total DS_P via potentiometric or conductometric titration, which was in agreement with the results of elemental analysis.

Moreover, it was also found that CP was formed during the direct dissolution of cellulose in phosphoric acid. Cellulose dissolution in phosphoric acid involves two main processes. One process is the esterification reaction between hydroxyl groups

Table 3. Schematic illustration and general methods for the synthesis of CP.

Starting material	Phosphating agent	Time [h]/Temp. [°C]	Water solubility	DS _p	Ref.
Cotton cellulose	POCl ₃ /pyridine	1–6/25–150	Insoluble	Up to 0.67	[67]
Cotton fabric cellulose	(NH ₄) ₂ HPO ₄ /urea	0.17/150	Insoluble	–	[68]
Filter paper ^{a)} and cotton cellulose	H ₃ PO ₄ /molten urea	0.5–8/150	Insoluble	0.59–2.0	[69]
Microcrystalline cellulose ^{b)}	H ₃ PO ₄ /NaOH	0.5/r.t.	Insoluble	0.56	[70]
	H ₃ PO ₃ /NaOH	0.5/r.t.	Insoluble	0.49	[70]
Microcrystalline cellulose ^{c)}	H ₃ PO ₄ /P ₂ O ₅ /Et ₃ PO ₄	72/30	Gel	Up to 2.9	[71]
Microcrystalline cellulose ^{d)}	H ₃ PO ₃ /molten urea	2–5/150	Soluble	0.62–1.06	[72]
Microcrystalline cellulose ^{e)}	H ₃ PO ₃ /urea	2/105	–	0.2–2.8	[73]

^{a)}80 mesh, Toyo Roshi Ltd., code No. 2; ^{b)}Avicel 101 (microcrystalline cellulose for tableting application) was obtained from Trademark FMC Corporation; ^{c)}Microcrystalline cellulose Avicel PH-101 was purchased from Fluka Chemie with the particle size of 50 μm; ^{d)}Microcrystalline cellulose Avicel PH-101 obtained from Acros Organics, Germany; ^{e)}Reactions performed in solvent-free microwave condition.

of cellulose and phosphoric acid to form CP. The other process is a competition of hydrogen-bond formation^[74] (a. the hydrogen-bond formation between hydroxyl groups of cellulose chains and b. the hydrogen-bond formation between hydroxyl groups of cellulose chain with water molecule or with hydrogen ion) and the side reaction of acid hydrolysis of cellulose. Moreover, it is observed that CP can be reversibly converted back to free phosphoric acid and amorphous cellulose without any significant phosphorylation.^[75]

In addition to molecular weights, total DS_p and the distribution of phosphate groups are important structural features affecting the

physicochemical properties of obtained CP. The total DS_p of CP can generally be calculated using the phosphorous contents determined via elemental analysis method as follows^[76]

$$\text{Total DS}_p = (162 * P\%) / (3100 - 84 * 84\%) \quad (2)$$

where P% is the content of phosphorous in wt%.

Similar as for CS, ¹³C, and ³¹P NMR spectra based on the chemical shifts of carbon and phosphor atoms at the “substituted” and “nonsubstituted” positions are efficient methods to qualify the partial DS_p and the distribution of phosphate groups within AGUs.^[77]

CP demonstrates similar advantageous physicochemical properties as CS, such as biocompatibility, nontoxicity, hydrophilicity and biodegradability. However, the solubility of CP highly depends on the DS_p in addition to the molecular weight, because too low DS_p will lack the sufficient hydrophilicity and too high DS_p results in gel formation due to crosslinking of phosphate groups. Nevertheless, phosphate group possess a few specific advantages, such as extraordinary binding ability to Ca²⁺ ions or growth factors,^[69,78] cytocompatibility with human osteoprogenitor cells,^[79] crosslinking ability with other polysaccharides^[66] and more potential negative charges shown by each phosphate group for specific binding with biologically active species.^[80] Due to those advantageous properties, CP can be

envisaged as a promising biomaterial, such as for bone tissue engineering and drug delivery.^[81]

Carboxymethyl Cellulose: Carboxymethyl cellulose (CMC), another important cellulose derivative obtained via carboxymethylation of hydroxyl groups on cellulose backbone, finds a broad range of application in foods additive,^[82] pharmaceutical additive,^[83] and with high potential in biomedical fields.^[84,85]

CMC can be generally synthesized after the reaction of cellulose and chloroacetic acid in alcoholic solution of sodium hydroxide. In addition to this conventional approach, a few other methods have been established for the synthesis of CMC (Table 4). In 1994, Heinze et al. synthesized CMC in LiCl/DMAc under homogeneous condition and developed a rapid and convenient protocol to determine the substituent patterns of CMC by means of high-performance liquid chromatography.^[86] This method also could be used to separate the mixture of CMC, such as CMC with tri-substitution, di-substitution, and mono-substitution in cellulose backbone. In 2005, Ramos et al. established a novel carboxymethylation method to modify cellulose in DMSO/tetrabutylammonium fluoride condition.^[87] This method led to CMC with a higher total DS ascribed to carboxymethyl groups (DS_{CM}). In 2009, Qi et al. studied the carboxymethylation of cellulose in the aqueous solution of 7 wt% NaOH/12 wt% urea.^[88] Water-soluble CMC with DS_{CM} of 0.20–0.62 with the distribution of carboxymethyl groups at 6-O- > 2-O- > 3-O-position was prepared from both Avicel cellulose and cotton linters. In 2010, they further modified the method to synthesize CMC in the aqueous solution of sodium monochloroacetate/LiOH/urea with DS between 0.36 and 0.65 and similar distribution of carboxymethyl groups.^[89]

The basic physicochemical properties of CMC highly depend on the molecular weight, the total DS_{CM}, the distribution of carboxymethyl groups along the cellulose backbone and at diverse positions within repeating units.^[92] Similar analytical methods as for CS and CP are generally used, e.g., using GPC for the analysis of their molecular weights. In order to determine the

Table 4. Schematic illustration and a few recent approaches for the synthesis of CMC.

Cellulose $\xrightarrow{\text{Carboxymethylation agents}}$ Carboxymethyl cellulose
R = CH₂COONa or H

Synthesis	Starting material	Carboxymethylation conditions	Time [h]/Temp. [°C]	DS _p	Ref.
Heterogeneous	Alkali cellulose	Sodium monochloroacetate	–	0.5–1.0	[90]
Heterogeneous	Avicel cellulose and cotton linters ^{a)}	Monochloroacetic acid/NaOH/urea, aqueous	5/55	0.2–0.62	[88]
Homogeneous	Spruce sulfite pulp cellulose ^{b)}	Monochloroacetic acid/DMAc/LiCl/NaOH	10–72/70	0.33–2.07	[86]
Homogeneous	sisal and cotton linters ^{c)}	Monochloroacetic acid/DMSO/TBAF ^{d)} /NaOH	4/70	up to 2.2	[87]
Heterogeneous	Microcrystalline cellulose ^{e)}	Sodium bromomalonate/isopropanol/water/NaOH	5/60	0.05–0.51	[91]
Homogeneous	Avicel cellulose and cotton linters ^{a)}	sodium monochloroacetate/LiOH/urea, aqueous	5/55	0.36–0.65	[89]

^{a)}Avicel (DP = 330), cotton linters 1 (DP 500), and cotton linters 2 (DP 2000); ^{b)}DP of cellulose was 320, 600, and 1400; ^{c)}Sisal cellulose (DP = 640) and cotton linters (DP = 400); ^{d)}Tetrabutylammonium fluoride; ^{e)}Microcrystalline cellulose (MN 400).

total DS_{CM} of CMC, titration using sodium hydroxide solution is used as the classical method.^[93] The determination of sodium content is another common method to analyze the total DS_{CM} of CMC, if CMC is completely converted to the sodium salt and no other impurity is present.^[94] The details of further analytic methods were also reviewed by Heinze and Koschella,^[95] which includes a few recent methods, such as HPLC^[86] and NMR spectrum.^[95] The partial DS_{CM} can also be determined according to the integrated areas of signals within the ¹³C NMR spectrum of CMC ascribed to “substituted” and “non-substituted” positions within AGUs, after measuring the D₂O solution of CMC.^[96]

3.1.2. Positively Charged Ionic Cellulose Derivatives

For the introduction of N-containing moieties that might be cationic either permanently or depending on the pH value of the system, diverse approaches were developed in the last years. A myriad of publications was summarized in reviews about synthetic cationic polyelectrolytes^[97] as well as cationized polysaccharides (as amino and ammonium hydroxypropyl ethers).^[98] Thus, we only scope recent typical examples of cellulose-based products related to the focus herein.

The simplest method is the esterification of the biopolymers with carboxylic acids containing an ammonium moiety. However, activated carboxylic acids, such as acyl chlorides or acid anhydrides are not appropriate due to their limited solubility, availability and the formation of acidic byproducts. An elegant path for the esterification with N-containing moieties is the application of imidazolides obtained from the corresponding carboxylic acid. Among others, the reaction with *N,N*-carbonyldiimidazole (CDI) as catalyst is a mild and efficient synthesis strategy.^[66] In one study, (3-carboxypropyl)trimethylammonium chloride was activated with CDI in DMSO at first and the intermediate product was then allowed to react with cellulose homogeneously in DMA/LiCl.^[99] Resulting cellulose (3-carboxypropyl)trimethylammonium chloride ester showed typical ¹³C NMR spectrum with a DS of 0.75 as shown in **Figure 4**.

Cellulose (3-carboxypropyl)trimethylammonium chloride esters can be adsorbed on cellulose films triggering subsequent

protein adsorption.^[100] The material adsorbed was quantified by using QCM-D (quartz crystal microbalance with dissipation monitoring, wet mass) and MP-SPR (multiparameter surface plasmon resonance, dry mass). Studies with BSA (fluorescence labeled) at different concentrations and pH values indicated that the interaction decreases in order pH = 5 > pH = 6 > pH = 7 and DS_{high} > DS_{low}. The amount of adsorbed BSA could be adjusted in a range from 0.6 to 3.9 mg m⁻² (dry mass). Thus, to achieve selective functionalization of cellulosic surfaces by antibodies, BSA may be applied as blocking agent. Moreover, this N-containing cellulose derivative was also used for the surface modification of pulp fibers to preserve the inherent bulk properties (e.g., low density, mechanical strength) and to improve the properties of the fiber surface, for instance wetting behavior and bacteriostatic activity.

These cationic cellulose derivatives with diverse N-containing moieties can also contain other functional groups to further improve their properties. A typical example is cellulose 2-[(4-methyl-2-oxo-2H-chromen-7-yl)-oxy]acetates prepared via CDI-catalyzed reaction with the corresponding carboxylic acid in DMA/LiCl, which were subsequently modified via CDI-catalyzed reaction with (3-carboxypropyl)trimethylammonium chloride yielding water-soluble and photoactive cellulose derivatives (**Figure 5a**).^[101] The partial DS values could be determined by a combination of UV-vis spectroscopy and elemental analysis. The DSs were between 0.05 and 0.37 for the photoactive moiety and between 0.19 and 0.34 for the cationic group.

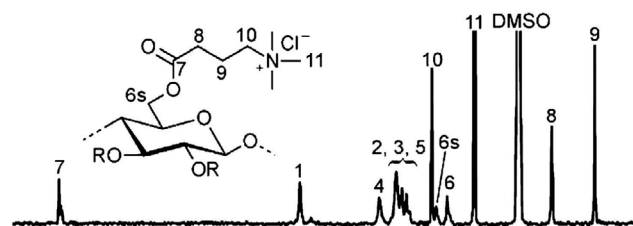


Figure 4. ¹³C NMR spectrum of cellulose (3-carboxypropyl)trimethylammonium chloride ester, degree of substitution 0.75 acquired in DMSO-d₆. Reproduced with permission.^[99] Copyright 2013, American Chemical Society.

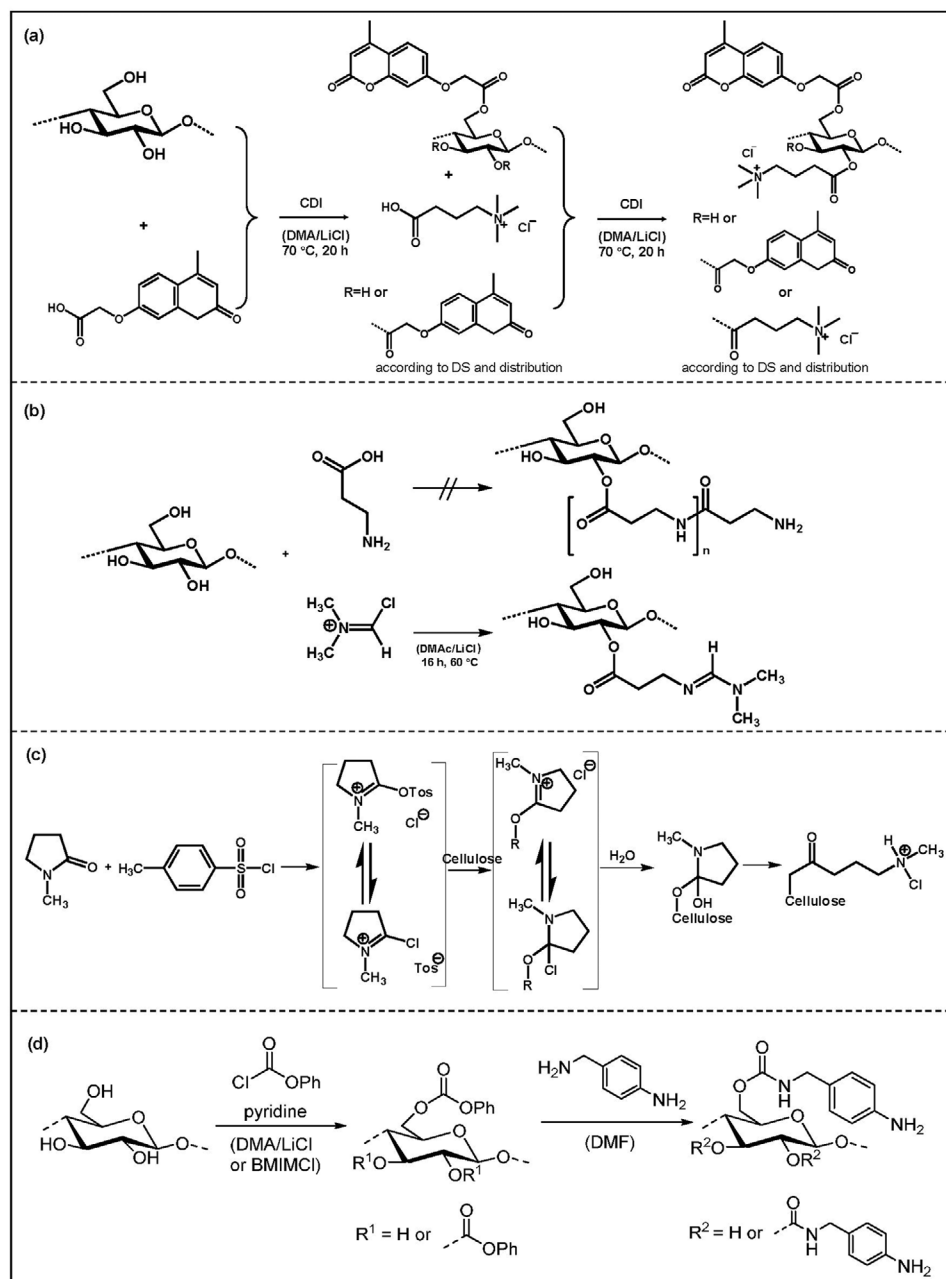


Figure 5. Diverse routes for preparing positively charged cellulose derivatives. a) Scheme for synthesis of cellulose 2-[(4-methyl-2-oxo-2H-chromen-7-yl)-oxy]- acetates and cellulose 2-[(4-methyl-2-oxo-2H-chromen-7-yl)oxy]-acetate-[4-(N,N,N-trimethylammonium) chloride] butyrates by in situ activation of 2-[(4-methyl-2-oxo-2H-chromen-7-yl)oxy]acetic acid and (3-carboxypropyl)trimethylammonium chloride with N,N-carbonyldimazole (CDI) in N,N-dimethylacetamide/LiCl (DMA/LiCl). Reproduced with permission.^[101] Copyright 2012, Springer Nature. b) Reaction pathway and structure of dextran N-[(dimethylamino)methylene]-β-alanine ester in one step. Reproduced with permission.^[102] Copyright 2016, Elsevier. c) Reaction scheme for the conversion of cellulose with N-methyl-2-pyrrolidone in the presence of p-toluenesulphonic acid chloride. Reproduced with permission.^[103] Copyright 2011, Springer Nature. d) Reaction scheme for the synthesis of cellulose phenyl carbonate and subsequent aminolysis applying p-aminobenzylamine to the corresponding cellulose carbamate. Reproduced with permission.^[104] Copyright 2014, Wiley-VCH.

Another synthetic approach is the esterification of polysaccharides with N-protected amino acids yielding nonviral vectors for gene delivery.^[105] Polysaccharide esters of β-alanine and L-lysine were able to interact electrostatically with DNA forming complexes of about 70–110 nm with positive zeta potential. L-Lysine esters showed more effective binding and protection of

DNA against enzymatic degradation compared to the β-alanine esters. However, luciferase reporter gene assays revealed higher transfection efficacies for β-alanine than for L-lysine esters. Even unprotected β-alanine was used for the one-step reaction on polysaccharides by iminium chloride, N-[(dimethylamino)methylene]-β-alanine esters of polysaccharides were selectively

formed, which are interesting nonviral gen-transfer vectors (Figure 5b).^[102]

Furthermore, the ring-opening of lactams in the presence of *p*-toluenesulphonic acid chloride is an efficient path to obtain cationic cellulose esters with DS in the range from 0.24 to 1.17.^[103] The transformation of cellulose can be carried out homogeneously in *N*-methyl-2-pyrrolidone (NMP)/LiCl or 1-butyl-3-methylimidazolium chloride containing NMP, with *N*-methyl-2-piperidone, ϵ -caprolactam and *N*-methyl- ϵ -caprolactam as reactive lactams forming a reactive intermediate in the presence of tosyl chloride according to the Vilsmeier–Haack reaction (Figure 5c). Subsequently, the iminium ion reacts with the hydroxyl groups of cellulose and subsequent ring opening by water occurs. Resulting cationic cellulose esters do not hydrolyze at pH values up to 7 and possess high adsorption capacity on cellulose surfaces at pH 7 ($\Delta f = -15$ to -17 Hz) at high ionic strength ($25\text{--}100 \times 10^{-3}$ M of NaCl) as studied by means of QCM-D.^[106] At lower ionic strength ($1\text{--}10 \times 10^{-3}$ M of NaCl), the adsorption decreases ($\Delta f = -2$ to -12 Hz) indicated by lower absolute values of the shifts in frequency.

The design of soluble amino cellulose derivatives was carried out after conversion of hydroxyl groups of cellulose into the good leaving groups, e.g., tosylate groups. Nucleophilic displacement reactions could be performed at C6 position using di- and oligoamines.^[107] The aqueous solutions of obtained 6-deoxy-6-(ω -aminoethyl)amino cellulose showed extraordinary properties as reversible association products, which typically occurs for proteins, discovered by analytical ultracentrifugation.^[108] Moreover, the formation of ultrathin and transparent films of amino celluloses takes place after their self-assembly on planar substrates, such as glass, gold and silicon wafer. A nanoscaled topography was obtained by dipping, spraying and spin coating using 5% aqueous solutions of amino celluloses.^[109,110] Moreover, self-assembled monolayers of amino celluloses were also obtained on various substrates from their dilute aqueous solutions (0.01–0.05%) that were stable against intensive rinsing with water.^[111]

An alternative path to synthesize soluble amino group-containing cellulose derivatives was established by the modifications of cellulose carbonates. Corresponding carbamates were formed via the reaction between cellulose and chloroformates followed by further aminolysis with an amino group-containing compound (Figure 5d).^[112] The aminolysis occurs efficiently with at least 90% of carbonate moieties converted into carbamate. Anilines, such as *p*-toluidine, do not react, while secondary amines yield crosslinked and hence insoluble products. Soluble products with terminal amino moieties could be obtained using aromatic amines, e.g., by using *p*-aminobenzylamine without any further protection (Figure 5d).^[113] The reaction of aliphatic diamines with cellulose carbonates could result in crosslinked products that can be avoided by using mono-protected diamines.^[114]

3.2. Application of Ionic Cellulose Derivatives as Biomaterials

3.2.1. Tissue Engineering

The biological activity of anionic cellulose derivatives has been studied with regard to various applications in the field of tissue

engineering. Based on the knowledge about sulfation pattern of natural GAGs, the binding affinity of CS toward growth factors was investigated by Peschel et al. and Zhang et al., especially regarding the substantial effects of regioselectivity and overall DS_S between 0.58 and 1.94 on growth factor binding and cellular activities.^[54,115,116] Studies showed that CS with overall DS_S more than 1.57 in addition to a gradual increase of sulfation at both the 2-O- and the 6-O-position exhibited a stronger binding ability toward FGF-2, while a higher affinity to BMP-2 was found for CS with intermediate DS_S and more sulfation at the 6-O-position, but lower sulfation at the 2-O-position.. Mitogenic and osteogenic activities of CS promoted cell proliferation and differentiation, which was comparative or even surpassing that of heparin (Figure 6a–c). Studying the working mechanism of CS toward growth factors, it was observed that CS protected growth factors from proteolytic cleavage that prolonged their half-life resulting in a sustained stability and bioactivity with increasing DS_S and concentration.^[117] Other groups studied the effect of regioselective sulfation of cellulose on in vitro vascularization of biomimetic bone matrices, but did not find any special cooperative effect with vascular endothelial growth factor (VEGF), although an improved angiogenesis was found in the presence of CS.^[118] Indeed, they speculated that the interaction with other growth factors could play a role, which could be FGF-2 that also plays a role in neovascularization and exhibited an enhanced activity by binding to CS.^[119] Peschel et al. found that the CS also enhanced cell growth in the absence of any exogenous addition of growth factors or serum to cell cultures, which further proved the enhanced activity of such growth factors by CS.^[116] A few other groups studied the effect of partially sulfated CS regarding its interaction with transforming growth factor- β (TGF- β), e.g., as electrospun blend fibers together with gelatin.^[120] They found stronger binding of TGF- β to these blend fibers due to postulated similarity of CS to chondroitin sulfate—a natural component of cartilage. They observed an improved chondrogenesis of mesenchymal stem cells cultured on these fibrous materials that was dependent on presence of CS and TGF- β . Similar findings toward binding of growth factors and effects toward chondrogenesis of MSCs were also observed with hydrogels made of CMC, sulfated CMC, and gelatin,^[121] which will be further discussed in the section about CMC. Other studies demonstrated that sulfation of cellulose significantly enhanced the interaction of scaffold materials with other growth factors, such as neuronal growth factor NGF comparing chondroitin A and C sulfated with lower (only at the 6-O-position of AGU) and fully sulfated CS.^[122] It was observed that binding of NGF increased with total DS_S, which was the highest for fully sulfated CS and led to maximum outgrowth of neurites. The findings that CS promotes the activity of growth factors and cells are strongly in line with statements on the activity of GAGs toward growth factors being dominated by ionic interactions.^[33]

Apart from the specific intrinsic bioactivity, the presence of negative charged sulfate groups in CS demonstrates other advantages. CS can be used as building blocks for adjustable fabrication of surface coatings, hydrogels and scaffolds via chemical and physical crosslinking reactions that mimic cell microenvironment or tissue structure.^[125] Recently, polysaccharide-based multilayers were assembled using oppositely charged polyelectrolytes via layer-by-layer (LbL) process.^[126]

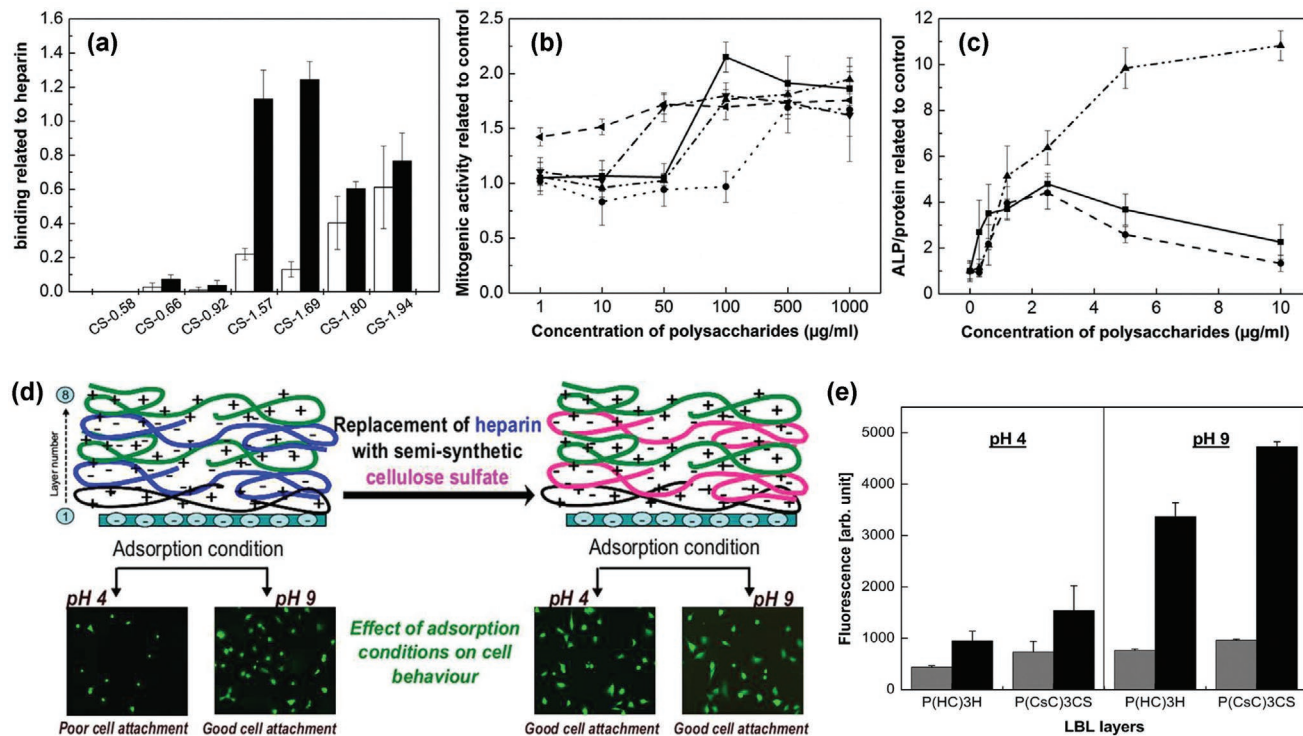


Figure 6. a) Comparative binding assay of cellulose sulfates versus heparin for FGF-2 (white bar) and BMP-2 (black bar). b) Mitogenic activity of selected cellulose sulfates measured by proliferation of 3T3 fibroblasts in the presence of 10 ng mL⁻¹ FGF-2 and increasing quantities of cellulose sulfates and heparin. CS-0.92: circle, dotted line; CS-1.57: triangles, dash-dot line; CS-1.80: rhombus, dash-dot line; CS-1.94: triangle, dashed line; heparin: square, solid line. c) Osteogenic activity of selected cellulose sulfates measured by expression phosphatase (ALP) normalized to protein content of cells in the presence of 200 ng mL⁻¹ BMP-2 and increasing quantities of cellulose sulfates and heparin. CS-1.57: triangles; CS-1.94: rhombus; heparin: square. a–c) Reproduced with permission.^[123] Copyright 2013, American Chemical Society. d) Schematic illustration for cell behaviors on multilayers built with chitosan and anionic polysaccharides. The illustration of multilayer formation at pH 4 or 9 based on electrostatic interaction between chitosan as polycation and heparin (left) or cellulose sulfate (right) as polyanion.^[124] e) Cell proliferation measurements after 1 (gray bars) and 3 (black bars) days of C2C12 cell culture in DMEM with 10% FBS on polyanion (heparin or CS) terminated multilayers prepared at diverse pH conditions. d,e) Reproduced with permission.^[124] Copyright 2013, American Chemical Society.

The film thickness, hydration and swelling properties mainly depend on deposition conditions, such as pH values and ionic strength, which alter the properties regarding protein adsorption, controlled release of bioactive molecules and cell responses.^[124,126,127] For example, multilayers constructed with CS of selected total DS_s (1.57 and 2.59) as polyanion and chitosan as polycation were more stable in a wide range of pH values compared to multilayers composed of heparin and chitosan. The CS-containing multilayers supported fibronectin adsorption, C2C12 myoblast adhesion and proliferation to a higher extent than those prepared with heparin as polyanion. Therefore, CS demonstrates to be a promising candidate for bioactive coatings in such multilayer systems that are feasible for growth factor loading in tissue engineering and biomimetic modification of implants (Figure 6d,e).^[124,128] Aggarwal et al. also explored distinct approaches to blend natural GAGs (e.g., heparin) with CS to regulate multilayer properties and cellular response.^[127]

While surface coatings provide an optimal platform for control of cell adhesion and growth on implant surfaces, 3D systems like scaffolds and hydrogels may be used in tissue engineering approaches to replace injured or lost tissues by a living substitute colonized by cells either in vitro or in vivo. The

stability and bioactivity of scaffolds made of CS was evaluated recently by Huang et al., who blended CS with gelatin to prepare scaffolds via electrospinning after further crosslinking.^[120] The crosslinked fibrous scaffolds exhibited excellent mechanical properties and stability in the hydrated state assessed by the analysis of tensile stress and elastic modulus close to the properties of electrospun collagen fibers. The interaction and binding affinity of TGF-β₃ were found to increase with the amount of CS in the scaffold. However, only 0.1% CS combined with gelatin could induce chondrogenic differentiation of human mesenchymal stem cells (hMSC) with TGF-β₃ dissolved in the medium. This was assumed to be due to stronger binding of TGF-β₃ with higher amounts of CS included in the scaffolds, which blocked release of this growth factor and thus inhibited chondrogenesis. Another report investigated the effect of regioselective sulfation of CS, particularly at 2-O-position, during the formation of porous collagen/hydroxyapatite nanocomposite scaffolds of optimal porosity (with a diameter of 100–200 µm).^[118] It was hypothesized that the polyelectrolyte complex (PEC) should promote the neovascularization in combination with VEGF. However, the evidences were not sufficient and required further studies regarding the cooperation between collagen and CS, which might trigger the interaction

between CS and VEGF. Very recently, chemically crosslinked hydrogels were constructed using oxidized CS and polyamines including carboxymethyl chitosan for embedding cells for potential replacement of soft tissues like cartilage.^[129]

Biocompatible and biodegradable CMC with anionic carboxyl groups can link with positively charged materials via electrostatic interaction to form polyelectrolyte complexes (PEC). Recently, PEC made by mixing CMC and chitosan have attracted tremendous interest for application in bone tissue engineering. For example, a chitosan/CMC scaffold possessed an improved stability for more than 30 days and suitable internal porosity allowing the diffusion of nutrients, which generated the potential for the regeneration of dental pulp tissue.^[130] Hydroxyapatite is a typical inorganic component of bone and the most common type of calcium phosphate (CaP) used in bone tissue engineering. The addition of CMC in nano-hydroxyapatite/chitosan (n-HA/CHI/CMC) scaffold with irregular network structure resulted in a compressive strength of 3.5 MPa and a porosity of 77.8%. In particular, the mechanical properties met the requirements not only for promoting hMSC proliferation *in vitro*, but also for the growth of blood vessels and integration of surrounding tissues, while the scaffold was gradually degraded within 4 weeks *in vivo* experiment.^[131] Furthermore, a composite derived from bioactive glass/CS/CMC showed similar hemostasis effect and even better performance of reconstruction of bone defect than bone wax at 9 weeks post-surgery with decreasing weight.^[132]

Moreover, Martinfar et al. developed multiphasic (biphase/triphase) CaP whisker-like fibers that were incorporated into crosslinked CHI/CMC scaffolds.^[133] The multiphasic CaP fibers stiffened the scaffold via ionic interaction and the formation of hydrogen bonds with PEC of chitosan/CMC, leading to a compressive strength of 150–260% greater than pure chitosan scaffold. In particular, such scaffold containing CaP fibers that contributed to calcium deposition similar as the composition of natural bone could further improve the cell biomineralization. Moreover, a group of novel composite nanofibrous scaffold using silk fibroin and CMC were fabricated after electrospinning, post-crosslinking and further treatment with CaCl₂ for nucleation of CaP through coordinated bonding between –COO[–] and Ca²⁺ in simulated body fluid, with the aim to provide aids for controlled biomineralization. The scaffolds exhibited a high level of mineralization and provided an osteogenic environment to promote MSC growth and differentiation. The strong ability of osteoblastic differentiation supported by the scaffolds was proved by measuring the expression of ALP, RUNX2 transcription factor, osteocalcin, and type 1 collagen.^[134]

Alternatively, CMC could be further modified with additional functional moieties to prepare diverse scaffolds with desired functionalities. Kageyama et al. engineered a perfusable hydrogel system by preparing gelatin/CMC hydrogels crosslinked by mixing hydrazide-modified gelatin (gelatin-ADH) and aldehyde-containing CMC (CMC-CHO).^[135] Such crosslinked gelatin/CMC hydrogels formed within 30 s that was much shorter than 30 min of gelation time required for making collagen gels and thus could avoid oxygen shortage during the process of engineering the structure. The gel was formed, while vascular endothelial cells (EC) attached on gold rods were placed inside the gel. Detachment of EC from the

gold rods was achieved by applying –1.0 V versus the Ag/AgCl reference, which transferred the cell layer to the internal surface of the hydrogel. After removal of the gold rods, EC formed a kind of vascular network after 4 days of perfusion culture. Therefore, such CMC-based hydrogels are of great interest for creating vascularized 3D tissues and organs.

CMC-based hydrogels were used also to load and release TGF- β 1 to reduce the inflammatory response in wounds applicable as wound dressings.^[84] In addition, sulfated CMC (sCMC) was synthesized to mimic sulfated GAGs with high affinity to proteins with regulatory function like growth factors. Arora et al. developed an enzymatically crosslinked hydrogels composed of sCMC/CMC/gelatin to enable the binding of TGF- β 1. The sCMS gels could retain more than 90% of TGF- β 1 during 4 weeks of *in vitro* experiments.^[121] MSCs and ACs were encapsulated in hydrogels with preloaded TGF- β 1 in hydrogels postloaded with TGF- β 1 supplemented from medium. Both approaches for the enrichment of TGF- β 1 promoted equivalent cell survival and chondrogenic differentiation, while the concentration of soluble TGF- β 1 added to the medium was 80 ng while the preloading amount was 50 ng only. This indicates that the binding between hydrogel components such as sCMC and TGF- β 1 is an essential advantage for chondrogenic differentiation of cells and may be also more relevant for a clinical application than addition of growth factors from outside (Figure 7).

3.2.2. Encapsulation of Cells for Immunoprotection

CS as a biocompatible polymer has been also used to prepare microcarriers to encapsulate and protect mammalian cells from immune reactions *in vivo* and to allow sufficient delivery of nutrients and oxygen to cells inside. The microsphere or microcapsule formation is based on the polyelectrolyte character of CS permitting the complexation with divalent cations including Ba²⁺ and Ca²⁺ ions or polycations, such as poly(diallyl dimethyl ammonium chloride) (pDADMAC). For example, Weber et al. prepared CS/pDADMAC microcapsules assembled on transient Ca²⁺/alginate beads after the complexation on this scaffold.^[136] The result showed an adequate stability and permeability of capsules with a molecular weight cutoff between 43 and 70 kDa for transfer of solutes. Transfected Chinese hamster ovary cells grown inside these capsules produced high levels of erythropoietin *in vivo*. This technique provided a feasible approach for the production of this hormone.^[137]

Polyelectrolyte complex microspheres with CS as polyanion and pDADMAC as polycation were also developed for porcine islet cell implantation. The permeable CS/pDAMAC microspheres allowed glucose in nutrient solution to pass to the encapsulated cells for glucose-dependent insulin production.^[138] Hyperbaric oxygenation (HBO) can increase microvascularization by stimulating VEGF production, which is helpful in the treatment of diabetic ulcers and other chronic wounds.^[139] As one potential application for CS/pDADMAC microspheres, the treatment with HBO and foam + VAC (vacuum-assisted wound closure) therapy was combined with them to create a local prevascularized site to support HEK293 cells, a human embryonic kidney cell line to survive in an *in vivo* setting. However, these studies focused on the function of microcapsules

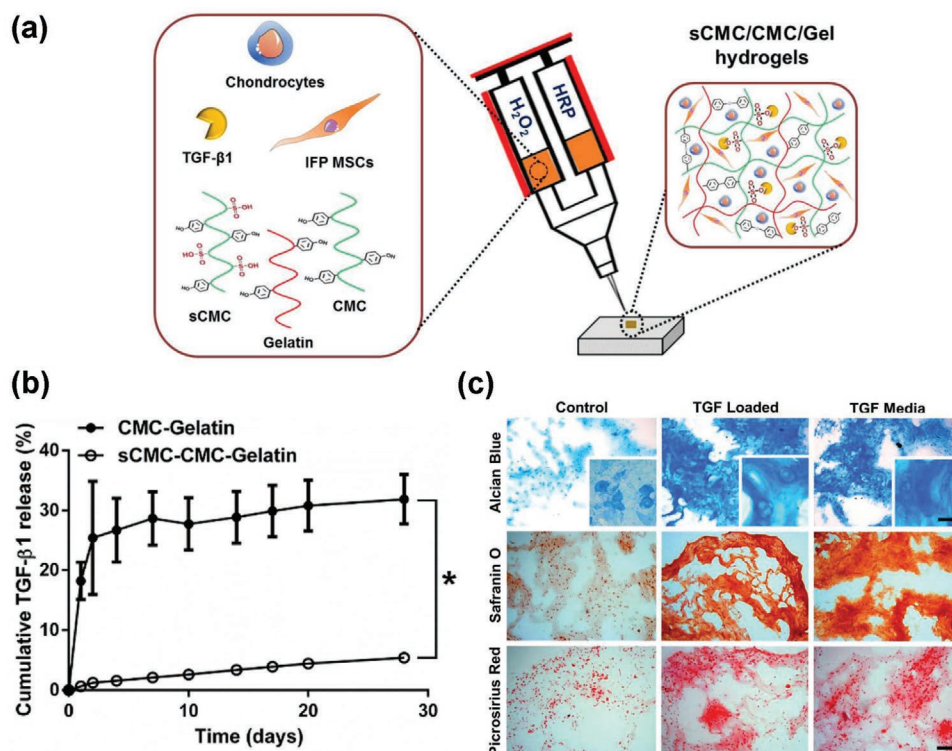


Figure 7. Preparation of sCMC/CMC/gelatin hydrogels and bioactivities. a) Scheme of enzymatically crosslinked sCMC/CMC/gelatin hydrogels for delivery of cells and TGF- β 1 for cartilage tissue engineering. b) Cumulative percentage release of TGF- β 1 from CMC/gelatin and sCMC/CMC/gelatin hydrogels. c) Histological analysis of cell-seeded hydrogels cultured for 28 days in vitro with and without TGF- β 1. a–c) Reproduced with permission.^[121] Copyright 2017, Elsevier.

or microspheres to protect transplanted xenogenic or allogenic cells from immune system of a potential recipient should include further xenotransplantation of porcine islet cells to ensure their response, because islet cells are more prone to hypoxia.^[140] Moreover, the kinetics of commercial CS-based capsules (Cell-in-a-Box) to release proteins with diverse molecular weights has been investigated in more details. Proteins with 10–70 kDa were retained in CS-based capsules and released consistently for up to 120 h, while larger proteins were not detectable. Low molecular cytokines, such as IL-2 (14–15.5 kDa) as an antitumor molecule produced by encapsulated Hut-78 human T cell lymphoma cells, could be effectively released from CS-based capsules, which is comparable to nonencapsulated cells upon stimulated fashion, e.g., using phorbol 12-myristate 13-acetate (PMA) and ionomycin.^[141] Therefore, cytokines released from encapsulated cells in CS-based capsules can be a promising technique for treatment of cancer or other diseases.

3.2.3. Anticoagulation

The anticoagulant properties of heparin rely on the interaction with AT III that inhibits thrombin, Factor Xa and other activated clotting factors. Common clotting assays measuring thrombin time (TT), prothrombin time (PT), and activated partial thrombin time (APTT) that use different activators can be used to assess the activity of the clotting system in a patient, but also to measure effects of anticoagulation. A more specific

approach is to monitor the specific inhibition of thrombin and factor Xa by AT III in the presence of heparin or other anticoagulants based on the use chromogenic substrates for specific clotting enzymes.^[142] Semisynthetic CS with a structural similarity to heparin can show a pronounced anticoagulant activity, which is dependent on overall DS regioselectivity of sulfation, on the molecular weight, and concentration. Groth and Wagenknecht found that CS with an overall DS_S of about 1.5 generated extraordinary anticoagulation when clotting times like TT and PTT were measured. Single factor testing using chromogenic substrates for measuring the activities of thrombin and factor Xa, showed that inhibition was acting through interaction of CS with AT III (Figure 8a). CS derivatives with distinct sulfation patterns exhibited relationships between the binding ability to AT III, and therefore anticoagulant potential, and the preferential sulfation positions as 2-O- > 3-O- > 6-O-position (Figure 8b). This result was in accordance with the affinity between AT III and heparin owing to sulfate ester at 3-O-position of GlcN for the main role in ionic pairing and sulfate groups at 2-O-position of IdoA for extra conformational change.^[142]

In addition, CS prolonged APTT and TT at even high concentrations compared to heparin and inhibited thrombin based on dose- and molecular weight-dependent binding with AT III in vivo.^[42,143,144] In contrast, it was found in the same study that CP did not show any remarkable anticoagulant effect.^[142] Although such CS cannot be applied without extensive preclinical and clinical testing as anticoagulant for intravenous use due to known complications related to contamination of

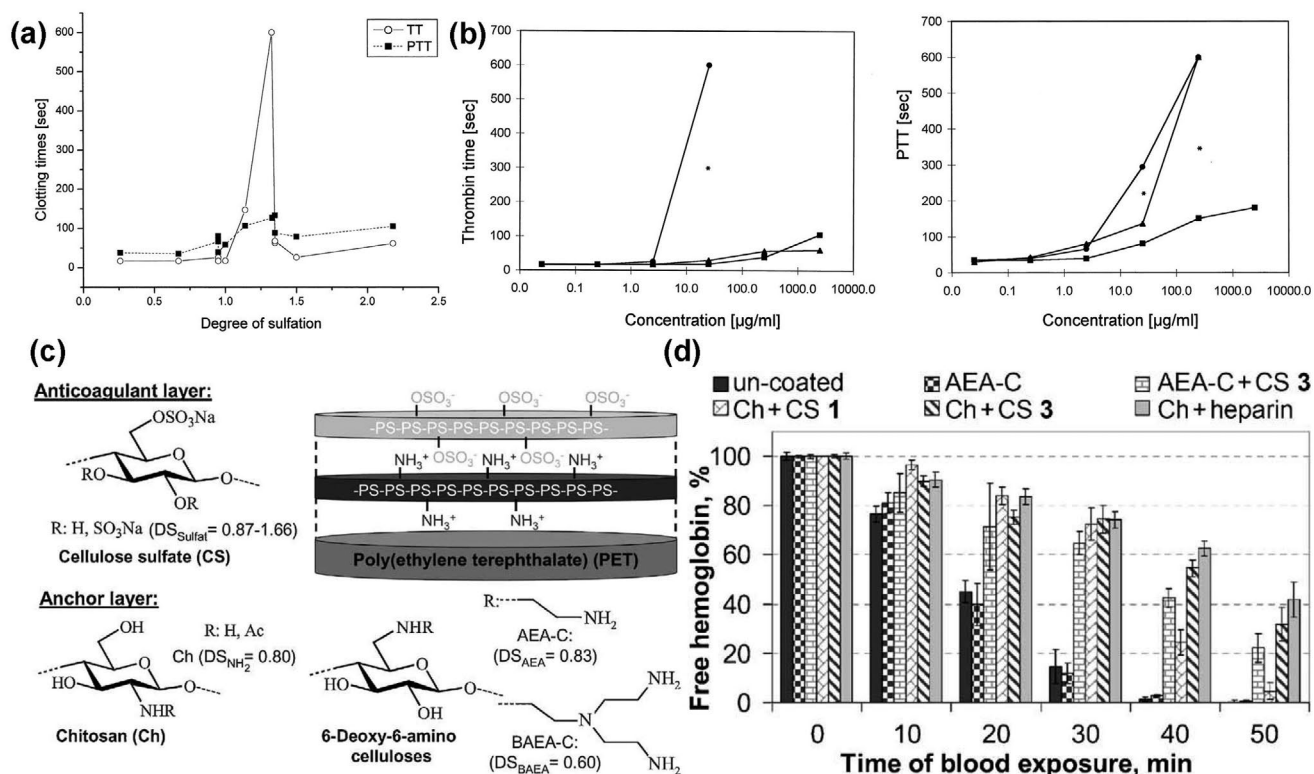


Figure 8. a) Thrombin time (○) and partial thromboplastin time (■) plotted versus DS_5 of CS at a sample concentration of $2.5 \mu\text{g mL}^{-1}$. b) Thrombin time (left) and partial thromboplastin time (right) of CS with total DS_5 of 0.95, but different distributions of sulfate groups within AGUs: (●) derivatization predominantly at 2-O-position; (■) derivatization only at 6-O-position, and (▲) derivatization to the same extent at 2-O-, 3-O-, and 6-O-position. a,b) Reproduced with permission.^[142] Copyright 2001, Elsevier. c) Schematic illustration for anticoagulant CS-coated PET surfaces prepared via layer-by-layer assembly of polysaccharides (CS: cellulose sulfate; Ch: chitosan; AEA-C: 6-deoxy-6-(2-aminoethyl)aminocellulose; BAEA-C: 6-deoxy-6-(2-aminoethyl)aminocellulose). d) Free hemoglobin released from nonmodified PET foils and ones coated with polysaccharides. c,d) Reproduced with permission.^[147] Copyright 2011, Wiley-VCH.

heparin preparations with highly sulfated GAG like chondroitin sulfate,^[145] it may be applied to improve blood compatibility of biomaterials that are commonly used to make all kind of blood linings and artificial blood vessels. Similar findings from other groups showed that anticoagulant activity of sulfated CMC was related to overall DS_5 with increasing anticoagulation with higher DS_5 and concentration of sCMC.^[146] This result further underlines the potential of sulfated cellulose derivatives for preparing blood-compatible surfaces.

Heinze and co-workers fabricated poly(ethylene terephthalate) (PET) foils coated with CS and aminopolysaccharides (chitosan or unbranched/branched aminocellulose) using LbL technique.^[147] Precoated aminopolysaccharides on PET could enhance CS adsorption, particularly when branched aminocellulose was applied due to complex formation of these polyelectrolytes. All PET foils coated with CS (with sulfate groups predominantly at 2-O- and 3-O-position) and heparin represented similar inhibition of coagulation within 30 min in contact with blood. However, CS-coated PET foils with lower DS_5 of 0.87 showed lesser inhibition after 40 min (Figure 8c,d). This study indicates that LbL-assembly of CS on PET surface with precoated aminopolysaccharides is a suitable approach to improve blood compatibility of PET-based artificial vascular grafts. Moreover, CS with outstanding blood compatibility and anticoagulant activity demonstrates enormous potentials to replace

heparin, which may cause bleeding in patients by the application for the treatment of thrombosis disorders and implantation of medical devices,^[148] such as cardio-pulmonary bypass circuits, heart lung oxy-generators and hemodialysis.

3.2.4. Antibacterial Activity and Application as Wound Dressings

Infection can cause serious problems and life-threatening complications during wound healing. Blending of silver nanoparticles (Ag NPs) in wound dressings is an effective approach to enhance their antibacterial activities, e.g., by mixing Ag NPs into hydrogels constructed with modified polysaccharides.^[149] Among others, CMC is an attractive candidate for the preparation of such hydrogels as potential wound dressings due to its advantageous chemical-physical properties that are compatible with Ag NPs for synergistic antimicrobial activities.^[150,151]

Recently, Anjum et al. presented an antimicrobial wound dressing based on a gel system composed of polyvinyl alcohol/poly(ethylene oxide)/CMC matrix by blending nanosilver nanohydrogels along with Aloe vera or curcumin and coating this dressing onto hydrolyzed polyester (PET) fabric.^[152] Aloe vera and curcumin were used to accelerate the healing process based on their advantageous properties for the removal of scars and antioxidant activities for the treatment of wound

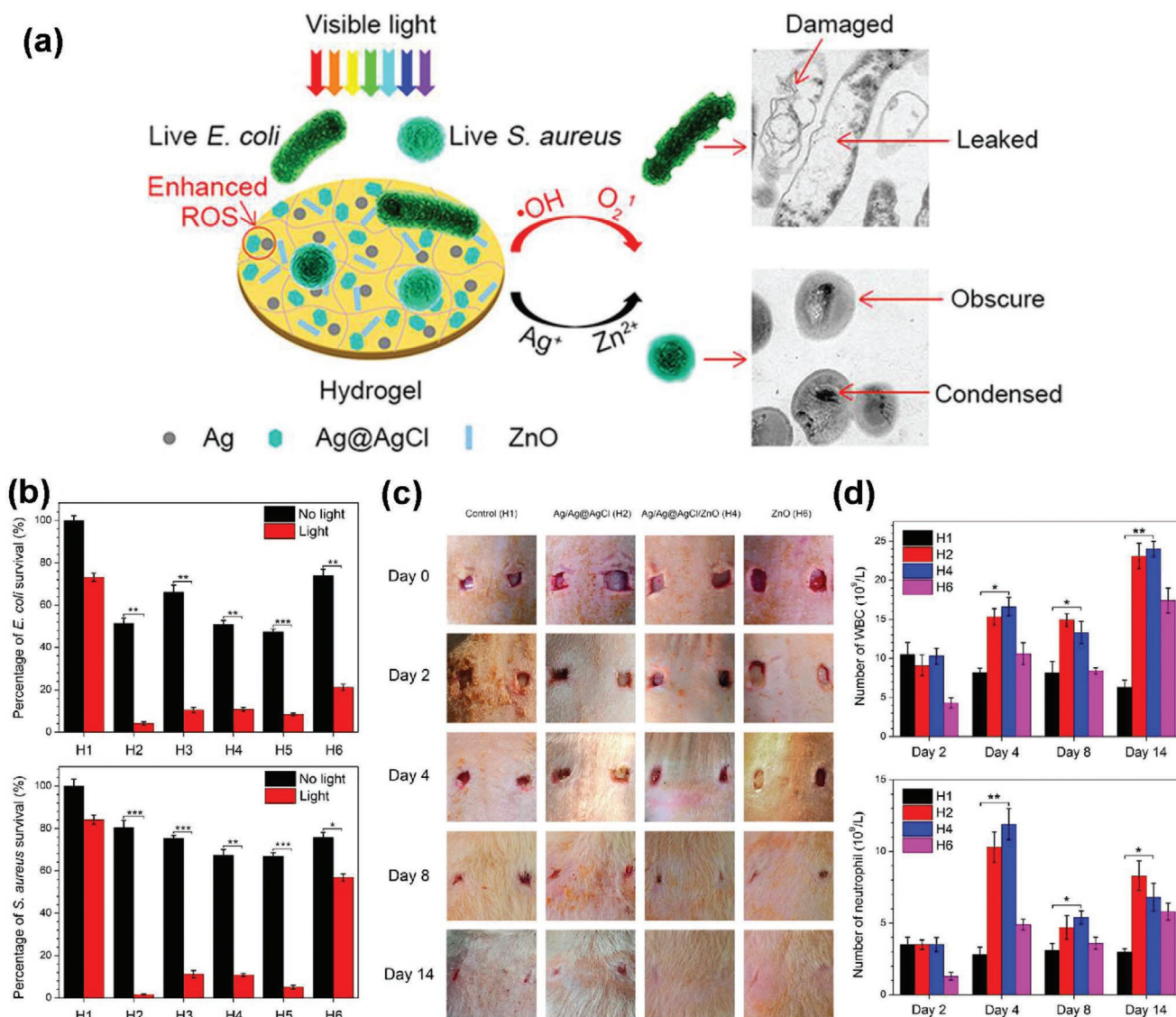


Figure 9. a) Scheme of Ag@AgCl/ZnO hydrogel to inhibit antibacterial activity. b) Ability of the hydrogels in killing *E. coli* and *S. aureus* under simulated sunlight for 20 min. c) In vivo study on the effects of treatment of *S. aureus*-induced wound infections by hydrogels and the corresponding wound photographs of rats at days 0, 2, 4, 8, and 14. d) In vivo analysis of blood of the numbers of white blood cells and neutrophils in whole blood extracted from rats after treatment with hydrogels for 2, 4, 8, and 14 days. H1: control hydrogel; H2: Ag@AgCl hydrogel; H4: the representative Ag@AgCl/ZnO hydrogel; H6: ZnO hydrogel. a–d) Reproduced with permission.^[157] Copyright 2017, American Chemical Society.

damage.^[153] Based on the bacterial-inhibiting activities (e.g., against *Escherichia coli* and *Staphylococcus aureus*) of nanosilver nanohydrogels, the dressing containing Aloe showed almost complete (100%) reduction of bacteria, while gel dressing containing curcumin was not as effective as the gel dressing containing Aloe and only inhibited around 80–90% bacterial. Likewise, the wound treatment reached 100% healing with gel wound dressing containing Aloe but only 80% for gel wound dressing containing curcumin, which was probably due to the protecting antioxidant properties of curcumin in contrast to the lethal effects of antibiotic nanosilver.^[154] This further indicated the great potential of such gel-based wound dressings containing nanosilver nanohydrogels and Aloe for biomedical applications.^[152]

Zinc oxide (ZnO) as another antimicrobial agent that can be incorporated together with Ag NPs into wound dressing could enhance photocatalytic activity and therefore antibacterial activity of reactive oxygen species (ROS) using visible light.^[155] In addition, Zn^{2+} ions released from ZnO can support fibroblast proliferation and differentiation for skin regeneration.^[156] Mao et al. developed CMC-based hydrogels with assembled Ag/Ag@AgCl/ZnO hybrids, which showed superior photocatalytic activity and high antibacterial activity upon visible light irradiation with altering pH values for reversible swelling-shrinking transition of the hydrogels (Figure 9a).^[157] The investigation on the release of Zn^{2+} and Ag^+ ions showed that 90% of Zn^{2+} ions were released in the acidic environment. Survived *S. aureus* and *E. coli* decreased significantly with the application of hydrogels

containing Ag/Ag@AgCl or Ag/Ag@AgCl/ZnO after the exposure to sunlight for 20 min, which was also attributed to the release of antibacterial ions (Ag^+ and Zn^{2+}) (Figure 9b). Wound healing studies were conducted with rats in the presence of *E. coli*. Ag/Ag@AgCl/ZnO CMC hydrogels exhibited the greatest ability for promoting wound healing and skin regeneration due to mitigation by ZnO within 14 day treatment (Figure 9c). The numbers of white blood cells including neutrophils highly increased after the treatment (Figure 9d). Therefore, modified polysaccharides including ionic cellulose derivatives showed great potential for the fabrication of hydrogels as platform for the integration of diverse antimicrobial compounds and thus for wound dressings with anti-infective properties.

Diverse positively charged cellulose derivatives have found particular attention regarding their antimicrobial activities. The ω -aminoethyl- and ω -aminoethyl-*p*-aminobenzyl cellulose carbamate exhibit a bactericide and fungicide activity in vitro. The ω -aminoethylcellulose carbamate showed a strong activity against *Candida albicans* and *S. aureus* (IC_{50} of 0.02 and 0.05 mg mL⁻¹, respectively) that could be improved by using *p*-aminobenzylamine as additional substituent. The mixed cellulose carbamate exhibits a high biocompatibility (LC_{50} of 3.18 mg mL⁻¹) and forms films on cotton and polyester, which exhibit a strong activity against *S. aureus* and *Klebsiella pneumoniae*.^[158] Moreover, 6-deoxy-6-trisaminoethyl-amino celluloses blended with PVA could be electrospun into nanofibrous webs with fiber diameters of 50–160 nm. Such nanofibrous webs showed strong reduction of *S. aureus* growth and a significant antibacterial efficiency against the Gram-negative *K. pneumoniae*.^[159] Furthermore, spraying of a dilute aqueous solution of 6-deoxy-6-tris(2-aminoethyl)amino cellulose (0.05 wt%) onto paper and subsequent drying yielded coated paper that exhibited significant antibacterial effects against *S. aureus*, *K. pneumoniae*, and *Pseudomonas aeruginosa*.^[160]

3.2.5. Drug Delivery

CMC as a pH-sensitive polymer due to the presence of a high amount of carboxyl groups is also feasible for the development of stimuli-responsive drug carriers. It was reported previously that CMC-based hydrogels had the capability to upload and release the drugs greatly depending on pH values and preferred to release drugs at acid condition.^[161] Recently, a popular approach to prepare CMC-based hydrogels is to generate physical crosslinking through coordination between metal ions and the carboxyl groups of CMC.^[162] For example, CMC/ZnO hydrogel beads with integrated antibacterial ZnO were prepared after the crosslinking with Fe^{3+} ions for the delivery of propranolol hydrochloride.^[163] It was shown that the swelling degree of hydrogel beads and the release of propranolol hydrochloride from the hydrogel beads were greater at higher pH (6.8) compared to lower pH (1.2). This was primarily due to the conversion of the carboxyl groups of CMC to negatively charged carboxylate ions at higher pH values, which led to stronger swelling due to penetration of more water into the hydrogel and could be used as trigger to control the drug release.

Rasoulzadeh and Namazi used a similar method to fabricate CMC/graphene oxide (CMC/GO) nanocomposite hydrogels

for loading and release of anticancer drug doxorubicin (DOX) (Figure 10).^[164] Increasing the content of GO efficiently enhanced the drug loading, indicating the formation of beneficial hydrogen bonding between carboxyl groups of GO and amino groups of DOX. DOX was released faster at pH 6.8 than at pH 7.4 due to the stronger hydrogen bonding at basic condition, which prevented the release of DOX. The biocompatible CMC/GO nanocomposite showed no cytotoxicity to human colon cancer cells (SW480), while CMC/GO nanocomposite loaded with DOX reduced cell viability. Different than directly loading DOX into matrix, its polymeric prodrug was conjugated with CMC in another study and the conjugate was used to form hydrogels after the crosslinking with citric acid.^[165] Such conjugated DOX/CMC hydrogels were found to be able to selectively kill cancer cells.

Furthermore, CMC has been found to reduce the high level of reactive oxygen species.^[166] CMC modified with a collagen peptide (CMCC) that can protect against oxidative free radicals was used to prepare hydrogels for loading an anti-inflammatory cytokine, IL-10 for H₂O₂-treated retinal cells (Figure 11).^[167] With the antioxidative CMCC gels, reactive oxygen species level in retina endothelial cells (rRECs) were greatly reduced. The injection of CMCC gel loaded with IL-10 (IL-10@CMCC) in vivo to treat retinal ischemia/reperfusion injury was observed to significantly attenuate the thinness of retina and assessed by enhancing the expression of antiapoptotic protein (Bcl-2 and Bax). However, a decreasing trend of apoptotic protein (Csp3) was detected in contrast to the gel without IL-10. Therefore, IL-10@CMCC with significant therapeutic effects alleviated retinal oxidative stress damage and downgraded the expression of inflammatory cytokines.

3.2.6. Immobilization of Bioactive Compounds

The surface modification using positively charged cellulose derivatives yields a reactive and protein-like environment, which make these layers well suitable to immobilize enzymes.^[168] A strong influence of the coupling agents on the enzymatic activities was found for glucose oxidase (GOD), lactate oxidase (LOD) and horseradish peroxidase (HRP), e.g., by applying *p*-phenylenediamine (PDA)-modified cellulose (Table 5 and Figure 12). The unstable LOD obtained its highest enzymatic activity after the immobilization with benzene-1,3-dicarboxylic acid dichloride. A similar influence of the coupling and the resulting activities was found for films formed by other amino celluloses.^[109,168,169]

ω -Aminocellulose carbamates are able to form layers on a gold surface depending on the pH values.^[171] It was possible to immobilize antibodies on layers of ω -aminocellulose carbamates of coated polyethylene-sintered filters as support material to design immunoassays (Figure 13). Anti-h CRP 6404 antibodies could be covalently attached onto layers of ω -aminocellulose carbamate using diverse coupling reagents to optimize their activities. The CRP determination could then be carried out by a very sensitive rapid flow-through immunoassay, which showed a detection limit of 5 ng CRP mL⁻¹ and a detection range of 5–250 ng CRP mL⁻¹ (Figure 14).^[172]

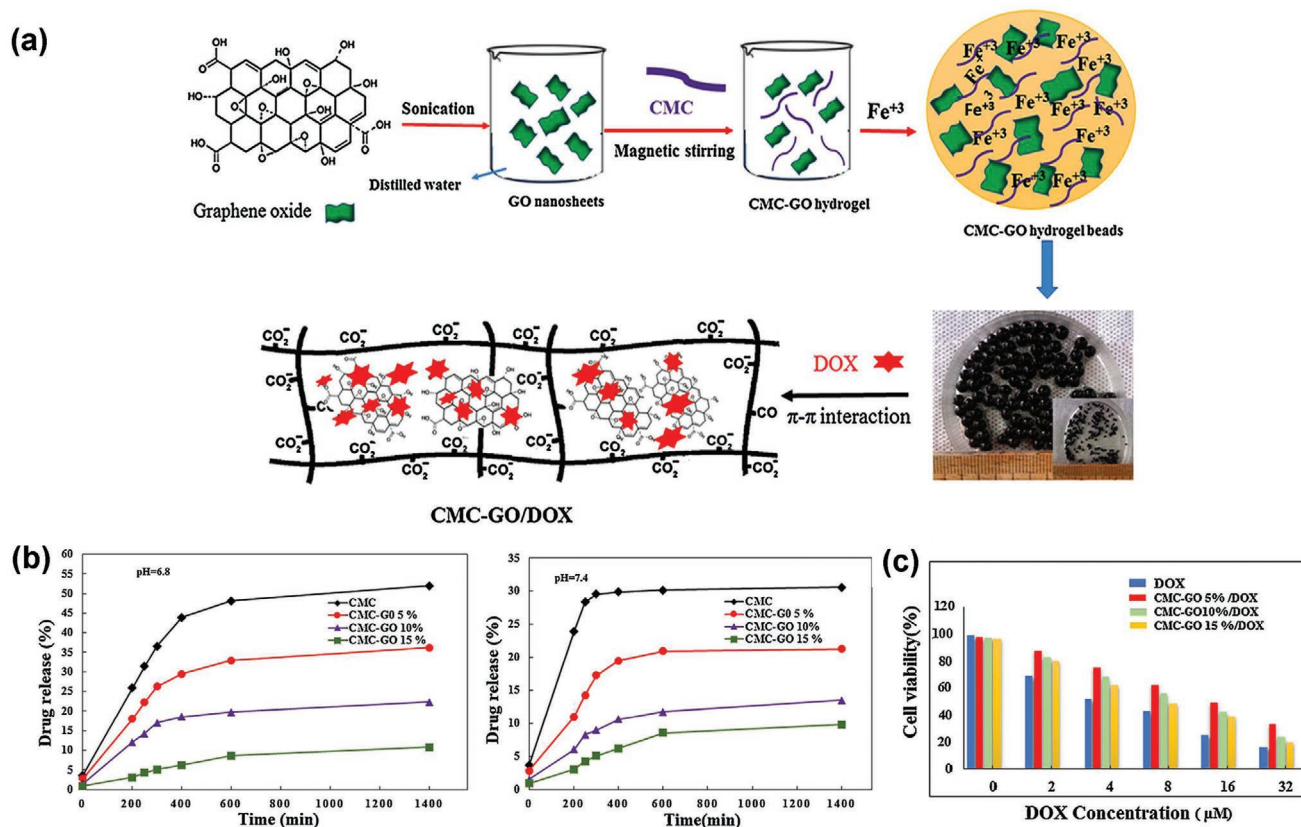


Figure 10. CMC/GO composite hydrogels for loading and release of DOX and the effect of anticancer ability. a) Schematic illustration for the preparation of DOX-loaded CMC/GO nanocomposites. b) DOX release from the CMC/GO nanocomposite hydrogel at pH 6.8 or pH 7.4 in PBS solutions. c) MTT viability assay of SW480 cells treated with free DOX and CMC/GO+DOX at corresponding concentrations of the complexes between 0 and 32×10^{-3} M. a–c) Reproduced with permission.^[164] Copyright 2017, Elsevier.

Biomedical and biotechnological applications of ionic cellulose derivatives, especially widely used CS and CMC as biomaterials, are further summarized in Tables 6 and 7.

4. Ionic Nanocellulose-Based Compounds and Their Applications as Biomaterials

Nanocellulose as the nanostructured cellulose, a type of unique and promising natural material extracted from native cellulosic raw materials (biosynthesized by plants, animals, and bacteria), has gained much attention for biomaterials in the last years thanks to its remarkable physicochemical properties and excellent biological properties, e.g., for tissue engineering, implants, drug delivery systems, cardiovascular devices and wound healing. Generally, nanocellulose can be divided into three types according to their morphology and sources as: 1) cellulose nanocrystals (CNCs; Figure 15a), 2) cellulose nanofibrils (CNFs; Figure 15b), and 3) bacterial cellulose (BC; Figure 15c).

Although there are many approaches, including mechanical, chemo-mechanical and enzymatic-mechanical treatment, to extract nanocellulose from the cellulose materials, chemical and chemomechanical treatments, such as acid hydrolysis, ionic liquid treatment, carboxymethylation and 2,2,6,6-tetramethylpiperidine-1-oxyl (TEMPO)-mediated oxidation are the

most frequently applied techniques to prepare nanocellulose and to modify the surface, where ionic charges are preferentially imparted to the cellulose backbone (Figure 15d). Herein, we briefly introduce at first the chemical treatments for the preparation of ionic nanocellulose with diverse ionic groups in adjustable amounts. Then, their applications as biomaterials is further described in more detail.

4.1. Synthesis of Ionic Nanocellulose

4.1.1. Negatively Charged Nanocellulose

Sulfated Nanocellulose: CNCs are rods or whiskers with the dimension typically ranging from 3 to 5 nm in width and 50 to 500 nm in length. A common procedure for the production of CNCs begins with alkali and bleaching pretreatments followed by acid hydrolysis, washing, centrifugation, dialysis, and ultrasonication to form a stable aqueous suspension. In acid hydrolysis, the hydronium ions penetrate into the disordered cellulose chains and hydrolytically cleave glycosidic bonds, releasing individual crystalline cellulose domains as CNCs.^[182] Most of disordered and some crystalline regions in native celluloses are removed during this process. Different strong acids have been successfully applied, such as sulfuric, hydrochloric, phosphoric,

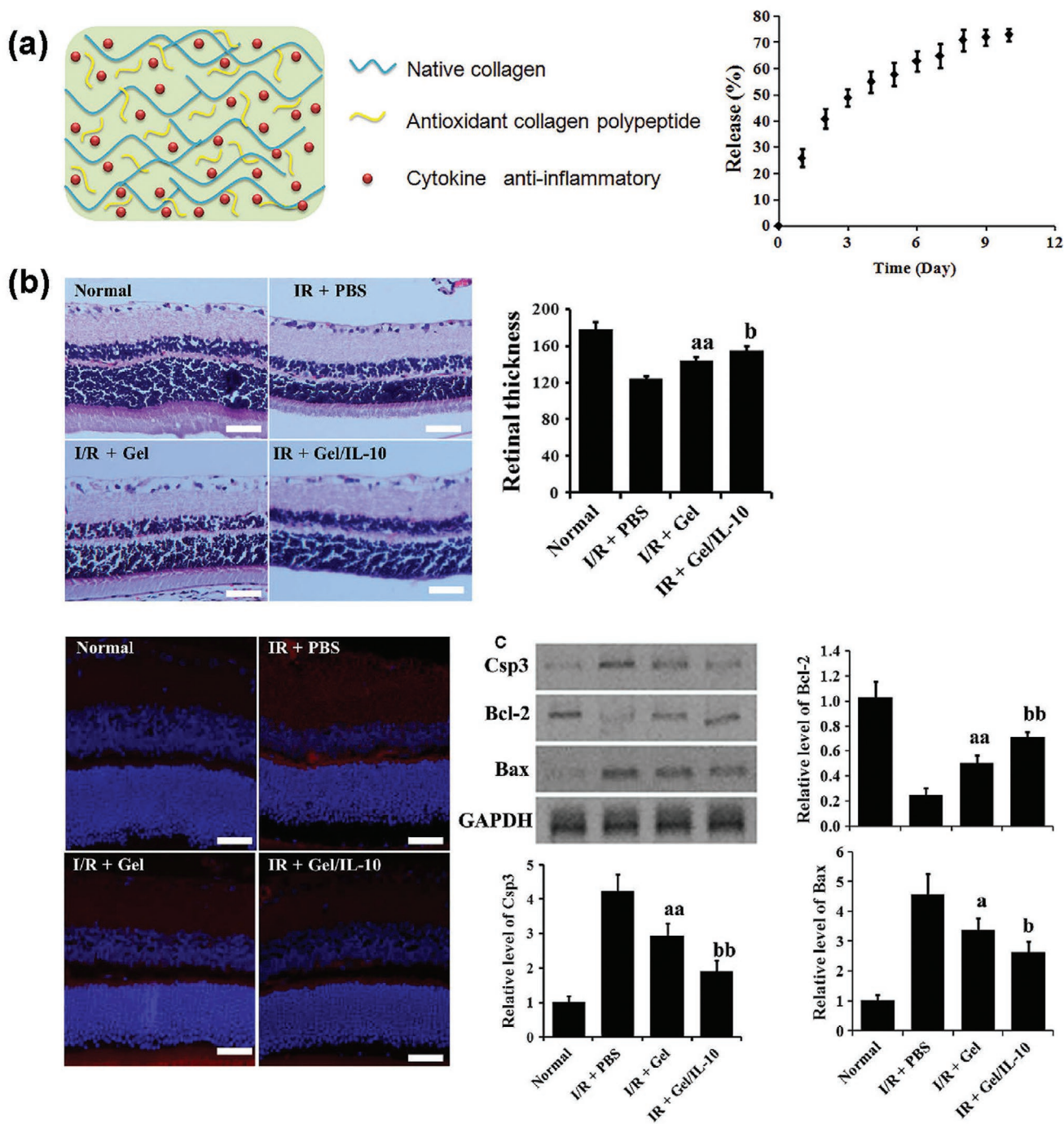


Figure 11. CMCC gels loaded with IL-10 and its effect on the retinal injury. a) IL-10 releasing measurement in vitro. b) Representative retinal section images of control, I/R + PBS, I/R + Gel or I/R + Gel/IL-10 group were attained by H&E staining and the corresponding quantitative total retinal thickness and western blotting analysis of apoptotic and antiapoptotic proteins of rRECs. a–c) Reproduced under the terms of the CC-BY Creative Commons Attribution 4.0 International License (<https://creativecommons.org/licenses/by/4.0/>).^[167] Copyright 2018, The Authors, published by John Wiley & Sons Ltd and Foundation for Cellular and Molecular Medicine.

hydrobromic, nitric acids, and a mixture composed of hydrochloric and organic acids.^[183] Due to the strong electrostatic stabilization of produced suspension, sulfuric acid is the most common and effective reagent reported for acid hydrolysis to date, which generally applies a sulfuric acid with the concentration of about 64%.^[183,184] Indeed, sulfuric acid could react with the surface hydroxyl groups of cellulose via the esterification

process by grafting anionic sulfate ester groups ($-\text{OSO}_3^-$) onto nanocellulose surface (with the content of sulfate groups of 0–0.4 mmol g^{-1})^[185,186] (Figure 16a), which endow strong electrostatic repulsion between individual nanocelluloses and promote their dispersion in solvents.

The content of sulfate groups on the surface of CNCs significantly affects their surface chemistry and physicochemical

Table 5. Covalent coupling of selected oxidoreductases to PDA cellulose films with various coupling agents (see Figure 12 for chemical structures). Reproduced with permission.^[168] Copyright 2000, Wiley-VCH.

Enzyme coupling	Activity [mU cm ⁻²]			
	(Y)	GOD	HRP	LOD
Diazo coupling	–	194	135	220
Glutaraldehyde	A	187	206	100
L-Ascorbic acid	I	185	200	192
Benzene-1,3-disulfonic acid chloride	L	168	48	–
4,4'-Biphenyldisulfonic acid chloride	K	27	35	–
Benzene-1,3-dicarboxylic acid dichloride	J	34	121	286
Benzene-1,4-dicarboxylic acid chloride	H	60	27	131
Cyanuric chloride	F	33	59	119
Benzene-1,3-dialdehyde	B	94	58	61
Benzene-1,4-dialdehyde	C	56	48	21
1,3-Diacetylbenzene	D	51	76	123
1,4-Diacetylbenzene	E	70	104	52

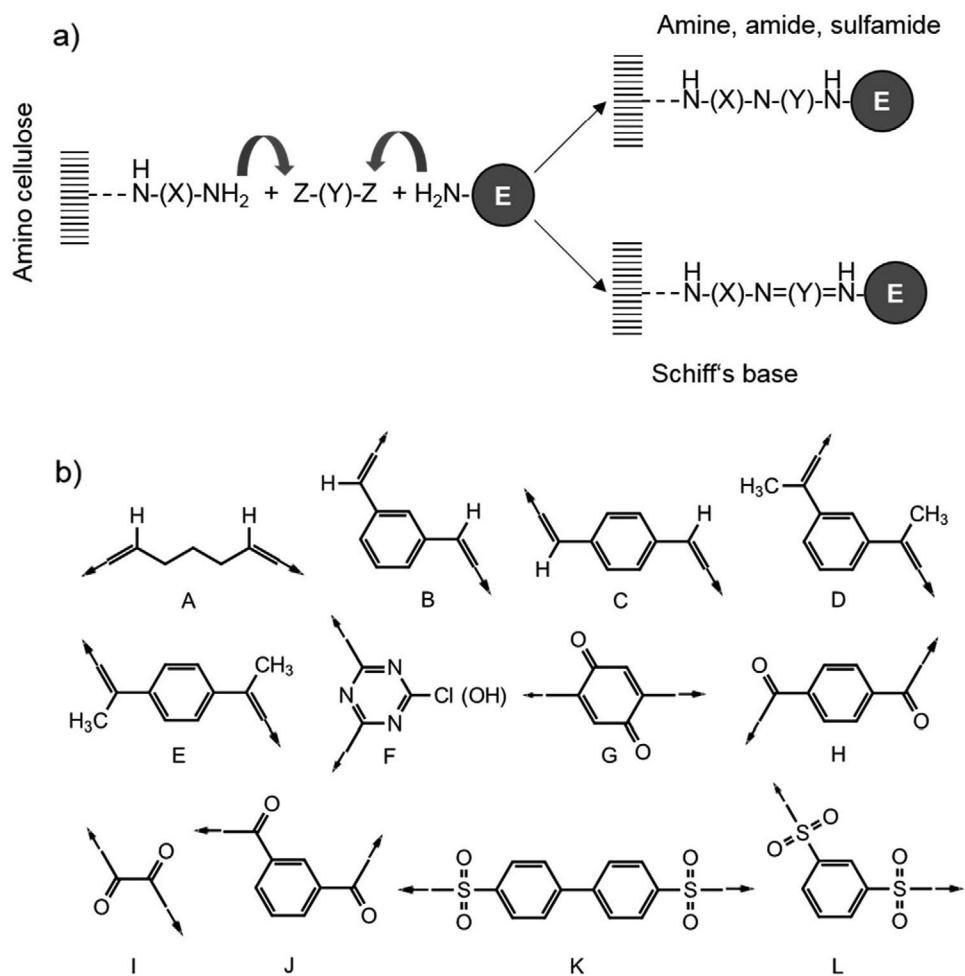


Figure 12. Schematic representation for a) the enzyme immobilization on amino cellulose surfaces and b) coupling agents. Reproduced with permission.^[170] Copyright 2019, John Wiley & Sons Ltd.

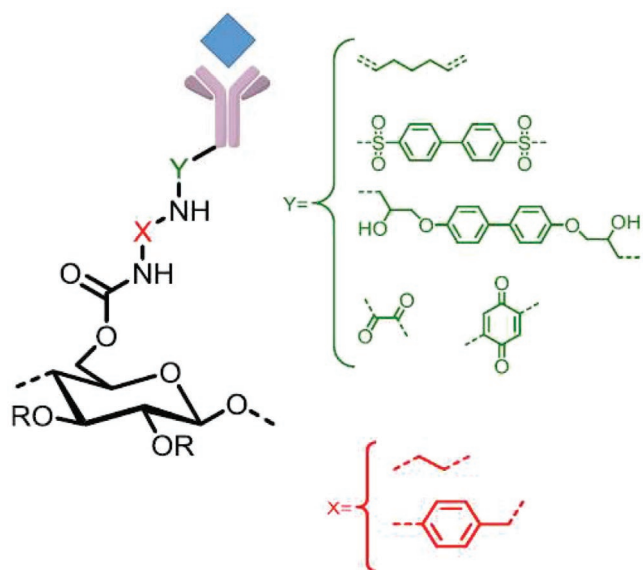


Figure 13. Schematic composition of a rapid flow-through immunoassay based on coatings of ω -amino cellulose carbamate. Reproduced with permission.^[170] Copyright 2019, John Wiley & Sons Ltd.

properties, such as surface charges, birefringence behaviors, thermal and colloidal stability, as well as rheological behaviors of their suspensions. The content of sulfate groups on the surface of CNCs is dependent on the hydrolysis time, temperature and sulfuric acid concentration.^[187] By increasing the harshness of the hydrolysis (time, temperature, acid concentration or acid-to-pulp ratio), smaller CNCs with higher sulfate contents are produced and in high yields. However, cellulose will be strongly degraded into sugars, when the harshness of the hydrolysis increases beyond a certain extent. Chlorosulfonic acid and hydrochloric acid were also used as a sulfating agent for the postsulfation of CNCs, which can further enhance the surface sulfation and avoid the intense degradation of CNCs induced by strong sulfuric acid (Figure 16b).^[188] In addition, the desulfation of CNCs, including solvolytic desulfation^[189] and alkaline desulfation (Figure 16c),^[190] was also sometimes used to adjust the contents of sulfate groups on the surface of CNCs. Lin and Dufresne used postsulfation and desulfation treatments to prepare CNCs with a gradient of sulfate groups on the surface.^[186]

The level of surface charge of CNCs could then be used to alter the viscosity of the suspension. It has been proved that the introduction of more sulfate groups on the surface of CNCs drastically reduced the viscosity of their aqueous suspensions

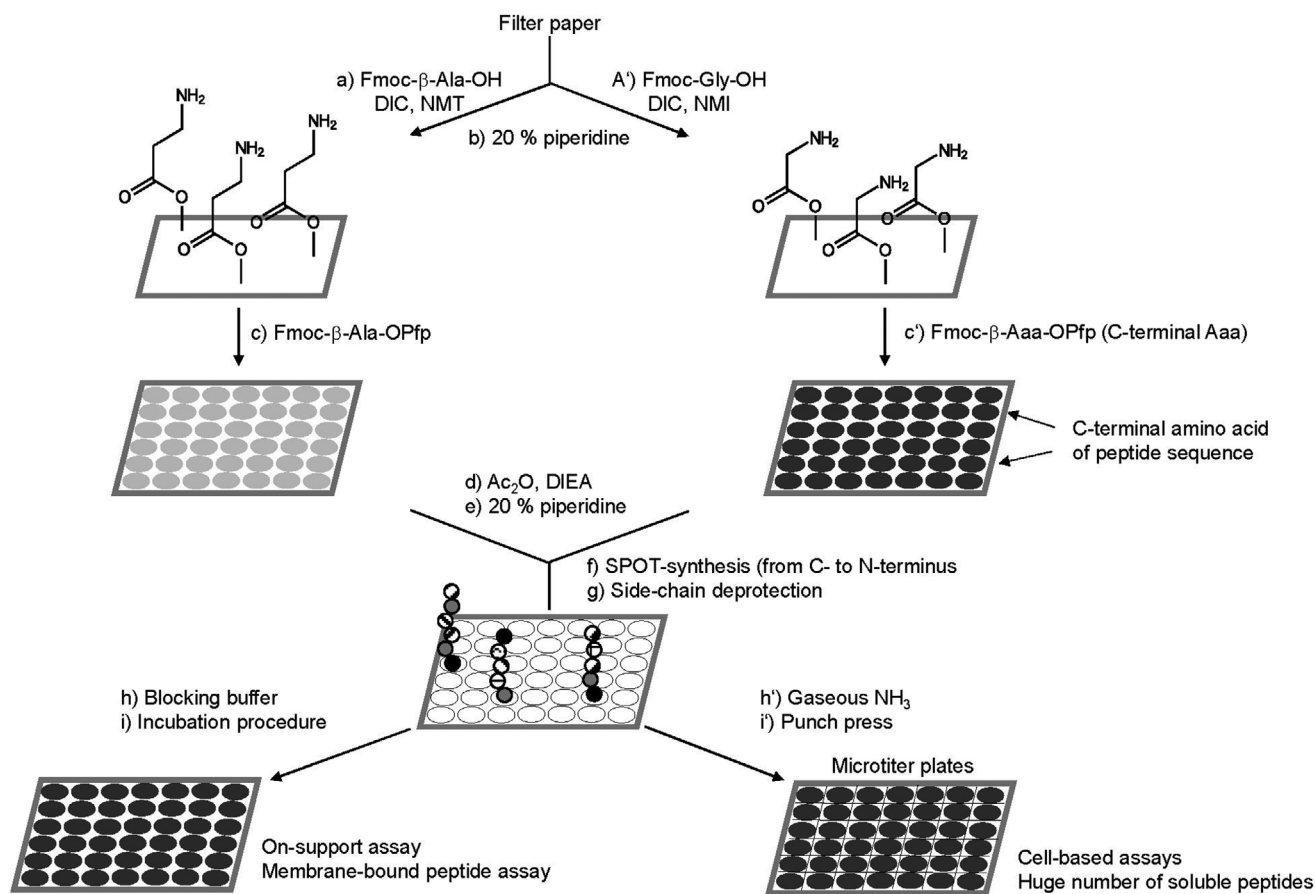


Figure 14. Schematic composition of a rapid flow-through immunoassay based on coatings of ω -aminocellulose carbamate. Reproduced under the terms of the CC BY Attribution 3.0 Unported license.^[172] Copyright 2013, The Authors, published by IntechOpen.

Table 6. Application of CS as biomaterials.

Materials	DSs	Modification of surface coating/scaffold	Applications	Ref.
Bioactivity				
CS	0.31–1.94		FGF-2 binding Promoting mitogenic activity BMP-2 binding Promoting osteogenic activity FGF-2 proteolytic protection	[116,117,173]
CMCS	0.41/0.31		FGF-2 binding (not significant)	[54]
COCS	0.4–0.92		Promoting mitogenic activity	[54]
Tissue engineering				
CS/chitosan multilayer	1.57	LbL	Fibronectin adsorption Myoblast C2C12 adhesion and proliferation	[124]
CS/chitosan multilayer	1.57/2.59	LbL	Fibronectin adsorption: CS1.57 > 2.59 Myoblast C2C12 adhesion: CS1.57 > 2.59 Myoblast C2C12 proliferation: CS1.57 < 2.59	[128]
Heparin-CS/chitosan multilayer	1.57/2.59	LbL	Myoblast C2C12 adhesion	[127]
Oxidized CS/CM chitosan hydrogel		Chemical crosslinking	Further studies to test their applicability to accommodate cells for use as in situ gelling, injectable hydrogels	[129]
CS/gelatin fiber		Electrospinning/ chemical crosslinking	TGF- β binding Promote hMSC chondrogenesis	[120]
CS in porous collagen/hydroxylapatite nanocomposite scaffold	CSA 80: 0.41 (mostly 2-O-sulfation) 13-TASC-1: 1 (mostly 2-O/3-O-sulfation)	PEC	VEGF-induced (with or w/o) vascular formation (coculture of endothelial cells and fibroblasts)	[118]
Anticoagulant				
CS	0.26–1.35		Anticoagulant Thrombin/factor Xa inhibition Antithrombin III interaction	[142]
CS	1.7		Anticoagulant Factor IIa/factor Xa inhibition Antithrombin III interaction	[143]
CS	1.59		Anticoagulant Factor IIa/factor Xa inhibition	[42]
CS-coated PET foils	0.87–1.66	LbL coating with aminopolysaccharides (chitosan or aminocellulose)	Anticoagulant	[147]
CS (dose-dependent)			Anticoagulant Factor IIa/factor Xa inhibition	[144]
Encapsulation for cell immobilization				
CS/pDADMAC			Chinese hamster ovary cell carrier for protein production	[136]
CS/pDADMAC		PEC	Immunoprotection (porcine islet cells) for xenotransplantation	[137]
CS/pDADMAC		PEC	Human endoderm kidney cell (HEK293) xenotransplantation	[140]
CS capsule (Cell-in-a-Box)			Immunoprotection (T cell lymphoma cell) for IL-2 production and release	[141]

and removed the time dependence.^[191] Moreover, the presence of acidic sulfate groups would decrease the thermal stability by the dehydration reaction.^[192] Usually, higher content of acidic sulfate groups leads to a stronger thermal degradation of cellulose at low temperatures.^[185,193] Although the thermal stability

can be improved by using hydrochloric acid to hydrolyze cellulose, obtained CNCs intend to aggregate due to the lack of sufficient charges at surface and therefore weaker electrostatic repulsion force.^[194] Wang et al. proposed two methods to improve the thermal stability of sulfated CNCs, including

Table 7. Application of CMC as biomaterials.

Materials	Modification of surface coating/scaffold	Applications	Ref.
Tissue engineering			
Chitosan/CMC scaffold	PEC	Pulp tissue engineering	[130]
n-HA (nano-hydroxyapatite)/chitosan/CMC scaffold	PEC	Osteoblasts and hMSC attachment, proliferation, bone regeneration	[131]
Sodium CMC scaffolds		Skin wound healing	[174]
Gelatin-ADH/CMC-CHO hydrogel	Chemical crosslinking	Engineering vascularized and cell-dense 3D tissues and organs (encapsulation of vascular endothelial cells)	[135]
CMC/MFC (microfibrillated cellulose)/pectin blend hydrogel	Crosslinking via Ca ²⁺ ions	Biocompatible composite scaffolds (NIH3T3 fibroblast)	[84]
Glass/chitosan/CMC	PEC	Bone regeneration, hemostasis	[132]
Sericin-CMC	Chemical crosslinking	TGF- β 1 loading TNF- α production Skin wound healing	[175]
Silk fibroin (SF)/CMC composite nanofibrous scaffold/CaP particles	Electrospinning/Chemical crosslinking	Osteoblastic differentiation (hMSCs)	[134]
CMC/chitosan/Zn ²⁺ microparticles		Osteoblasts attachment, proliferation	[176]
CMC/sCMC/gelatin hydrogels	Chemical/enzymatic crosslinking	TGF- β 1 loading for cartilage tissue engineering (coculture of MSC, articular chondrocytes)	[121]
CMC/CaP sheets (with loaded calcium phosphate)		Osteoblast differentiation of human mesenchymal stromal cells (hMSCs), bone regeneration	[177]
Chitosan/CMC/CaP fibers scaffolds	PEC/chemical crosslinking	Enhancing cell adhesion and proliferation, mineralization (MG63 (human osteosarcoma))	[133]
Drug delivery			
CMC/poly(allylamine hydrochloride)		Protein delivery (positive bovine serum albumin (BSA))	[178]
CMC/poly(acrylic acid) hydrogel		Oral insulin delivery	[161]
CMC/ZnO hydrogel beads	Physical crosslinking	Propranolol hydrochloride delivery	[163]
CMC/graphene oxide hydrogel beads	Physical crosslinking	Doxorubicin delivery (anticancer drug)	[164]
CMC/DOX	Chemical crosslinking	Doxorubicin delivery (melanoma cancer cells)	[165]
Collagen peptide modified CMC	Chemical crosslinking	IL-10 delivery against retinal ischemia/reperfusion injury	[167]
Antibacterial activity and wound healing			
CMC hydrogel with loaded AgNPs		High antibacterial activity against Gram positive and Gram negative bacteria	[151]
PVA/polyethylene oxide/CMC matrix blend with AgNPs, Aloe vera and curcumin		Antibacterial activity against <i>S. aureus</i> and <i>E. coli</i> Wound healing	[154]
CMC hydrogel embedded with Ag/Ag@AgCl/ZnO nanostructures		Antibacterial activity against <i>S. aureus</i> and <i>E. coli</i> Wound healing	[157]

diminishing the acidic sulfate groups by desulfation and neutralizing them by using aqueous NaOH solution.^[195] The results showed that the thermal stability of the hydrogen form of CNCs (as CNCs–SO₃H) can be improved by exchanging a hydrogen atom with sodium to obtain the sodium form (as CNCs–SO₃Na) through neutralization.

Combination of periodate and bisulfite oxidation is another method to introduce negatively charged sulfate ester groups (–OSO₃[–]) onto the surface of nanocellulose and can be used to enhance the fibrillation process. Liimatainen et al. treated bleached kraft hardwood pulp with periodate and bisulfite (Figure 16d), and obtained CNFs with sulfonated functionality (with the content of sulfonated groups of 0.18–0.51 mmol g^{–1}) via high pressure homogenization.^[196] In a similar manner,

periodate oxidation and bisulfate addition also can be used as pretreatment for CNCs.^[197]

Carbonylated and Carboxylated Nanocellulose: Nanocellulose can be oxidized by converting primary hydroxyl groups into carboxylic form. Three main approaches are generally applied for the oxidation of surface hydroxyl groups of nanocellulose, including TEMPO-mediated oxidation, APS oxidation and periodate-chlorite oxidation.

TEMPO-oxidation method has been extensively used for the preparation of CNFs, where TEMPO acts as a catalyst for regioselective oxidation of primary hydroxyl groups at C6 position of cellulose into carboxyl groups.^[198] The oxidation process with TEMPO coupled with NaBr/NaClO leads to functionalization on the surface of microfibrils with a significant amount

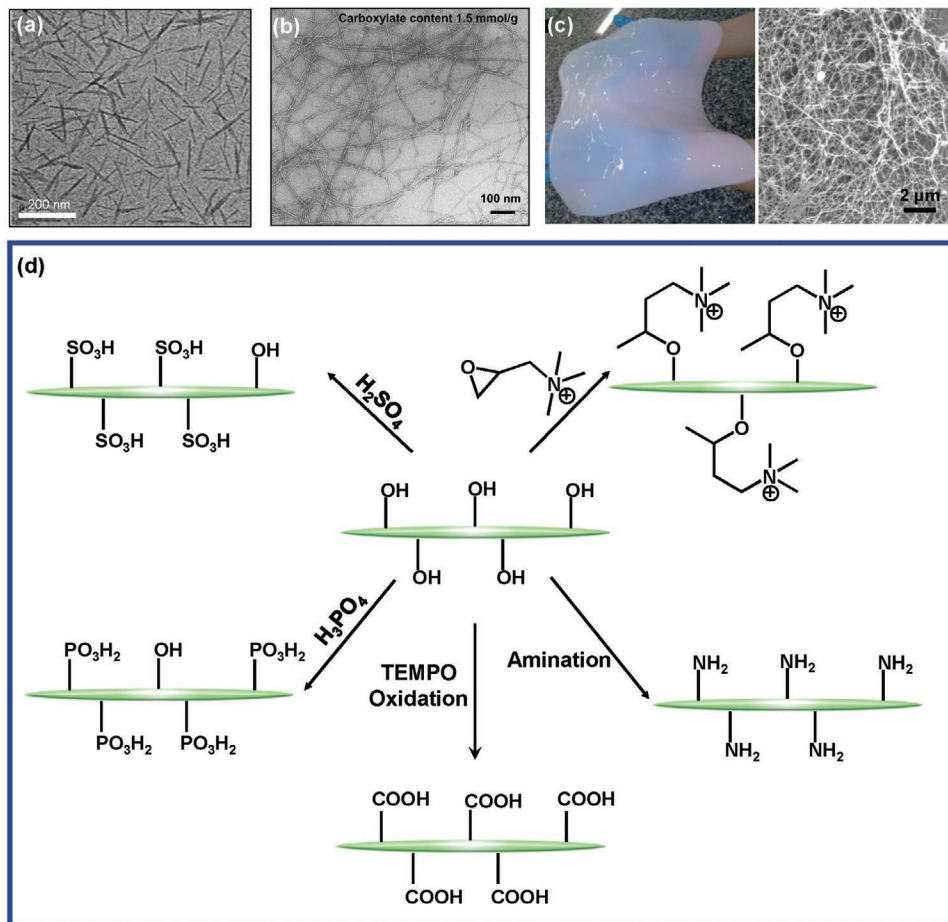
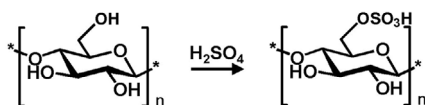


Figure 15. Morphology of three main kinds of nanocellulose: a) TEM image of CNCs. Reproduced with permission.^[179] Copyright 2012, Elsevier. b) TEM image of CNFs. Reproduced with permission.^[180] Copyright 2007, American Chemical Society. c) BC pellicle and SEM image. Reproduced with permission.^[181] Copyright 2016, Elsevier. d) Various ionic nanocellulose prepared by diverse surface modification techniques, including sulfonation, phosphorylation, oxidation, amination and cationic modification.

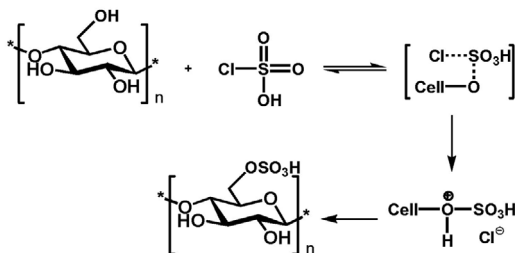
of sodium carboxylate groups (0–1.7 mmol g⁻¹) and a small amount of aldehyde groups. Unlike CNCs, CNFs contain many nonordered regions and have the widths ranging from ten to a few hundred nanometers and lengths on the micrometer scale. Mechanical, chemical, and biological approaches have been applied to produce CNFs, among which mechanical treatments are the most common methods. They are typically high-pressure homogenization, cryocrushing and grinding. TEMPO-mediated oxidation is mostly used as a cost-efficient chemical treatment prior to the mechanical process in order to facilitate the individualization of the fibers. TEMPO-mediated oxidation was first applied by de Nooy et al. to water-soluble polysaccharides such as starch, amylopectin and pullulan to oxidize the primary hydroxymethyl groups.^[199] This method selectively converts the exposed primary hydroxyl group at C6 position of AGUs to a carboxylic acid, while the secondary hydroxyl groups remained unaffected. The oxidation reaction is generally carried out at room temperature under ambient conditions for several hours at pH 9–11. The basic principle of TEMPO/NaBr/NaClO treatment is the oxidation of cellulose fibers by the nitrosonium ion (⁺N=O), which is generated in situ through the reaction of TEMPO radical with the oxidants. Consequently, the primary

alcohol groups of cellulose are converted into aldehydes, which are further oxidized to carboxyl groups (Figure 17a).^[198,200] However, side reactions including remarkable depolymerization are inevitable in TEMPO/NaBr/NaClO oxidation system under alkaline conditions, leading to lower DP that is important for the strength, length, and flexibility of individual cellulose fibrils and their properties. Moreover, the aldehyde groups formed as intermediates always remain in this system, which are thermally unstable and cause discoloration of the oxidized cellulose when heated or dried at more than 80 °C. Moreover, the residual aldehyde groups disturb the dispersion of the individual oxidized CNFs in water by partial formation of hemiacetal linkages between the fibrils. Saito et al. reported the use of TEMPO/NaClO/NaClO₂ system for cellulose oxidation, under neutral or weakly acidic conditions at 60 °C for up to 72 h.^[201] NaClO₂ is used as the primary oxidant, which immediately oxidized aldehyde groups to carboxyl groups under weakly acidic or neutral conditions. NaClO oxidizes TEMPO to the N-oxoammonium ion, which further oxidizes the primary hydroxyl to aldehyde group forming the hydroxylamine. The aldehyde group is then further oxidized to carboxyl group by the primary oxidant NaClO₂ with itself transformed into NaClO, and the

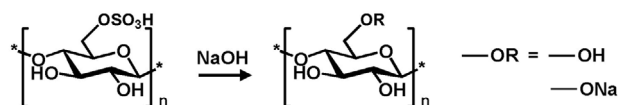
(a) Sulfuric acid hydrolysis



(b) Surface postsulfation



(c) Surface desulfation



(d) Periodate-bisulfite treatment

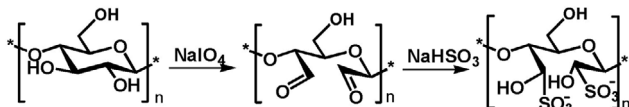


Figure 16. a–d) Sulfonation (a,b,d) and desulfation (c) process of nanocellulose.

hydroxylamine is oxidized to the N-oxoammonium ion again by the NaClO thus generated (Figure 17b). Due to stronger oxidizing feasibility, no aldehyde group remains in the oxidized products, and depolymerization of cellulose chains caused by β -elimination is expected to be avoided. Notably, it has been proved that the internal cellulose crystallinity and the crystal sizes were not affected after this TEMPO oxidation.

TEMPO-mediated oxidation also can be used for preparation CNCs with surface-attached carboxyl groups and the oxidative carboxylation should be combined with mechanical disintegration or acid hydrolysis since TEMPO-mediated oxidation cannot break down the nonordered regions completely.^[202] In fact, TEMPO-mediated oxidation of cellulose fibers involves a topologically confined reaction sequence. As a consequence of two-fold screw axis of the cellulose chain, only half of the accessible hydroxymethyl groups are available to the oxidation, where the other half are buried within the crystalline particles.^[183]

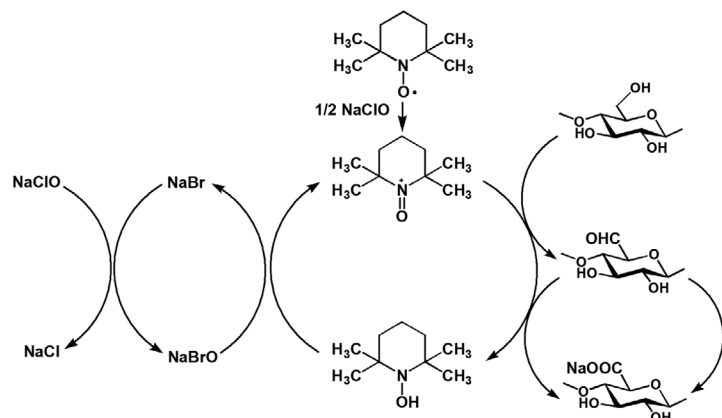
Leung et al. proposed another one-step oxidation method to prepare CNCs with surface-attached carboxyl groups, where APS was used as a strong oxidant to degrade the nonordered regions.^[203] The yield of CNCs was found to highly associated with cellulosic raw materials. The principal mechanism of APS method for isolation and oxidation of nanocellulose depends on the formation of free radicals ($\text{SO}_4^{\bullet-}$), hydrogen peroxide (H_2O_2), and HSO_4^- during heating (Figure 17c).^[204] These free radicals and H_2O_2 are capable of penetrating the nonordered regions to break down the nonordered cellulose to form CNCs. In addition, both the free radicals and H_2O_2 also open the

aromatic rings of lignin to decolorize this material. Thus, the removal of noncellulosic plant contents by pretreatment, such as via acid hydrolysis, can be avoided. Such technique of APS-based oxidation has relatively mild conditions compared with acid hydrolysis and lower energy consumption in comparison to mechanical ways. Moreover, it could carry significant benefits in terms of the improved properties, such as thermostability, high crystallinity, transparency, water resistance and oxygen barrier property.^[205]

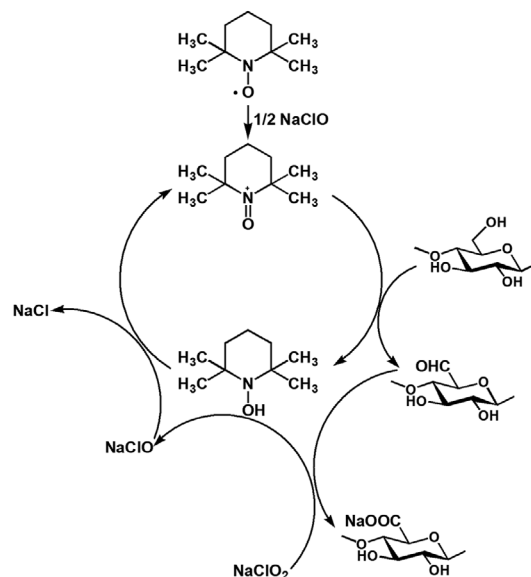
Besides, periodate-chlorite oxidation is another way for the carboxylated CNCs. The periodate was first employed to oxidize the hydroxyl groups at C2 and C3 positions of AUGs in cellulose and simultaneously break the corresponding carbon–carbon bond of the glucopyranose ring to form 2,3-dialdehyde cellulose (DAC) (Figure 17d). The aldehyde groups of DAC exhibit high reactivity toward further modifications, e.g., they can be oxidized to acids to form 2,3-dicarboxylic acid cellulose (DCC). Yang et al. prepared CNCs with carboxyl content between 3.6 and 6.6 mmol g^{-1} through the periodate-chlorite oxidation.^[206] Liimatainen et al. employed periodate and chlorite oxidation as an efficient pretreatment to enhance nanofibrillation of cellulose pulp through homogenization.^[207] The carboxyl content of the oxidized nanocelluloses can be up to 1.75 mmol g^{-1} . It should be noted that this method leads to the opening of the glucopyranose ring without decreasing the strength properties of CNFs. Recently, Zhang's group developed a novel method for the efficient production of CNCs containing carboxy groups of up to 0.49 mmol g^{-1} by selective alkaline periodate oxidation at $\text{pH} = 10$.^[208] The carboxy groups on the surface of produced CNCs were independent on the reaction time and raw materials. This method allows direct production of CNCs from diverse sources, in particular lignocellulosic raw materials including sawdust, flax and kenaf, in addition to microcrystalline cellulose and pulp. Besides, this method doesn't need any complicated pre/post-treatments.

Furthermore, carboxylated CNCs and CNFs also can be obtained by hydrolysis using concentrated organic acids through esterification (Figure 17e). Iwamoto and Endo reported preparation of carboxylated CNFs with carboxyl groups of 1.9 mmol g^{-1} after the mechanical disintegration of wood flour that was esterified with maleic anhydride in advance.^[209] Sehaqui et al. prepared carboxylated CNFs with high content of carboxyl groups of 3.8 mmol g^{-1} via the esterification of wheat fibers with cyclic anhydrides (maleic, phthalic, and succinic) followed by mechanical disintegration process.^[210] The DS ascribed to carboxyl groups of the resultant CNFs is generally around 0.67, which is higher than CNFs prepared via APS oxidation (0.11–0.19). Compared with the CNFs from TEMPO-mediated oxidation, esterified CNFs have a higher molar mass (viscosity average DP (DP_v)) and a better thermal stability due to the lower content of carboxylic acid. Chen et al. reported the production of highly thermal stable (at 322 °C) and functional CNCs and CNFs using dicarboxylic acids.^[211] The carboxyl groups of the resultant CNCs with contents of 0.1–0.4 mmol g^{-1} facilitated further functionalization and also the dispersion in aqueous solutions for successive processing. Koshani et al. presented a facile method to isolate CNCs with carboxylated surfaces from cellulose materials by adding hydrogen peroxide as an oxidant and copper(I) sulfate as catalyst in acidic medium

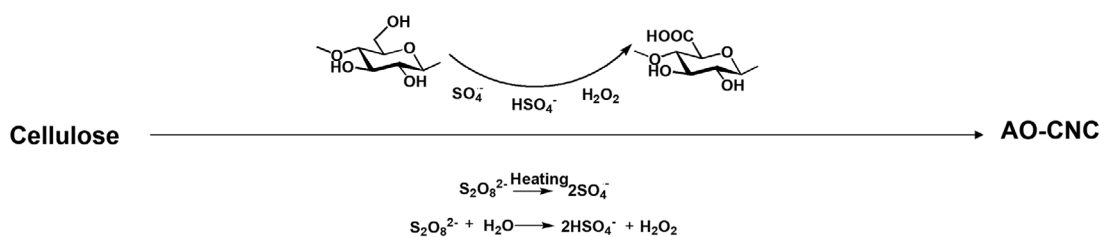
(a) TEMPO/NaBr/NaClO oxidation



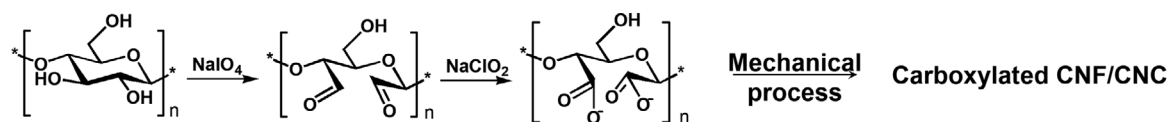
(b) TEMPO/NaClO/NaClO₂ oxidation



(c) APS oxidation



(d) Periodate-chlorite oxidation



(e) Esterification

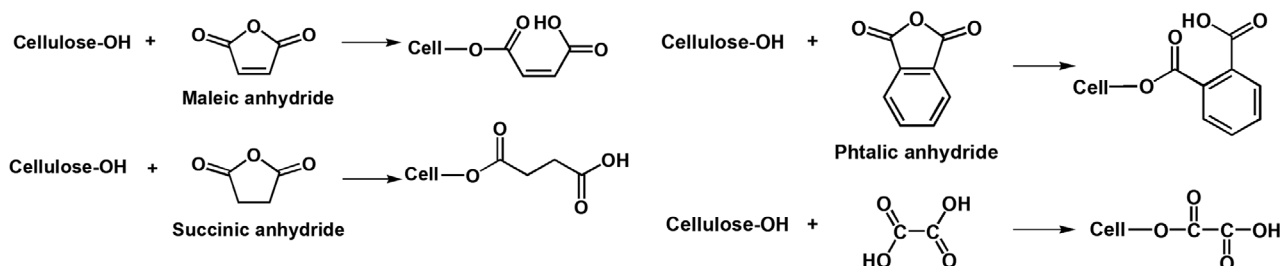


Figure 17. Diverse routes to prepare carboxylated nanocellulose. Schematic diagrams for the oxidation of cellulose by: a) TEMPO/NaBr/NaClO in water at pH of 10–11. b) TEMPO/NaClO/NaClO₂ in water at neutral or slightly acidic pH values. c) APS oxidation, d) periodate and chlorite oxidation, and e) esterification using organic acids, respectively. a,b) Reproduced with permission.^[198] Copyright 2011, Royal Society of Chemistry. e) Reproduced with permission.^[210] Copyright 2016, American Chemical Society.

under mild thermal conditions.^[212] The metal catalysts in H₂O₂ oxidation can facilitate the formation of radicals, which can react with cellulose and introduce aldehyde and carboxyl groups.

Phosphorylated Nanocellulose: In comparison to sulfated and carboxylated nanocellulose, the introduction of phosphate groups to the nanocellulose received little attention. Similar as sulfuric acid, phosphoric acid is employed to introduce negative charges by modifying the surface of nanocellulose with phosphate ester groups. As shown above, diverse cellulose phosphorylation methods have been developed during the past decades. Phosphorylating agents, such as phosphorus oxychloride (POCl₃), phosphorus pentoxide (P₂O₅), phosphoric acid (H₃PO₄), diammonium hydrogen phosphate ((NH₄)₂HPO₄), and organophosphates, have been employed individually or in combination.^[213] Compared with other phosphorylating agents, (NH₄)₂HPO₄ has less toxicity and causes less cellulose hydrolysis. Excess amounts of urea were used to prevent the degradation of cellulose caused by the released phosphoric acid at an elevated temperature.^[213,214] Phosphorylation usually takes place in the presence of organic solvents, such as *N,N*-dimethylformamide (DMF), pyridine, or urea, which are used to swell cellulose fibers to increase the homogeneity of the phosphorylation reaction. Introduced amounts of phosphate groups heavily depend on the amounts of the phosphorylating agents, reaction time and temperature.

Espinosa et al. obtained phosphorylated CNCs containing 10.8 ± 2.7 mmol kg⁻¹ of phosphate groups using phosphoric acid.^[215] These CNCs exhibited a much higher thermal stability than sulfated CNCs and were more resistant to coloration at high temperatures. Not just phosphorylated CNCs but also phosphorylated CNFs and BC have been reported. Oshima et al. prepared the phosphorylated BC in the mixture of DMF and urea, and found that the phosphorylation degrees increased with a higher amount of urea and phosphoric acid.^[216] Moreover, the method for drying the BC materials is an important factor for effective phosphorylation, because it affects the aggregation of fibrous structure of cellulose. Besides, phosphoric acid and/or urea are more accessible to BC than to plant cellulose, probably due to the different morphology of the fibers. Ghanadpour et al. obtained phosphorylated CNFs with a width of 3–4 nm at a maximum yield of 60% after the phosphorylation of sulfite softwood pulp with urea and (NH₄)₂HPO₄, followed by nanofibrillation using a high-pressure homogenizer under controlled pH values of the phosphorylated pulp slurry at 9.5.^[213,217] The presence of phosphate groups in the structure showed the improved flame retardancy.

4.1.2. Positively Charged Nanocellulose

The intrinsic negative surface charges of CNCs prevent the direct use of electrostatic interactions for the binding or self-assembly with negatively charged biomacromolecules, nucleic acids, and certain proteins.^[218] Hence, the development of cationic functional CNCs may open up more opportunities for biomedical applications. Up to now, there are mainly three reported pathways for the cationization of the surface of CNCs. The first pathway by Hasani et al. uses epoxy moiety of (2,3-epoxypropyl)-

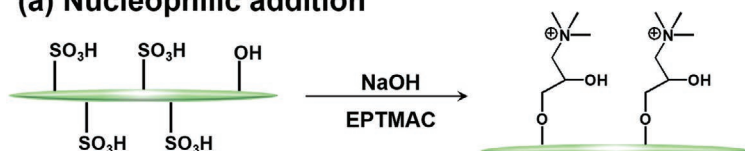
trimethylammonium chloride (EPTMAC) to introduce quaternary ammonium onto CNCs (Figure 18a).^[219,220] The H₂SO₄-hydrolyzed CNCs needed to be alkali-activated before the cationization, where the anionic sulfate ester groups on the surface of CNCs were removed by solvolytic desulfation or alkaline solution. In the desulfation process, the alkaline concentration should be carefully controlled in order to completely remove the surface sulfate esters of CNCs and at the same time to avoid the transformation of cellulose type I to type II. 27.6% of the surface hydroxyl groups of CNCs were replaced by cationic hydroxypropyl-trimethylammonium groups, indicating that most of C6 positions was functionalized with cationic groups during the modification. After the surface cationization, the zeta potential of CNCs changed from -50 ± 7.7 to 37.3 ± 5.4 mV. Furthermore, the thermal degradation temperatures (*T_d*) for desulfated and cationic CNCs increased by 60 °C (from 140 to 202 °C) in comparison with that of pristine CNCs, showing the improved thermal stability, which may be partially due to the protection and shielding effects by polymeric chains.^[192] In order to circumvent the issue of a low total surface charge density of the above cationized CNCs, Zaman et al. proposed an aqueous semidry method with similar synthetic strategy, where dry CNCs and sodium hydroxide were ground together prior to the addition of cationic agent.^[179] A strongly enhanced charge density of 2.05 meq g⁻¹ were achieved, making the modified CNCs well dispersed and stable in aqueous media.

The second route, reported by Eyley and Thielemans, was realized via click chemistry to introduce imidazolium groups on the surface of CNCs without the removal of sulfate groups (Figure 18b).^[221] This pathway forms imidazolium-grafted-CNCs through copper(I) catalyzed azide–alkyne cycloaddition involving three steps: chlorination, azidation, and grafting. Selective modification of the primary hydroxyl groups on the surface of CNCs with a high yield was realized. Significantly increased cationic surface charge (1.17 e nm⁻²) and surface imidazolium concentration of 0.53 mmol g⁻¹ were obtained, which are feasible for ionic exchange application. Instead of chlorination, Feese et al. applied tosylation of CNCs to further synthesize the CNCs functionalized with a cationic porphyrin.^[222] Resulting insoluble CNC-Por (5) showed excellent efficacy for photodynamic inactivation of *Mycobacterium smegmatis* and *S. aureus*. The advantages of a covalent attachment of the porphyrin to the surface of CNCs include conferring longer lasting or permanent antimicrobial properties, minimizing the leaching of the biocidal agent into surrounding environment, and prevention of porphyrin aggregation. In addition, Jasmani et al. proposed the cationization route with the simple and one-pot reaction system to produce positively charged CNCs by grafting of pyridinium moieties.^[223] The resultant CNCs retain their crystallinity and maintain the integrity of their original morphology.

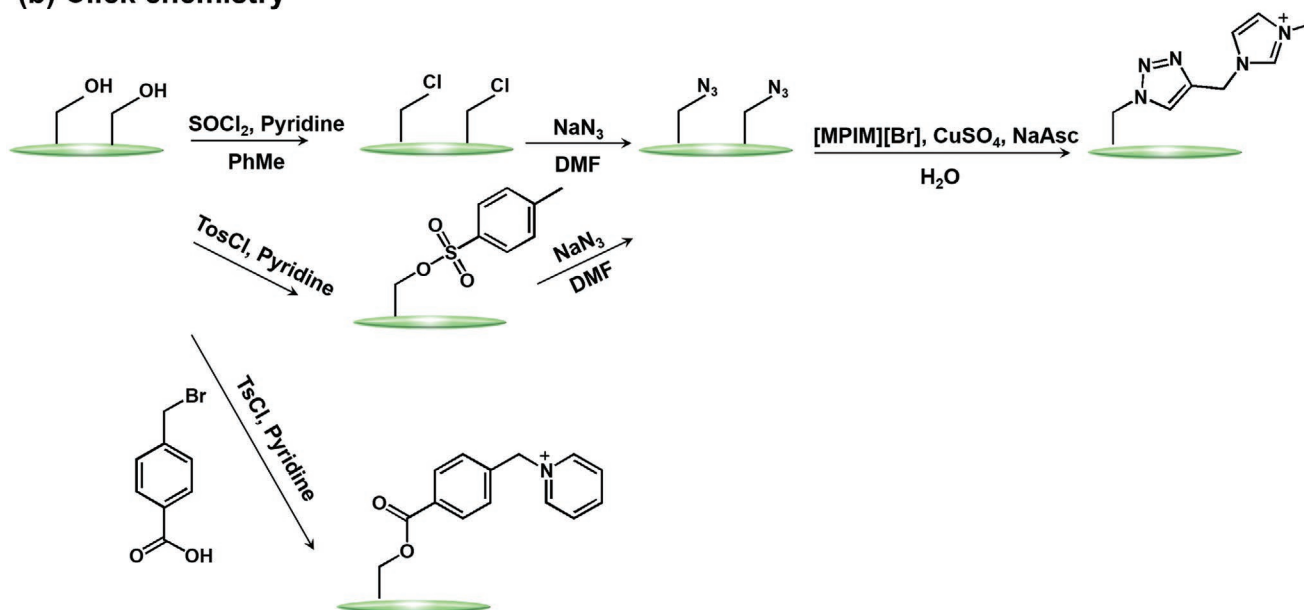
The last route to prepare the cationic CNCs via covalent linkages was to graft polymer chains onto the surface via grafting to, grafting from, and grafting through approaches, e.g., via living radical polymerization or reversible deactivation radical polymerization techniques.^[224] Surface-initiated atom transfer radical polymerization (SI-ATRP) and single-electron transfer living radical polymerization are the most widely used methods for grafting from of polymer chains onto the surface of CNCs.

Covalent interactions

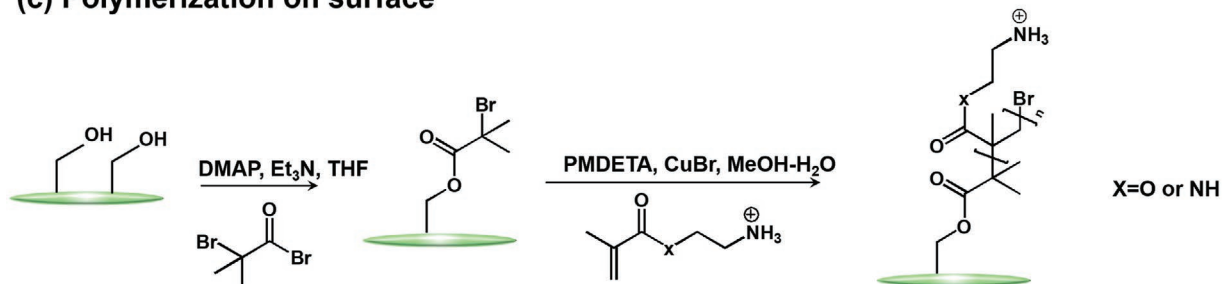
(a) Nucleophilic addition



(b) Click chemistry



(c) Polymerization on surface



Noncovalent interactions

(d) Physical adsorption

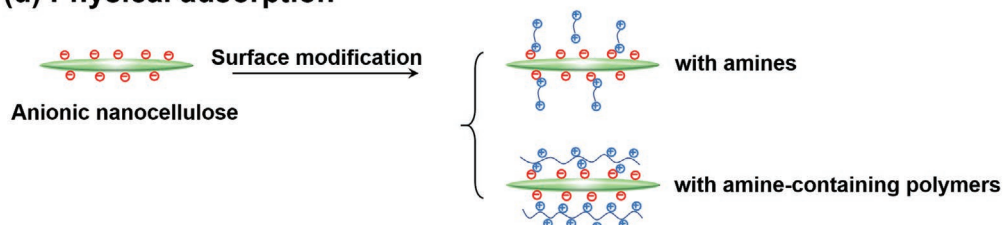


Figure 18. Synthetic routes for cationic CNCs via covalent and noncovalent interaction: a) cationic modification of nanocellulose using chemical grafting by nucleophilic ring-opening of the epoxide moiety, b) click chemistry, c) polymerization on the surface, and d) surface modification of nanocellulose using physical adsorption with cationic molecules or polymers.

For instance, poly(*N,N*-dimethylaminoethyl methacrylate) (PDMAEMA) was grafted onto the surface of CNCs using the free radical polymerization method in the presence of APS as the initiator.^[225] Hemraz et al. grafted cationic polymers from CNCs surface via the surface-initiated single-electron-transfer living radical polymerization technique using cationic monomers, namely, 2-amino-ethyl methacrylate hydrochloride and 2-aminoethyl-methacrylamide hydrochloride (Figure 18c).^[226] These cationic CNC-based compounds were further exploited as a nanoplatform for gold deposition and both of them still allow sufficient cell viability at low concentrations, which made them suitable for potential biomedical applications. Moreover, Rosilo et al. prepared cationic CNCs by surface-initiated ATRP of PDMAEMA.^[218]

In addition to chemical modifications for the covalent linkages, the surface cationization of CNCs can also be achieved by physical adsorption using cationic molecules or polymers via electrostatic interaction, hydrophilic affinity, van der Waals interaction or hydrogen bonding (Figure 18d).^[220,227]

For instance, the physical adsorption of polyethylenimine (PEI) on the surface of CNC was achieved by the electrostatic interactions between cationic polymer chains and negative sulfate groups.^[220] The pH of the mixture was then adjusted to 1.5 with HCl to enhance the ionic interaction between CNC and PEI chains. Alternatively, CNCs with surface-attached carboxyl groups also can be used for the cationization via physical absorption. Zhou and co-workers utilized four quaternary ammonium cation surfactants bearing long alkyl, phenyl, glycidyl, and diallyl groups to modify CNCs with surface-attached carboxyl groups through ionic exchange process.^[228] Obtained CNCs modified with quaternary ammonium salts bearing octadecyl chains showed higher static water contact angle (71°) than that of unmodified CNCs (12°), which can be redispersed and individualized in an organic solvent such as toluene.

4.2. Applications for Biomaterials

4.2.1. Biological Properties

In comparison to water-soluble polymeric cellulose derivatives that have been intensively studied regarding their fundamental biological properties, nanocellulose still needs more long-term evaluation regarding these critical biological properties, i.e., biocompatibility, cytotoxicity and biodegradability. In spite of this, lots of studies already proved the great application potential of nanocellulose as biomaterials.

Previous studies on nanocellulose-based materials utilized experiments on cell cultivation, through the growth, propagation and further cell activities to evaluate their biocompatibility.^[220,229] Biocompatible and antioxidant characteristics of longer BC after the functionalization with sulfate groups through acetosulfation have been verified by cell viability, antioxidant, and hemocompatibility assays.^[230] Such sulfated BC was found to be highly blood compatible, because it did not lyse human red blood cells (RBC) and maintained the integrity of cells after treatment. The size of CNCs would allow the prolonged circulation of CNCs in the bloodstream and sufficiently delays its clearance by the mononuclear phagocytic

system.^[231] With its anticipated production and application at a larger scale, bioeffects and safety of CNCs to the environment and human health must be thoroughly investigated in vitro, before they can be used in vivo.

Moreover, many studies have been conducted to analyze the cytotoxicity of CNCs. Different results were achieved due to the application of different cell lines, cellulose sources, preparation procedures of CNCs, postmodification and even post-processing.^[232] These factors affect the physicochemical properties, size dimensions, and surface chemistries of obtained CNCs, which have distinct effects on cell viability.

Many efforts have also been devoted to improving the in vitro biodegradability of nanocellulose, e.g., through further oxidation. BC was modified by periodate oxidation to produce biodegradable 2,3-dialdehyde bacterial cellulose (DABC).^[233] The nanonetwork in such modified DABC was able to degrade into porous scaffold with micro-sized pores in water, phosphate buffered saline (PBS) and the simulated body fluid (SBF).

4.2.2. Gene Delivery

In gene therapeutic application, cationic gene vectors, as effective alternative to viral vectors, have been widely studied due to their low cost, easy preparation and low immunogenicity. Polycations are always a double-edged sword for gene delivery.^[234] On the one hand, the negative-charged pDNA can be condensed by polycations to form nanoparticles (NPs), avoid enzymatic degradation and facilitate cellular uptake. On the other hand, polycations can disturb negatively charged cell membrane structures due to the electrostatic interaction. The major challenge is the lack of ideal gene vectors that possess high transfection efficiency but low cytotoxicity. Hence, new efficient delivery nanocarriers developed with biobased materials have become very interesting. CNCs can be good candidates for nanocarriers with low cytotoxicity for efficient gene and drug delivery due to their characteristic nanosized and rod-like particles as well as good biocompatibility.

Hu et al. designed cationic CNC-based gene vectors by wrapping the surface of CNCs with disulfide bond-linked dense PDMAEMA brushes.^[235] Prior to SI-ATRP with PDMAEMA, sulfated CNCs were modified in two steps (Figure 19): 1) reaction of cystamine with CDI-activated CNCs to obtain CNC-SS-NH₂ and 2) amidation reaction of CNC-SS-NH₂ with α -bromoisobutyric acid (BIBA) to produce CNC-SS-Br. The resulting CNC-graft-PDMAEMA vectors (CNC-SS-PD) were evaluated for their gene condensation abilities, reduction sensitivities, cytotoxicities, gene transfection efficiencies, cellular uptake, in vitro and in vivo antitumor effects. In intracellular reducing conditions, disulfide bonds between PDMAEMA chains and CNCs can be broken, promoting pDNA released from complexes. Therefore, the cationic CNCs exhibited good transfection efficiency and low cytotoxicities compared to PEI, H-PD, and CNC-PD, showing good potential for gene/drug delivery systems.

Furthermore, they designed a multifunctional nanovector of gold NPs (Au NPs)-conjugated heterogeneous polymer brush-wrapped CNCs.^[234] In this system, poly[poly(ethylene glycol)ethyl ether methacrylate] (PPEGEEMA) and PDMAEMA

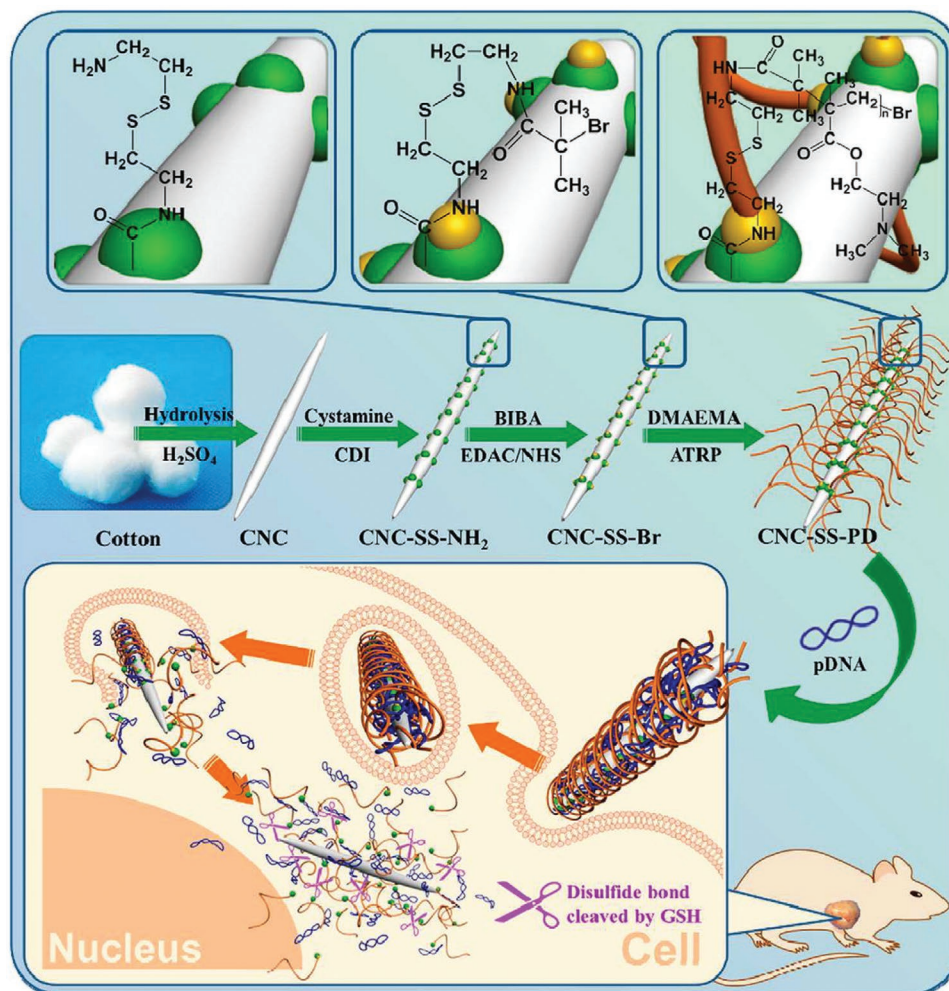


Figure 19. Schematic diagram depicting the synthesis of CNC-graft-PDMAEMA (CNC-SS-PD) via SI-ATRP and the gene delivery process. Reproduced with permission.^[235] Copyright 2015, American Chemical Society.

brushes were individually grafted from CNCs. The cationic PDMAEMA chains can effectively complex with genes, while the uncharged PPEGEEMA brushes spread outward and significantly reduce the cytotoxicity. In order to impart computed tomography (CT) imaging of CNCs, Au NPs as CT contrast agents were in situ formed on the CNC-based carriers by using the amine groups of PDMAEMA chains as reducing and protective agents. Similarly, by physical adsorption with amines and amine-containing polymers, the cationic bacterial CNCs with low toxicity at a concentration of 0.1 mg mL^{-1} were fully complexed with siRNA, showing the big potential as nucleic acid nanocarriers.^[227]

4.2.3. Drug Delivery

The ability of nanomedical techniques to target specific sites depends highly upon the particle size, surface charge, surface chemistry and hydrophobicity, which in turn determine their interaction with the cell membrane and their penetration across the physiological drug barriers. CNCs has a rod-like shape with

sizes in the range of 100–300 nm long and 5–50 nm wide, which would allow for a prolonged circulation of CNCs in the bloodstream and sufficiently delays its clearance by the mononuclear phagocytic system.^[231] Their biodegradability, cytotoxicity to human cells and the cellular uptake as the delivery system need to be critically evaluated. The cellular uptake of negatively charged fluorescein isothiocyanate (FITC)-labeled CNCs was compared with that of positively charged rhodamine B isothiocyanate-labeled CNCs (RBITC) in human embryonic kidney 293 (HEK 293) and *Spddoptera frugiperda* (Sf9) cells. The results showed that the positively charged CNC-RBITC conjugate was uptaken by the cells without affecting the integrity of the cell membrane and there was no noticeable cytotoxic effect observed according to the cell viability assay and cell-based impedance spectroscopy (Figure 20), whereas the negatively charged CNC-FITC conjugate resulted in no significant internalization at physiological pH, but the effector cells were surrounded by CNC-FITC, leading to eventual rupture and showing the importance of the surface charge of CNCs in cellular uptake and cytotoxicity.

CNC-based nano-prodrugs can be prepared by the chemical conjugation between *cis*-aconityl-DOX (CAD) and amidated

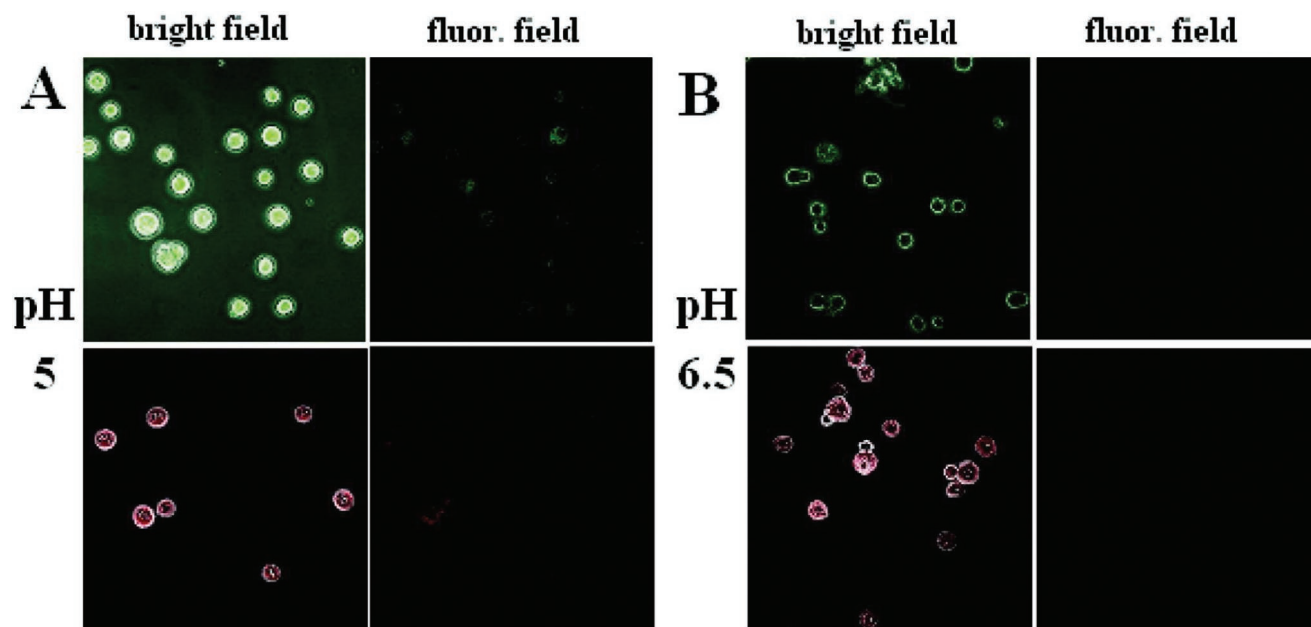


Figure 20. A,B) Mixed field and fluorescence-microscopy images comparing the uptake of CNC-FITC (upper) with CNC-RBITC (lower) by Sf9 cells at pH (A) 5 and pH 6.5 (B). Cells were incubated with CNC-FITC or CNC-RBITC during 3 h experiment at corresponding pH values, and then fixed for confocal microscope measurement. A,B) Reproduced with permission.^[231] Copyright 2010, American Chemical Society.

CNCs, as reported by Li et al.^[236] CAD was synthesized by the ring-opening reaction between *cis*-aconitic anhydride (CAA) and the amino group of DOX. Amidation reaction occurred between the 6-carboxyl groups of CAD and the amino groups on the surface of aminated CNCs. *cis*-Aconityl amide linkages are ideal pH-sensitive linkages for DOX prodrugs, because they are sensitive to a small change of pH values in diverse cellular compartments and can realize intracellular controlled drug release. Hence, the nano-prodrugs showed enhanced cellular uptake and lysosomal pH-triggered drug release, in addition their fluorescence nature. To further increase the cellular uptake and drug loading of CNC-based nanocarriers, hybrid folate/CAD@PEI@CNC were built up using the building blocks folate, CAD, PEI, and CNCs via the robust LbL assembly technique.^[237] The drug loading reached a content of 11.3 wt%, almost 20-folds higher than that of CNC-based nano-prodrugs. Moreover, these nanocarriers showed lysosomal pH-controlled drug release profiles over 24 h *in vitro*, and had a higher (9.7-fold) mean fluorescent intensity than that of DOX-HCl, with enhanced cytotoxicity and decreased IC₅₀ against MCF-7. In addition, these nanocarriers could deliver more DOX to the nucleus than the control groups, due to the β -carboxylic acid-catalyzed cleavage of pH-labile *cis*-aconityl amide linkage in CAD.

In another approach, ionic nanocomplexes are used to deliver drugs, for instance by using the conjugates of β -cyclodextrin (β -CD) and CNCs as nanocarriers to trap target molecules via the formation of host-guest complexes. β -CD can be immobilized onto the surface of CNCs by three routes: 1) by an amidation reaction for covalently binding β -CD to amine-modified CNCs,^[238] 2) by loading premodified cationic β -CD onto the surface of sulfuric acid-hydrolyzed CNCs via ionic interaction,^[239] and 3) by using epichlorohydrin (EPI) as coupling agent.^[240] In one typical study, such nanocomplex formed after trapping

curcumin and exhibited an antiproliferative effect on colorectal and prostatic cancer cell lines, where the IC₅₀ was found to be lower than that of curcumin alone.^[239]

Wang et al. reported a further strategy to modify CNCs with hydrophilic poly(ethyl ethylene phosphate) (PEEP) through a “grafting onto” process, in which a combination of ring-opening polymerization (ROP) and Cu(I)-catalyzed azide-alkyne cycloaddition (CuAAC) “click” chemistry was used.^[241] Resulting negatively charged CNCs (CNC-g-PEEP) were used to encapsulate DOX by electrostatic interactions and deliver it to the HeLa cells. The hydrophilic PEEP chains provided favorable stability to the DOX-loaded CNCs in blood circulation. Besides, the diameter of CNC-g-PEEP nanocrystals was around 30–40 nm, which allowed them to be internalized by tumor cells. In the tumor acidic environment, the electrostatic interaction was destroyed by the attack of ions (e.g., H⁺ or Cl⁻ ions) in the cytoplasm and PEEP segments were degraded, leading to a pH-triggered release of DOX. The system showed a pronounced biocompatibility to both HeLa cells and L929 cells and exhibited an anticancer activity against HeLa cells.

In addition to the presence as nanocarriers for drug delivery, ionic nanocellulose also can be used for the preparation of microparticulate drug delivery systems. LbL films made with negatively charged CNCs and positively charged chitosan have also been employed as microcapsules for controlled drug delivery, including water-soluble anticancer drug DOX hydrochloride and lipophilic curcumin.^[242] A high encapsulation efficiency of up to 97% of the drug indomethacin was achieved with the drug release process sustained over 30 days. Lin et al. prepared double membrane hydrogels based on sodium alginate with cationic CNCs to increase structure stability and control the delivery of drugs.^[220] Two drugs were introduced into the different membranes of the hydrogels, which ensured the

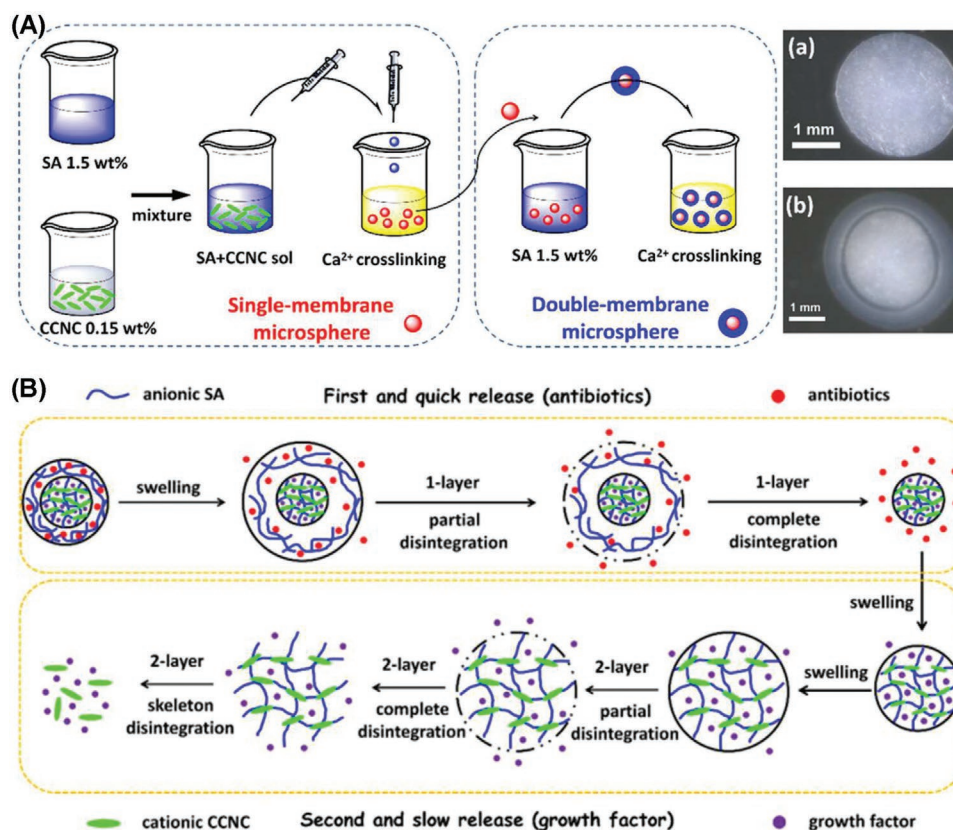


Figure 21. A) Preparation routine of single-membrane and double-membrane microsphere hydrogels and the images of: a) SA (sodium alginate)/CCNC (cationic CNCs) single-membrane microsphere hydrogel and b) SA/CCNC-1 h double-membrane microsphere hydrogel; B) proposed complexing drug release model for the double-membrane hydrogel with the formation of cationic CNCs and anionic alginate at pH 7.4. A,B) Reproduced with permission.^[220] Copyright 2016, American Chemical Society.

complexing drug codelivery and the varied drugs release behaviors from two membranes as rapid drug release from the outer hydrogel and prolonged drug release from the inner hydrogel (Figure 21). The double-membrane hydrogels were biocompatible and realized the complexing drugs release with the first quick release of one drug and the successively slow release of another drug.

4.2.4. Wound Dressings

Over the past few decades, wound repair has become a realm of extensive research among biomedical applications. In clinical practices, effective wound healing materials must meet the requirements that can provide moist environment to wound, permit gaseous diffusion, prevent microbial infection, remove excess of exudates, and can be readily removed from the wound site without causing much pain or other side effects.^[243] Among others, BC membranes have been used as excellent topical wound dressings, thanks to their appealing properties including high purity, good tensile strength for never-dried films, high exudates capacity, and a unique nanofibril morphology network structure.^[244] However, their lack of ability to prevent bacterial infection in wound area, mainly restricts their application in wound dressings.^[245,246]

Recently, ionic nanocellulose has been applied for wound dressings. Because hydrophilic CNCs are also lack of antimicrobial activities and cannot effectively prevent microbial infection around moist wound milieu, Singla et al. developed nanobiocomposites in films and ointment forms by in situ synthesis of Ag NPs within the matrix of CNCs isolated from bamboo.^[243] Obtained nanobiocomposites with good water absorption capacity and strong antibacterial activity showed synergistic effect on in vivo skin wound healing and documented faster wound closure on mice. Moreover, those nanobiocomposites containing a low amount of Ag (0.05 ± 0.01 wt%) exhibited lesser inflammation and early vasculogenesis at day 3 coupled increased fibroblasts and collagen content at day 8, leading to faster neo-epithelization by day 14. In addition, they also found that the CNCs isolated from different sources showed varying healing performance.^[247]

Although there are many forms of wound dressing materials, e.g., films, foams, hydrogels, hydrocolloids, and so on, hydrogels are among them promising materials to facilitate wound healing, because they can absorb and retain the wound exudate and sustain an ideal moist environment for healing while protecting the wound sites.^[245] Within the last years, CNC- and CNF-based hydrogels have received extensive attention for wound dressing applications.^[248] To improve the antimicrobial activity of hydrogels containing ionic nanocellulose, Basu et al.

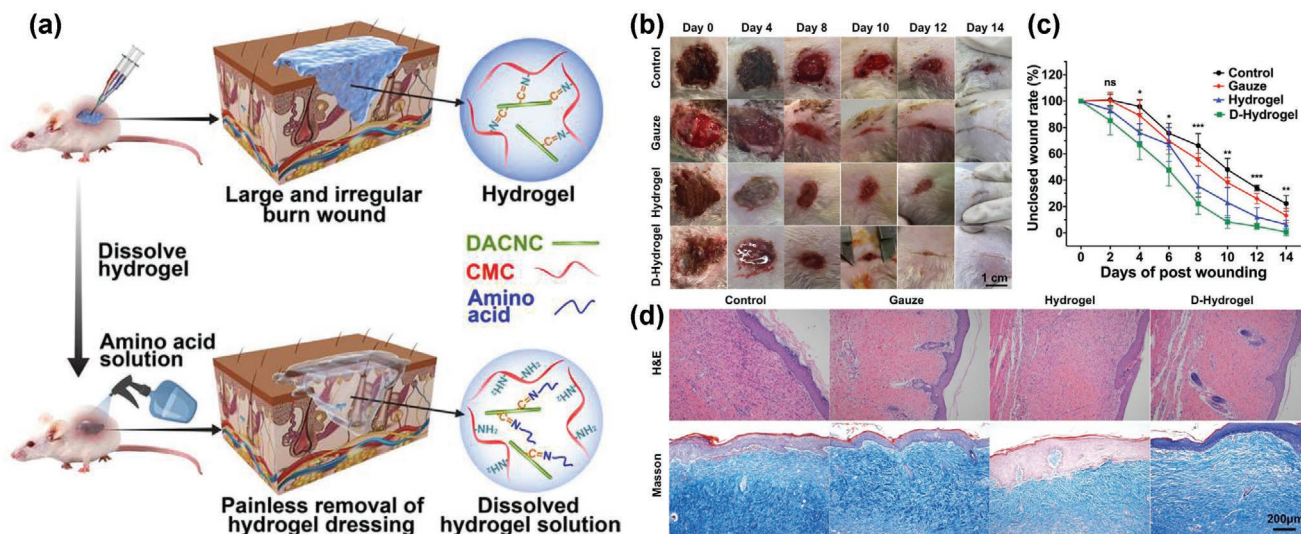


Figure 22. a) Schematic illustration of on-demand dissolvable self-healing hydrogels for deep partial-thickness burn wound healing. b–d) Wound healing process: b) images of a representative wound site from each group taken on the postinjury days 0, 4, 8, 10, 12, and 14. c) unclosed wound area rate of an initial wound untreated or treated with petrolatum gauze, hydrogel, and hydrogel with glycine on the day 0, 2, 4, 6, 8, 10, 12, and 14. Values are mean \pm standard deviation (SD) for each group. ns $p > 0.05$, * $p \leq 0.01$, *** $p \leq 0.001$. d) Hemotoxylin and eosin (H&E) staining and Masson's trichrome staining of wounds on day 14. a–d) Reproduced with permission.^[252] Copyright 2018, American Chemical Society.

prepared CNF-based hydrogels for wound dressings after the crosslinking using metal cations.^[249] They found that different crosslinking agents (calcium or copper ions) could strongly affect their antibacterial properties against diverse kinds of bacterial strains.^[250] Liu et al. developed a kind of composite hydrogels by introducing the aminated Ag NPs and gelatin to carboxylated CNFs. The hydrogel dressing with 0.5 mg mL⁻¹ amino modified Ag NPs demonstrated stronger mechanical, self-recovery and antibacterial properties, satisfactory hemostatic performance, and appropriate balance of fluids on the wound bed (2093.9 g m⁻² per day). The in vitro and in vivo wound healing model evaluation of these hydrogels showed an outstanding biocompatibility and wound healing efficacy.^[251] To solve the problem in currently available hydrogels that they cannot quite match the deep and irregularly shaped wounds and neither can they reach to some special areas, such as joint and cavity wounds, Huang et al. developed a kinds of self-healing hydrogels for deep partial-thickness burn wound healing.^[252] The hydrogels based on carboxymethyl chitosan and dialdehyde-modified CNCs, are crosslinked by dynamic Schiff-base linkages between amines and aldehydes. with the presence of Schiff-base, the hydrogels could be removed by on-demand dissolving using amino acid solution by wound dressing changes, which could accelerate deep partial-thickness burn wound healing, avoid pain during wound dressing changes, and prevent scar formation (Figure 22a). In the animal model, burn wounds covered by the dissolved hydrogel exhibited more rapid skin regeneration and fewer visible scars compared with the control, gauze, and hydrogel groups, as shown in Figure 22b–d.

4.2.5. 3D Bioprinting

Recent advances have enabled 3D printing of biocompatible materials, cells and supporting components into complex 3D

functional living tissues, which affords potential applications of 3D printing in tissue engineering and regenerative medicine.^[253] Nanocellulose stands out as a substrate and also a component in bioink owing to its biocompatibility, low cytotoxicity and especially excellent mechanical strength for 3D bioprinting. It should be mentioned that collapsing and shape fidelity are common challenges in 3D printing.^[254] Collapsing is typical for biobased hydrogels, and it is usually because of low dry-matter contents. Shape fidelity, in turn, is related to the viscoelastic properties of the printing paste.

CNFs can form hydrogels due to the abundant hydroxy groups, as well as sufficient flexibility and propensity for fibril entanglement. In particular, the high zero shear viscosity and strong shear thinning properties make CNFs ink appropriate for 3D printing.^[253] Rees et al. used homogenized CNFs for bioink, which was prepared with combined carboxymethylation and periodate oxidation to yield C-periodate nanocellulose with reduced viscosity in aqueous suspensions.^[255] In contrary to the TEMPO nanocellulose, C-periodate nanocellulose formed a more solid structure with defined tracks, whilst the TEMPO nanocellulose tended to collapse probably because of the lower consistency of the material (0.95%) than C-periodate nanocellulose (3.9%). These 3D nanocellulose structures form tracks with open porosity and the potential to carry and release antimicrobial components. It was demonstrated that the nanocellulose assessed in this study did not support bacterial growth and therefore had advantages for wound dressing applications.

To print nanocellulose scaffolds as dominant matrix with tunable mechanical properties and stability in the wet state, Xu et al. proposed a dual-crosslinking strategy.^[256] The crosslinking was conducted first with Ca²⁺ ions for the complexation and then via chemical crosslinking with 1,4-butanediol diglycidyl ether (BDDE) during the postprinting to print CNFs hydrogel scaffolds with tunable mechanical strength in the range of 3–8 kPa. Recently, 3D printed nanocellulose

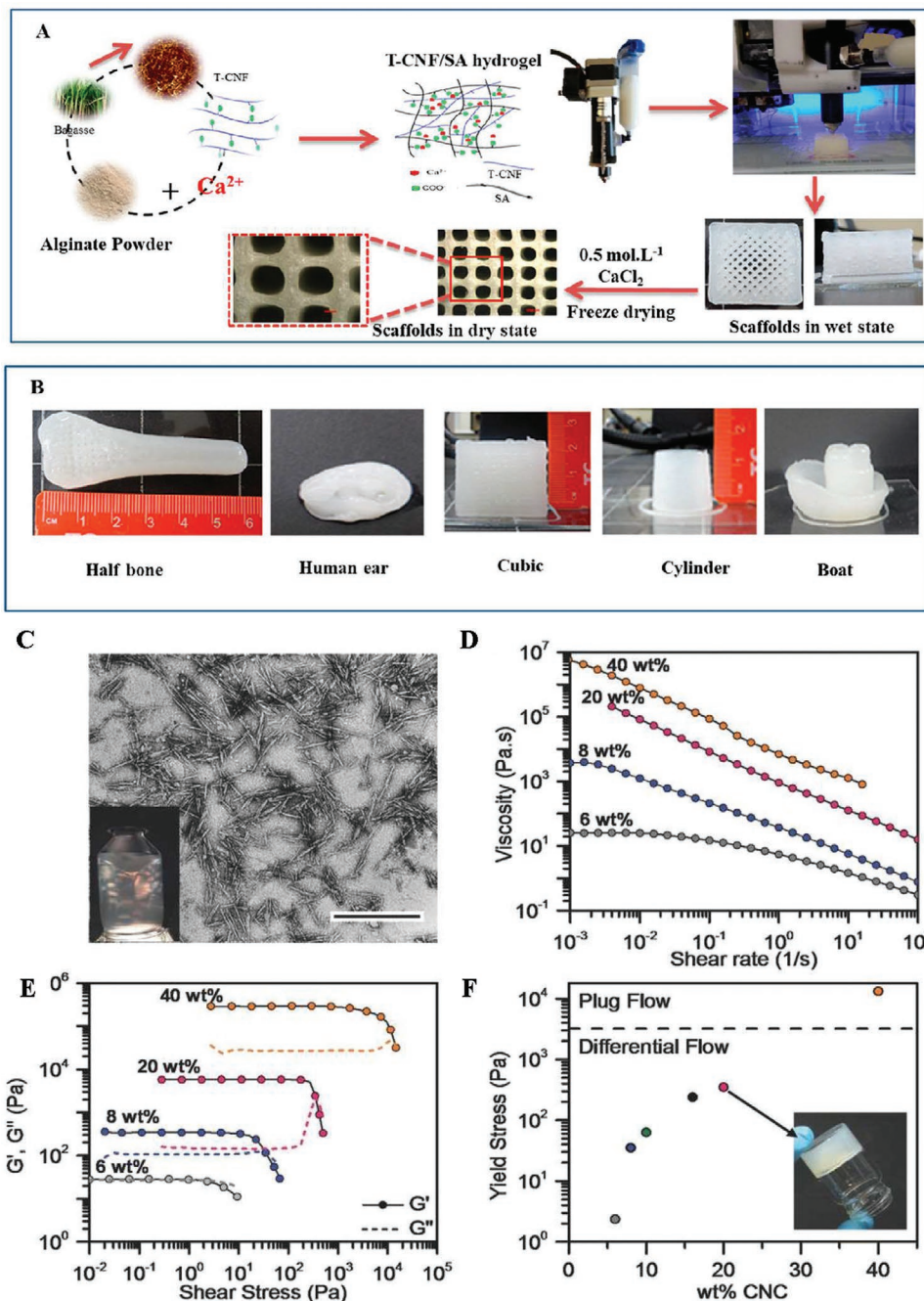


Figure 23. A) Fabrication process for 3D printing scaffolds using TEMPO CNF/alginate hydrogels. B) Scaffolds printed in diverse forms and designs from the optimum hydrogel formulation. Morphology of wood pulp CNFs and rheological behaviors of aqueous CNC inks of varying solid loading. A,B) Reproduced with permission.^[257] Copyright 2018, American Chemical Society. C) Transmission electron image of the anisotropic CNC particles (scale bar: 500 nm). Inset: Photograph of an aqueous dispersion of wood pulp CNFs (0.1 wt%) placed between cross-polarizers. D) Steady-shear and E) oscillatory rheological measurements (frequency = 1 Hz) for the aqueous CNC inks of increasing solid loading (6, 8, 20, and 40 wt% CNCs). F) Shear yield stress of these CNC inks (note: dotted lines in (F) denote the transition from differential to plug flow; inset: 20 wt% aqueous CNC ink in glass vial with 2.5 cm in diameter). C–F) Reproduced with permission.^[258] Copyright 2017, Wiley-VCH.

scaffolds were prepared by partial crosslinking of TEMPO CNFs/alginate hydrogels with Ca^{2+} ions while maintaining the shape, fidelity and preventing the collapse of the filaments (Figure 23A,B).^[257] Ca^{2+} ions were employed immediately after printing to crosslink the scaffolds to provide the sufficient

rigidity of the hydrogels and to assure long-term stability. The viscosity recovery measurement showed that the viscosity recovery for pure alginate hydrogels was only 16% of the initial value and the TEMPO-CNFs/alginate hydrogels showed 66% viscosity recovery. Moreover, the composite hydrogels were

Table 8. Preparation and properties of antimicrobial biomaterials based on ionic nanocellulose with inorganic antimicrobial agents.

Inorganic NPs	Size	Reducing agent	Nanocellulose	Ref.
AgNPs	12 nm	Formaldehyde	TEMPO-oxidized CNFs	[263]
AgNPs	15–20 nm	Pyrrrole	TEMPO-oxidized CNFs	[264]
AgNPs	25 nm	Glucose	Sulfuric acid hydrolyzed CNCs	[265]
AgNPs	–	DMSO	1,4-Diaminobutane-modified BC	[266]
AgNPs	10–90 nm	Dopamine	Dopamine-TCNFs	[267]
Ag NPs/dendritic particles	1–10 nm	CNCs	Sulfuric acid hydrolyzed CNCs	[268]
AgNPs	6 nm	Dopamine	Polydopamine-coated CNCs	[269]
AgNPs	6 nm	NaBH ₄	TEMPO-oxidized CNFs	[270]
AgNPs	15 nm	NaBH ₄	TEMPO-oxidized CNCs	[271]
AgNPs	20–45 nm	Aldehyde groups of CNCs	Periodic-oxidized CNCs	[272]
ZnO–AgNPs	9–35 nm	–	Sulfuric acid hydrolyzed CNCs	[271]

much stronger and harder against potential collapse compared with alginate scaffolds.

Because of the inherently entangled state of concentrated CNFs suspensions, the commonly used concentration of CNFs for hydrogel-based inks is 0.8–2.5 wt%.^[258,259] Thickening agents, such as fumed silica,^[260] laponite,^[261] or high molecular weight polymers,^[262] have been employed to achieve the desired rheological properties for 3D printing. By contrast, CNCs may offer advantages over CNFs since higher solid loading can be achieved at a given viscosity and storage modulus due to the absence of physical entanglements. Siqueira et al. used aqueous CNC inks (20 wt%) to print 3D cellular architectures (Figure 23C).^[258] Figure 23D reveals that inks composed of 8 wt% or higher undergo pronounced shear thinning behaviors. The 20 wt% CNC ink exhibits a plateau value of $G' \approx 5.75 \times 10^3$ Pa that exceeds G'' by about one order of magnitude at low shear stress (Figure 23E) and well-defined dynamic yield stress (τ_y) of 349 Pa, as shown by the crossover point between the storage and loss moduli measured under oscillatory conditions at the frequency of 1 Hz (Figure 23F). Such CNC inks can yield structures with a high degree of alignment and improved mechanical property along the printing direction.

4.2.6. Antimicrobial Materials

Nanocellulose-based antimicrobial biomaterials are generally achieved by the conjunction of antimicrobial agents and nanocellulose using physical or chemical approaches. According to the various types of antimicrobial agents, nanocellulose-based antimicrobial biomaterials can be divided in two parts as nanomaterials with incorporated inorganic and organic antimicrobial agents. Table 8 summarizes the antimicrobial biomaterials based on ionic nanocellulose with inorganic antimicrobial agents. Inorganic NPs, such as noble metal NPs (Au and Ag) and metal oxide NPs (TiO₂, CuO, ZnO, and MgO) are widely used in nanocellulose-based antimicrobial materials. They can be released from the composites and contact with bacteria. They can be synthesized via chemical reduction of metal ions in situ on the ionic nanocellulose, which immobilize the metal ions by electrostatic adsorption. Resulting nanocomposites generally

showed excellent antibacterial efficacy against common bacteria, such as *E. coli* and *S. aureus*.

In addition to inorganic NPs, the antimicrobial properties of nanocellulose also can be realized by modifying with organic antibiotics. The most frequently used antibiotics are shown in Figure 24. All three groups of nanocellulose have been employed to undergo the functionalization with antibiotics. In order to control the release rate and acquire better antibacterial effect, clathration is an effective method for the preparation of antibiotic nanocellulose-based materials. CNFs with absorbed titania NPs and different types of loaded antibiotic compounds (tetracycline, phosphomycin, diclofenac sodium, and penicillamine-D) were successfully prepared by Galkina et al., which showed antibacterial activity against *S. aureus* and *E. coli*.^[273] CNFs functionalized with β -cyclodextrin (β -CD) by using succinic acid and fumaric acid as bridging agents were also used to load and release antibacterial molecules (Danofloxacin) for long periods of time.^[238]

In addition to the modification with inorganic NPs and organic antibiotics, nanocellulose with aldehyde groups and quaternary ammonium also exhibits antimicrobial properties. After the sodium periodate oxidation of TEMPO-CNFs, 2,3-dialdehyde CNFs (DACNF) was obtained and found to show antimicrobial activity against both *S. aureus* and multi-drug-resistant *S. aureus* (MRSA), which increased with higher aldehyde contents.^[275] Other antibacterial nanocellulose was developed by grafting quaternary ammonium compounds onto nanocellulose surface. For instance, cationic porphyrin (CP) was appended onto CNCs via Cu(I)-catalyzed Huisgen–Medal–Sharpless 1,3-dipolar cycloaddition between azide groups on CNCs and porphyrinic alkynes.^[222,276] Resulting cationic nanocellulose showed excellent efficacy toward the photodynamic inactivation of *M. smegmatis* and *S. aureus*. In another study, Bespolova et al. employed chloroacetylation and subsequent reaction with tertiary amines to produce quaternary ammonium modified CNCs.^[277] It was found that modified CNCs with alkyl chains longer than ten carbons were effective antimicrobial agents against *S. aureus* and *E. coli*. Pure CNCs and quaternary ammonium modified CNCs with alkyl chain length of ten or less were not able to inhibit bacteria growth. Moreover, Fu and co-workers transferred the tertiary amines of

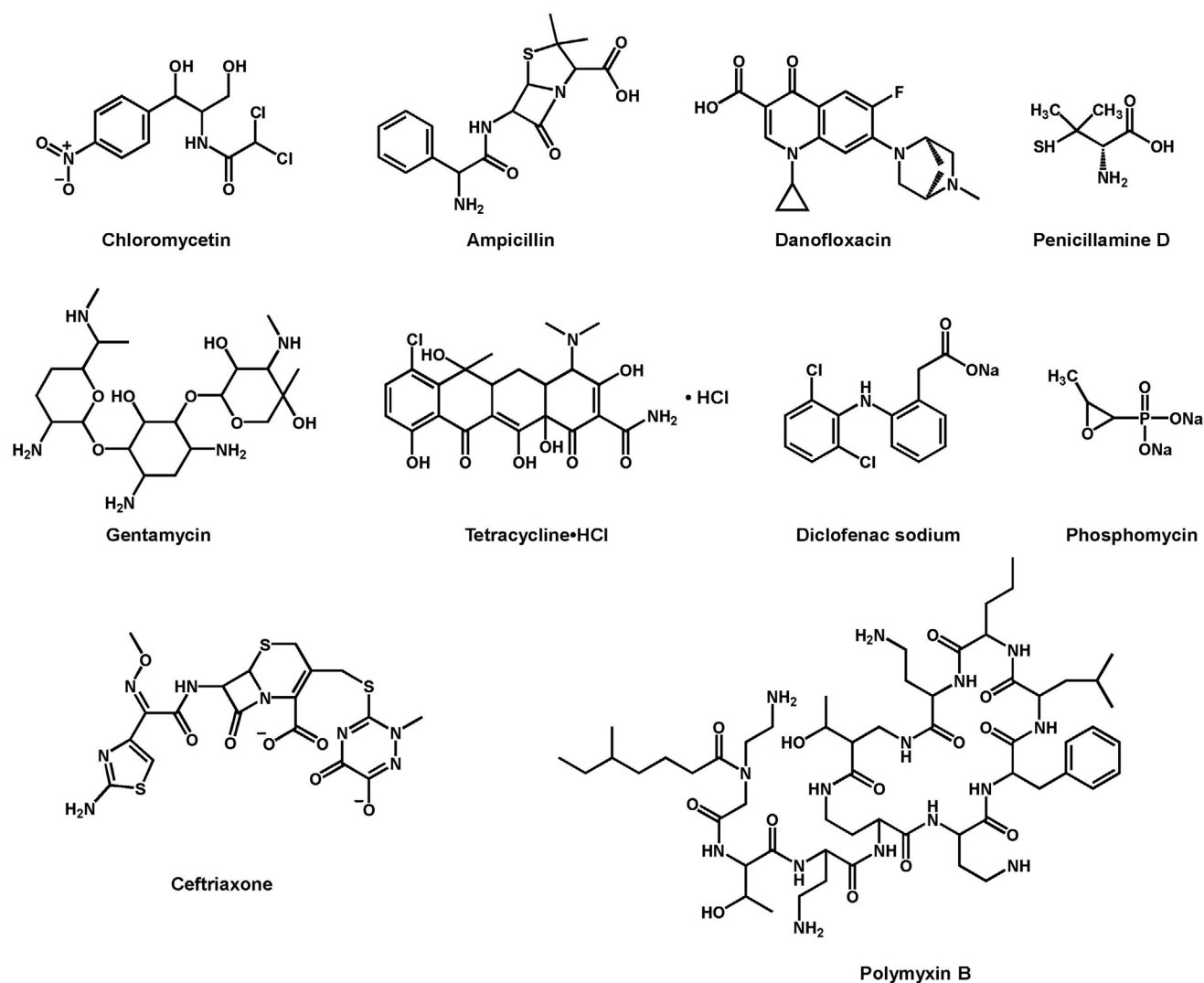


Figure 24. Organic antibiotics widely used in nanocellulose-based antimicrobial materials. Reproduced with permission.^[274] Copyright 2018, Wiley-VCH.

CNC-g-PDMAEMA into quaternary ammonium groups with three different alkyl bromides ($n = 10, 14,$ and 18).^[278] They found that the antibacterial activity depended on the length of alkyl chains of the quaternary ammonium groups and the hydrophobicity of the materials.

4.2.7. Tissue Engineering

Scaffolds, tissue cells and growth factors are dispensable factors for successful tissue engineering. To mimic the ECM of cartilage, scaffolds serve as substrates to interact with cells, support the newly formed tissues, supply nutrients and promote cell invasion. Polysaccharide-based biomaterials have been recognized as promising scaffold materials in recently years because of their low immunogenicity when implanted in vivo. They have showed promising results to process into complex 3D structures, such as artificial blood vessels/vascular grafts for bone and cartilage regeneration.^[279] BC- and CNF-based hydrogels/sponges support the adhesion and proliferation of human

liver cells (HepG2 and Hepa RG),^[280] human pluripotent stem cells (hPSCs),^[281] mouse fibroblasts (NIH-3T3),^[282] and so on.^[283]

Recently, Walther et al. demonstrated significant progress in two complementary directions.^[284] First, they introduced a simple and straightforward way to make complex hydrogels with mathematically defined pore geometries via a simple reverse templating approach and showcased the applicability of this methodology to fabricate gyroidal hydrogel scaffolds using TEMPO-CNFs and surface-deacetylated cationic chitin nanofibrils (Figure 25A,C). The pore size in the hydrogel is sufficient to allow nutrient diffusion and potentially also intercellular communication within the matrix. Supercritical drying is not mandatory to transfer the scaffolds into a new medium as they readily recover their shapes after air drying and re-exposure to water (Figure 25A,B,D). Second, they established important differences in terms of cell attachment of HSMCs on the surfaces of chitin nanofibrils versus cellulose nanofibrils (Figure 25E–P).

The mimicry of the anisotropic structure that characterizes tissues such as cartilage, tendons, or ligaments is extremely

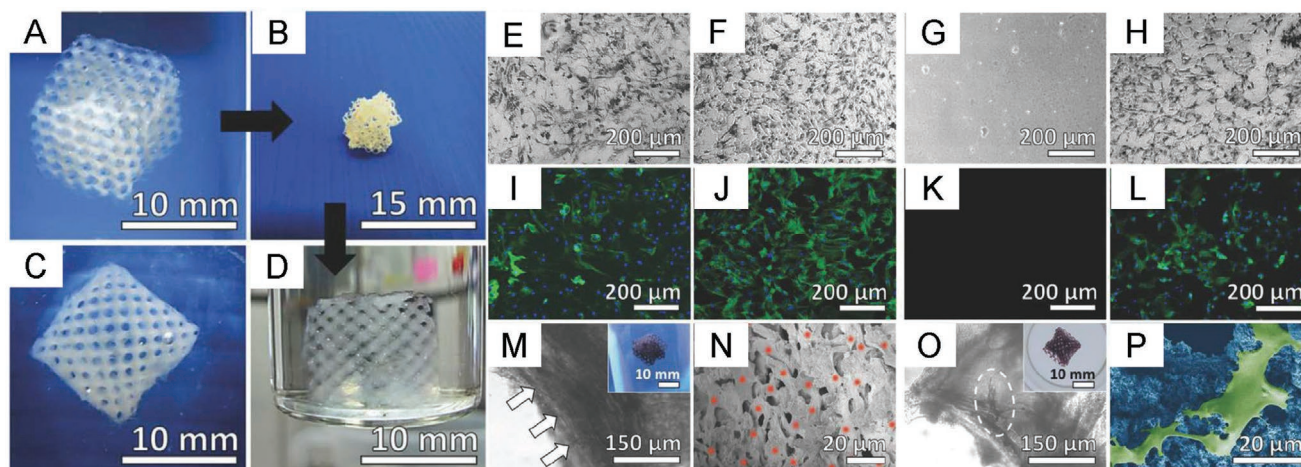


Figure 25. A,B,D) Shape recovery behavior of a CNF scaffold. A,C) Photographs of CNFs and chitin nanofibril scaffolds with 10 mm edge length. E–H) Bright-field microscopy after ALP live staining and I–L) fluorescence microscopy after staining the actin filaments with Alexa Fluor 488 Phalloidin (green) and nuclei with DAPI (blue) of: E,I) CNF films, F,J) CNF–Gel–CaPO₄ films, G,K) chitin film, and H,L) chitin–Gel–CaPO₄ films. M,O) Bright-field microscopy after ALP live staining of CNF–Gel–CaPO₄ and chitin–Gel–CaPO₄ scaffolds after sectioning to 1 mm thickness (the insets show the homogeneous ALP live stain in the scaffolds; scale bars 10 mm). N,P) SEM images of a confluent cell layer in a CNF–Gel–CaPO₄ scaffold and well-adherent HSMCs on a less densely populated area of the chitin–Gel–CaPO₄ scaffold. A–P) Reproduced with permission.^[284] Copyright 2015, Wiley-VCH.

important because their ordered ECM architecture and cellular organization play an essential role in the biomechanical and biological functions of these tissues.^[285,286] Recently, CNCs have been receiving more and more attention as reinforcing nanofillers in aligned scaffolds for tissue engineering to enhance the strength and to introduce high surface areas, tunable surface chemistry, and a hydrophilic interface for controlling interactions with the gel environment. Gomes and co-workers used sulfated CNCs as reinforcing nanofillers in aligned electrospun scaffolds for tendon tissues based on poly- ϵ -caprolactone (PCL)/chitosan matrix.^[287] The incorporation of small amount of CNCs (up to 3 wt%) into tendon mimetic nanofiber bundles showed a remarkable toughening effect ($85\% \pm 5\%$, $p < 0.0002$) and raised the mechanical properties of scaffolds to the relevant range as tendon/ligament ($\sigma = 39.3 \pm 1.9$ MPa and $E = 540.5 \pm 83.7$ MPa, $\rho < 0.0001$). Aligned PCL/chitosan/CNC nanocomposite scaffolds not only meet the mechanical requirements for tendon tissue engineering application, but also provide tendon mimetic ECM topographic cues, which is a key feature for maintaining tendon cell's morphology and behaviors. Furthermore, due to their highly crystalline structure, CNCs have both a negative diamagnetic anisotropy and a giant dipole moment, making them susceptible to alignment in electromagnetic fields. Based on this feature, Gomes and co-workers developed a gelatin-based multiphasic hydrogel system.^[285] In each phase, hydroxyapatite particles or CNCs were incorporated into enzymatically crosslinked gelatin networks to mimic bone or tendon tissues, respectively. Stiffer hydrogels were produced with the incorporation of mineralized particles, and magnetically aligned CNCs resulted in anisotropic structure. The evaluation of the biological commitment with human adipose-derived stem cells toward the tendon-to-bone interface revealed an aligned cell growth and higher synthesis and deposition of tenascin in the anisotropic phase (Figure 26), while the activity of the secreted alkaline phosphatase and the expression of osteopontin were induced in the mineralized phase.^[285] Hoare

and co-workers demonstrated an injectable nanocomposite hydrogel with tunable nanoscale anisotropy facilitated by the application of an external magnetic field.^[288] CNCs were shown to align in situ on the order of minutes within a rapidly gelling poly(oligoethylene glycol methacrylate) (POEGMA) hydrogel matrix. The hydrogel containing CNCs exhibit higher swelling, lower shear moduli and higher compressive moduli relative to isotropic CNC-POEGMA hydrogels. Furthermore, the alignment of CNCs leads to a significant improvement in myotube orientation both on 2D and within 3D of the hydrogels, which can be applied for engineering orientated tissues.

4.2.8. Other Biomedical Applications

Immobilization and Recognition of Enzymes/Proteins: To overcome the problem of instability and rapid loss of catalytic and biological activity of enzymes and proteins, the immobilization of enzymes/proteins on carriers has been considered as a powerful technique in diverse fields ranging from food technology to biomedical and biosensor engineering. An ideal carrier material for the immobilization of enzymes/proteins should be biocompatible without compromising the protein structure and biological activities.^[47] Furthermore, such carriers should be easily processed to enhance the loading capacity of enzymes/proteins as well as their stability in both operation and storage. A key point in enzyme/protein immobilization is the selection of immobilization method, such as adsorption, entrapment, or covalent binding on carrier materials. Available hydroxyl groups and possible negative charges on the surface of nanocellulose provide the possibility of enzyme/protein immobilization. The methods for enzyme/protein immobilization onto nanocellulose surfaces can be broadly divided into three main routes: a) physical interactions between the protein and nanocellulose; b) affinity interactions between the protein and ligand; and c) covalent interactions.^[289] Covalent immobilization of

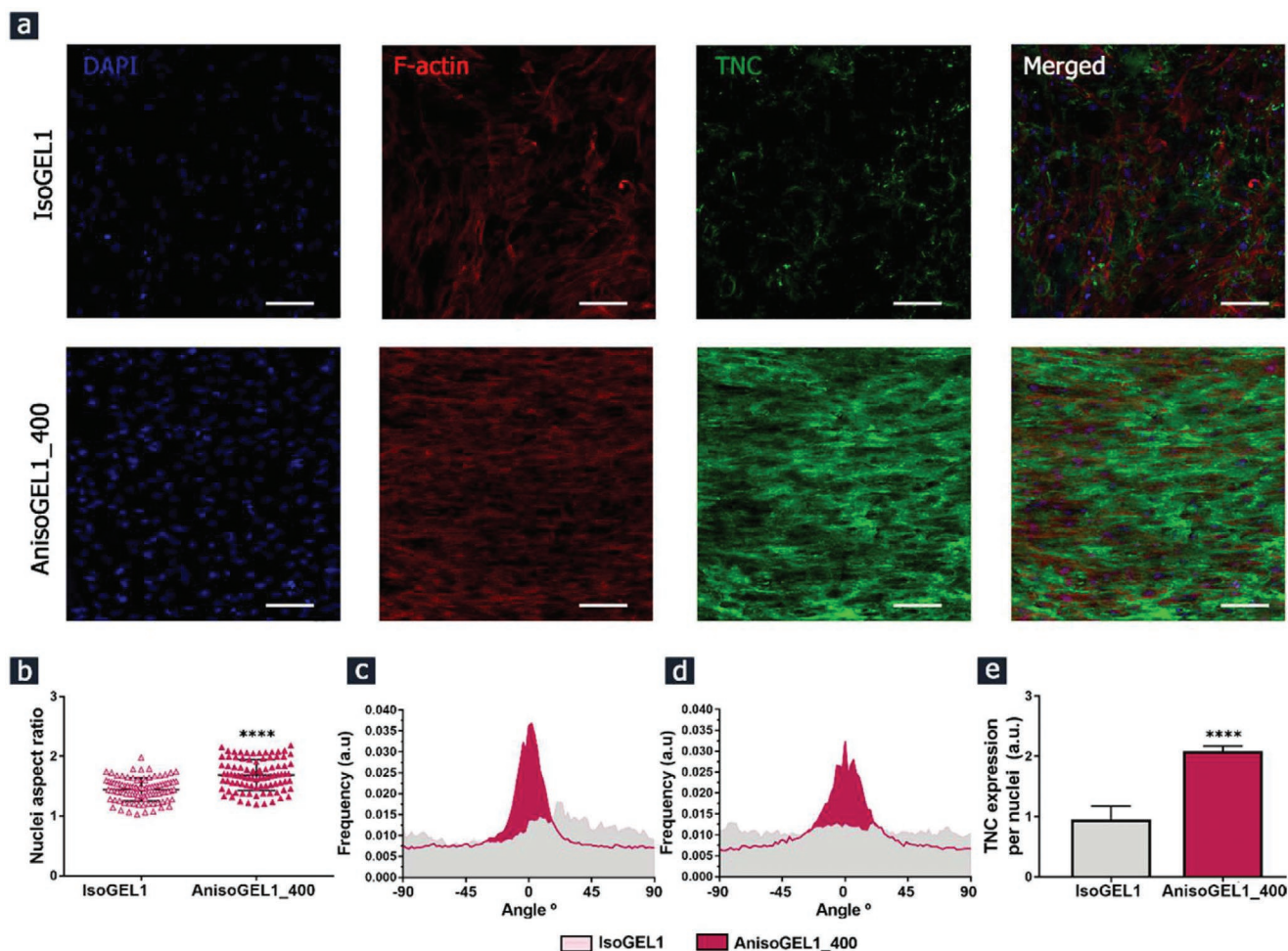


Figure 26. Biological characterization of the nanocomposite 3D hydrogels using encapsulated hASCs after 21 days of culture. a) Confocal images of immunolabeled samples against TNC (green), cell nuclei (blue), and cytoskeleton (scale bars = 200 μm). b) Nuclei aspect ratios of cells cultured in isotropic and anisotropic (400 mT) hydrogels reinforced with 1% (w/v) CNCs. Evaluation of cytoskeleton c) and the TNC deposition d) directionality by the encapsulated cells. e) Quantification of tendon-related marker TNC expression normalized with nuclei area. Statistical significance: **** $p < 0.0001$. a–e) Reproduced with permission.^[285] Copyright 2019, American Chemical Society.

enzyme/protein on nanocellulose can provide significant high loading capacity and excellent stability, but often requiring complicated chemistry procedure. Physical approach is simple, cheap and allows better preservation of the original structure of enzymes/proteins, but with limited loading capacity and efficiency of immobilization.^[47]

Conjugation of CNCs with nanomaterials has provides excellent hybrid supports for enzymes. AuNPs can for example be readily functionalized with thiolated molecules containing further carboxyl groups, which in turn can be conjugated with amine groups of proteins/enzymes. The CNCs/AuNPs as a catalytic platform exhibited significant biocatalytic activity and preservation of original activity with excellent stability and recovered specific activity (70–95%) for CGTase and alcohol oxidase.^[290] Furthermore, magnetic CNCs (containing Fe₃O₄ NPs) functionalized with AuNPs were used as a magnetic support for the covalent conjugation of papain and facilitated recovery of this immobilized enzyme.^[291] The conjugated materials retained high enzymatic activity, good stability and reusability.

Biomedical applications often require controlled immobilization of recognition molecules on the substrate and antifouling properties, mainly to lower nonspecific adsorption of biomolecules and to minimize interference. A promising method to control specific and nonspecific adsorption involves the installation of multifunctional polymers incorporating surface-binding and surface-passivating domains.^[292] Vuoriluoto et al. passivated TEMPO-CNFs toward human immunoglobulin G (hIgG) after the modification with block and random copolymers of PDMAEMA and POEGMA.^[293] Compared to common commercial blocking agents, copolymers with short PDMAEMA segments and large POEGMA blocks were found to be very effective in preventing nonspecific human immunoglobulin G (hIgG) binding.

Fluorescent Labeling: By means of introducing fluorescent molecules on the surface, nanocellulose can be converted to fluorescent nanomaterials with labeling ability. It is expected that the fluorescent modification on nanocellulose enables the potential use in biomedical fields, such as optical bioimaging, biosensors, and photodynamic therapy. Moreover, fluorescent

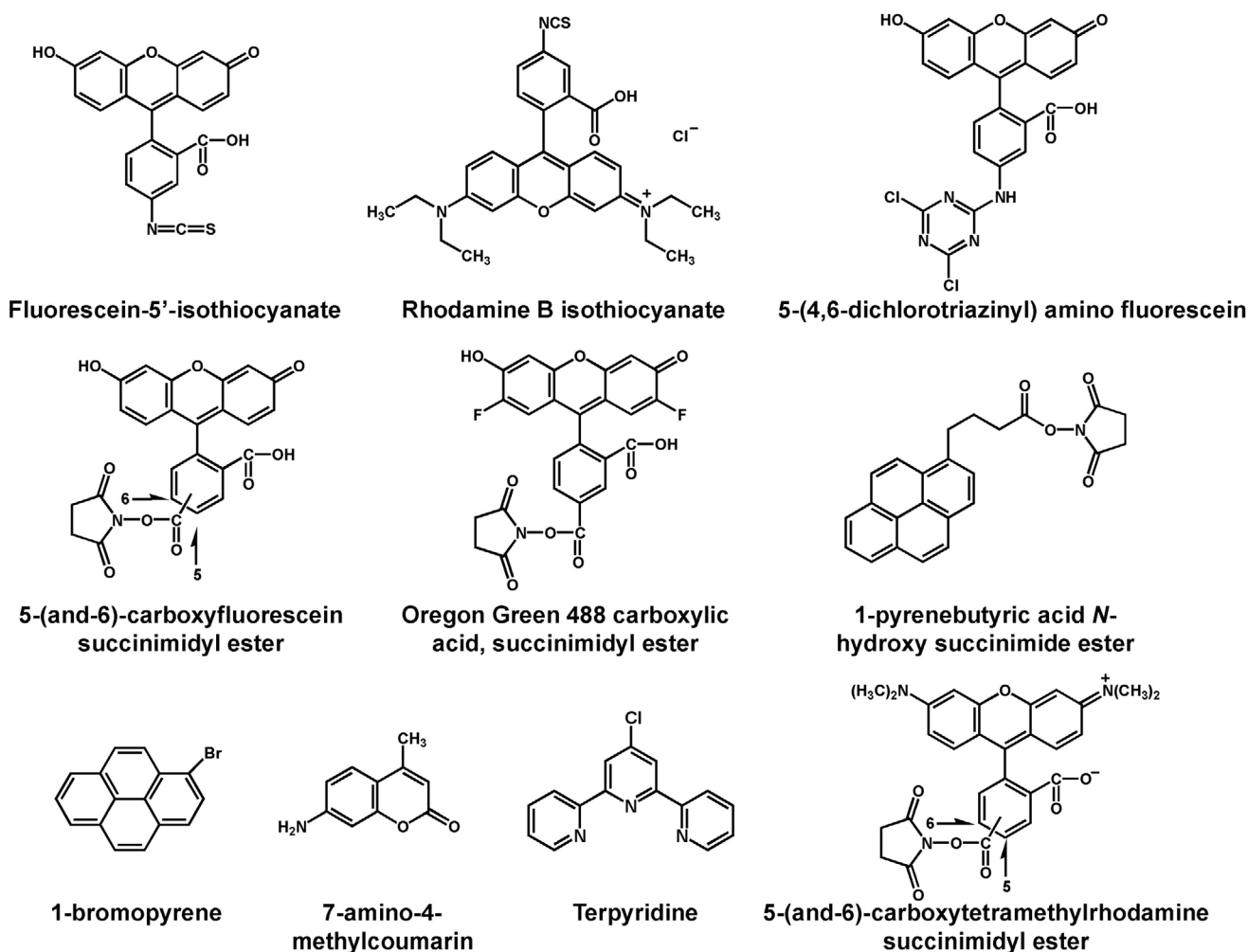


Figure 27. Chemical structure of fluorescent labeling molecules grafted on CNCs. Reproduced with permission.^[47] Copyright 2014, Elsevier.

labeled nanocellulose is easier to be traced and evaluated for toxicity and bioactivity in materials. Since the first report of fluorescent labeling on CNCs with fluorescein-5'-isothiocyanate (FITC) molecule,^[294] diverse fluorescent molecules have been covalently attached on the surface of CNCs, including Rhodamine B isothiocyanate,^[231,295] pyrene dyes,^[296] terpyridine, and its derivatives,^[297] 1-pyrenebutyric acid N-hydroxy succinimide ester,^[298] 5-(and-6)-carboxyfluorescein succinimidyl ester, succinimidyl ester,^[299] 5-(4,6-dichlorotriazinyl) amino-fluorescein,^[300] and 7-amino(hydrazine/mercapto)-4-methylcoumarin.^[301] **Figure 27** summarizes the chemical structures of a few typical fluorescent molecules that have been grafted on CNCs.

5. Conclusion and Future Perspectives

Our aim here was to describe the current state of research to provide some hints for future development of ionic cellulose-based compounds, including polymeric cellulose derivatives and surface-functionalized nanocellulose for application as biomaterials. As shown herein, ionic cellulose-based compounds

possess remarkable features that can surpass those of synthetic polymer-based materials, including lower cost, highly controllable composition and properties as well as excellent biocompatibility and biodegradability by far. The past two decades have witnessed significant progress in the development of ionic cellulose materials and their great potential for biomedical applications as wound dressings, drug delivery and diagnostic devices, implant materials and tissue engineering.

The working mechanisms of these compounds are not always clear regarding the precise interaction of the ionic moieties with the targets, e.g., proteins, cells and tissues, though there are more and more studies shedding a light on the interaction of ionic cellulose compounds with biological matter. Indeed, the chemical composition, surface chemistry, polymeric or even nanoscaled architecture of these cellulose-based materials significantly influences behavior of cells and tissues *in vitro* and *in vivo*. In addition, in contrast to other nanoparticulate systems like carbon nanotubes, ionic nanocellulose materials are not inherently dangerous, though more *in vitro* and *in vivo* studies are still required to evaluate any potential pharmaceutical side effects and cytotoxicity of these promising biomaterials. Consequently, more systematic studies on relationship between

chemical compositions and structures of these compounds with biological entities like proteins and cells are required, in order to tailor the bioactivity of ionic cellulose derivatives and nanocellulose and to achieve desired functionalities for biomedical applications.

Although ionic cellulose derivatives and nanocellulose are known as biocompatible and nontoxic and hence useful for many biomedical applications, materials like cellulose sulfate with extraordinary bioactivity, still have seldom been investigated in clinical studies. This should be overcome to realize their immense potential for medical applications.

Thus, despite the significant developments in the area of ionic cellulose-based materials that are of great biomedical interest, this field is still in its infancy regarding their application as medically and clinically acceptable products. We believe that cellulose and their ionic derivatives will attract and still need more exploration to realize their potential as biomaterials and to open further avenues to apply them in medical diagnostics and care.

Acknowledgements

Y.Y., Y.-T.L., and K.Z. contributed equally to this work. Thomas Groth and Kai Zhang thank Deutsche Forschungsgemeinschaft for the financial support for the project under Grant Nos. GR1290/12-1 and ZH546/3-1, respectively. Kui Zeng thanks China Scholarship Council and Yi-Tung Lu the International Graduate School AGRIPOLY supported by the European Regional Development Fund (ERDF) and the Federal State Saxony-Anhalt for the financial support of their PhD grants.

Conflict of Interest

The authors declare no conflict of interest.

Keywords

biomaterials, cellulose, ionic, nanocellulose

Received: January 31, 2020

Revised: February 25, 2020

Published online:

- [1] R. J. Moon, A. Martini, J. Nairn, J. Simonsen, J. Youngblood, *Chem. Soc. Rev.* **2011**, *40*, 3941.
- [2] a) H. L. Zhu, W. Luo, P. N. Ciesielski, Z. Q. Fang, J. Y. Zhu, G. Henriksson, M. E. Himmel, L. B. Hu, *Chem. Rev.* **2016**, *116*, 9305; b) Z. Gui, H. L. Zhu, E. Gillette, X. G. Han, G. W. Rubloff, L. B. Hu, S. B. Lee, *ACS Nano* **2013**, *7*, 6037.
- [3] P. Fagette, *ASAIO J.* **1999**, *45*, 238.
- [4] D. Lavanya, P. Kulkarni, M. Dixit, P. K. Raavi, L. N. V. Krishna, *Int. J. Drug Formulation Res.* **2011**, *2*, 2.
- [5] A. Mahiout, H. Meinhold, M. Kessel, H. Schulze, U. Baurmeister, *Artif. Organs* **1987**, *11*, 149.
- [6] A. Varki, *Glycobiology* **2017**, *27*, 3.
- [7] N. Volpi, *Molecules* **2019**, *24*, 1447.
- [8] B. Lepenies, J. A. Yin, P. H. Seeberger, *Curr. Opin. Chem. Biol.* **2010**, *14*, 404.
- [9] A. Varki, *Nature* **2007**, *446*, 1023.

- [10] R. Malhotra, *Biochem. Anal. Biochem* **2012**, *1*, 1000108.
- [11] A. Kowitsch, G. Y. Zhou, T. Groth, *J. Tissue Eng. Regener. Med.* **2018**, *12*, e23.
- [12] K. Gulati, K. M. Poluri, *Glycoconjugate J.* **2016**, *33*, 1.
- [13] a) J. Schlessinger, A. N. Plotnikov, O. A. Ibrahim, A. V. Eliseenkova, B. K. Yeh, A. Yayon, R. J. Linhardt, M. Mohammadi, *Mol. Cell* **2000**, *6*, 743; b) R. A. A. Smith, S. Murali, B. N. Rai, X. H. Lu, Z. X. H. Lim, J. J. L. Lee, V. Nurcombe, S. M. Cool, *Biomaterials* **2018**, *184*, 41; c) J. Spratte, M. Schonborn, N. Treder, F. Bornkessel, M. Zygmunt, H. Fluhr, *Fertil. Steril.* **2015**, *103*, 1363; d) A. E. I. Proudfoot, T. M. Handel, Z. Johnson, E. K. Lau, P. LiWang, I. Clark-Lewis, F. Borlat, T. N. C. Wells, M. H. Kosco-Vilbois, *Proc. Natl. Acad. Sci. USA* **2003**, *100*, 1885; e) A. E. I. Proudfoot, S. Fritchley, F. Borlat, J. P. Shaw, F. Vilbois, C. Zwahlen, A. Trkola, D. Marchant, P. R. Clapham, T. N. C. Wells, *J. Biol. Chem.* **2001**, *276*, 10620; f) B. A. Dalton, C. D. Mcfarland, P. A. Underwood, J. G. Steele, *J. Cell Sci.* **1995**, *108*, 2083; g) A. D. Gibson, J. A. Lamerdin, P. Zhuang, K. Baburaj, E. H. Serpersu, C. B. Peterson, *J. Biol. Chem.* **1999**, *274*, 6432; h) K. Kouzi-Koliakos, G. Koliakos, E. Tsilibary, L. T. Furcht, A. Charonis, *J. Biol. Chem.* **1989**, *264*, 17971.
- [14] a) D. Aviezer, A. Yayon, *Proc. Natl. Acad. Sci. USA* **1994**, *91*, 12173; b) S. Salek-Ardakani, J. R. Arrand, D. Shaw, *Blood* **2000**, *96*, 1879.
- [15] R. Garcia-Olivas, J. Hoebeke, S. Castel, M. Reina, G. Fager, F. Lustig, *Histochem. Cell Biol.* **2003**, *120*, 371.
- [16] S. S. Deepa, Y. Umehara, S. Higashiyama, N. Itoh, K. Sugahara, *J. Biol. Chem.* **2002**, *277*, 43707.
- [17] T. M. Handel, Z. Johnson, S. E. Crown, E. K. Lau, M. Sweeney, A. E. Proudfoot, *Annu. Rev. Biochem.* **2005**, *74*, 385.
- [18] A. Hienola, S. Tumova, E. Kuleskiy, H. Rauvala, *J. Cell Biol.* **2006**, *174*, 569.
- [19] a) R. Y. Xu, A. Ori, T. R. Rudd, K. A. Uniewicz, Y. A. Ahmed, S. E. Guimond, M. A. Skidmore, G. Siligardi, E. A. Yates, D. G. Fernig, *J. Biol. Chem.* **2012**, *287*, 40061; b) M. Teran, M. A. Nugent, *J. Biol. Chem.* **2015**, *290*, 16451; c) X. Y. Jiao, P. C. Billings, M. P. O'Connell, F. S. Kaplan, E. M. Shore, D. L. Glaser, *J. Biol. Chem.* **2007**, *282*, 1080; d) M. Gotte, *FASEB J.* **2003**, *17*, 575; e) D. P. Dyer, E. Migliorini, C. L. Salanga, D. Thakar, T. M. Handel, R. P. Richter, *Open Biol.* **2017**, *7*, 160286; f) C. E. WilkinsPort, P. J. McKeownLongo, *Biochem. Cell Biol.* **1996**, *74*, 887; g) A. Utani, M. Nomizu, H. Matsuura, K. Kato, T. Kobayashi, U. Takeda, S. Aota, P. K. Nielsen, H. Shinkai, *J. Biol. Chem.* **2001**, *276*, 28779.
- [20] a) S. F. Penc, B. Pomahac, T. Winkler, R. A. Dorschner, E. Eriksson, M. Herndon, R. L. Gallo, *J. Biol. Chem.* **1998**, *273*, 28116; b) K. R. Taylor, J. A. Rudisill, R. L. Gallo, *J. Biol. Chem.* **2005**, *280*, 5300; c) G. S. V. Kuscher, F. Coulin, C. A. Power, A. E. I. Proudfoot, R. E. Hubbard, A. J. Hoogewerf, T. N. C. Wells, *Biochemistry* **1999**, *38*, 12959.
- [21] a) C. I. Gama, S. E. Tully, N. Sotogaku, P. M. Clark, M. Rawat, N. Vaidehi, W. A. Goddard, A. Nishi, L. C. Hsieh-Wilson, *Nat. Chem. Biol.* **2006**, *2*, 467; b) L. Djerbal, H. Lortat-Jacob, J. C. F. Kwok, *Glycoconjugate J.* **2017**, *34*, 363; c) T. Miyazaki, S. Miyauchi, A. Tawada, T. Anada, S. Matsuzaka, O. Suzuki, *J. Cell. Physiol.* **2008**, *217*, 769; d) C. J. Rogers, P. M. Clark, S. E. Tully, R. Abrol, K. C. Garcia, W. A. Goddard, L. C. Hsieh-Wilson, *Proc. Natl. Acad. Sci. USA* **2011**, *108*, 9747; e) K. Takagaki, H. Munakata, I. Kakizaki, M. Iwafune, T. Itabashi, M. Endo, *J. Biol. Chem.* **2002**, *277*, 8882.
- [22] A. Weyers, B. Yang, K. Solakyildirim, V. Yee, L. Y. Li, F. M. Zhang, R. J. Linhardt, *FEBS J.* **2013**, *280*, 2285.
- [23] S. M. Ruppert, T. R. Hawn, A. Arrigoni, T. N. Wight, P. L. Bollyky, *Immunol. Res.* **2014**, *58*, 186.
- [24] a) M. Kisiel, M. M. Martino, M. Ventura, J. A. Hubbard, J. Hilborn, D. A. Ossipov, *Biomaterials* **2013**, *34*, 704; b) A. Washio,

- C. Kitamura, E. Jimi, M. Terashita, T. Nishihara, *Exp. Cell Res.* **2009**, 375, 3036.
- [25] I. Capila, R. J. Linhardt, *Angew. Chem., Int. Ed.* **2002**, 41, 390.
- [26] N. S. Gandhi, R. L. Mancera, *Chem. Biol. Drug Des.* **2008**, 72, 455.
- [27] S. Thompson, B. Martinez-Burgo, K. M. Sepuru, K. Rajarathnam, J. A. Kirby, N. S. Sheerin, S. Ali, *Int. J. Mol. Sci.* **2017**, 18, 1692.
- [28] M. R. Morgan, M. J. Humphries, M. D. Bass, *Nat. Rev. Mol. Cell Biol.* **2007**, 8, 957.
- [29] In *Progress in Molecular Biology and Translational Science*, Vol. 93 (Eds: L. J. Zhang), Elsevier, London, UK **2010**, pp. 1–510.
- [30] J. D. Esko, R. J. Linhardt, in *Essentials of Glycobiology*, 2nd ed. (Eds: A. Varki, R. D. Cummings, J. D. Esko, H. H. Freeze, P. Stanley, C. R. Bertozzi, G. W. Hart, M. E. Etzler) Cold Spring Harbor Laboratory Press, Cold Spring Harbor, NY, USA **2009**.
- [31] R. J. Linhardt, R. E. Hileman, *Gen. Pharmacol.: Vasc. Syst.* **1995**, 26, 443.
- [32] E. L. Shipp, L. C. Hsieh-Wilson, *Chem. Biol.* **2007**, 14, 195.
- [33] D. S. da Costa, R. L. Reis, I. Pashkuleva, *Annu. Rev. Biomed. Eng.* **2017**, 19, 1.
- [34] a) M. Hricovini, M. Guerrini, A. Bisio, G. Torri, A. Naggi, B. Casu, *Semin. Thromb. Hemost.* **2002**, 28, 325; b) A. Zamfir, D. G. Seidler, H. Kresse, J. Peter-Katalinic, *Glycobiology* **2003**, 13, 733.
- [35] D. Hachim, T. E. Whittaker, H. Kim, M. M. Stevens, *J. Controlled Release* **2019**, 313, 131.
- [36] J. Hirabayashi, T. Hashidate, Y. Arata, N. Nishi, T. Nakamura, M. Hirashima, T. Urashima, T. Oka, M. Futai, W. E. G. Muller, F. Yagi, K. Kasai, *Biochim. Biophys. Acta, Gen. Subj.* **2002**, 1572, 232.
- [37] T. Miller, M. C. Goude, T. C. McDevitt, J. S. Temenoff, *Acta Biomater.* **2014**, 10, 1705.
- [38] V. González-Motos, K. A. Kropp, A. Viejo-Borbolla, *Cytokine Growth Factor Rev.* **2016**, 30, 71.
- [39] D. Vigetti, E. Karousou, M. Viola, S. Deleonibus, G. De Luca, A. Passi, *Biochim. Biophys. Acta, Gen. Subj.* **2014**, 1840, 2452.
- [40] a) A. C. Rapraeger, A. Krufka, B. B. Olwin, *Science* **1991**, 252, 1705; b) M. C. Kiefer, J. C. Stephans, K. Crawford, K. Okino, P. J. Barr, *Proc. Natl. Acad. Sci. USA* **1990**, 87, 6985; c) F. M. Zhang, J. S. McLellan, A. M. Ayala, D. J. Leahy, R. J. Linhardt, *Biochemistry* **2007**, 46, 3933; d) D. L. Rabenstein, *Nat. Prod. Rep.* **2002**, 19, 312; e) J. P. Hodde, S. F. Badylak, A. O. Brightman, S. L. Voytik-Harbin, *Tissue Eng.* **1996**, 2, 209.
- [41] a) G. Y. Zhou, M. S. Niepel, S. Saretia, T. Groth, *J. Biomed. Mater. Res., Part A* **2016**, 104, 493; b) G. Y. Zhou, H. Al-Khoury, T. Groth, *Int. J. Artif. Organs* **2016**, 39, 37.
- [42] Z. M. Wang, K. J. Xiao, L. Li, J. Y. Wu, *Cellulose* **2010**, 17, 953.
- [43] N. D. Christensen, C. A. Reed, T. D. Culp, P. L. Hermonat, M. K. Howett, R. A. Anderson, L. J. D. Zaneveld, *Antimicrob. Agents Chemother.* **2001**, 45, 3427.
- [44] N. L. V. Carreño, A. M. Barbosa, B. S. Noremborg, M. M. S. Salas, S. C. M. Fernandes, J. Labidi, in *Advances in Nanostructured Cellulose-Based Biomaterials, Springer Briefs in Applied Sciences and Technology*, Springer, Cham, Switzerland **2017**, pp. 1–32.
- [45] M. Roman, *Ind. Biotechnol.* **2015**, 11, 25.
- [46] a) S. J. Lee, C. Broda, A. Atala, J. J. Yoo, *Biomacromolecules* **2011**, 12, 306; b) L. Zhou, I. Pomerantseva, E. K. Bassett, C. M. Bowley, X. Zhao, D. A. Bichara, K. M. Kulig, J. P. Vacanti, M. A. Randolph, C. A. Sundback, *Tissue Eng., Part A* **2011**, 17, 1573; c) H. M. Avila, E. M. Feldmann, M. M. Pleumeeckers, L. Nimeskern, W. Kuo, W. C. de Jong, S. Schwarz, R. Muller, J. Hendriks, N. Rotter, G. J. V. M. van Osch, K. S. Stok, P. Gatenholm, *Biomaterials* **2015**, 44, 122.
- [47] N. Lin, A. Dufresne, *Eur. Polym. J.* **2014**, 59, 302.
- [48] M. Singh, A. R. Ray, P. Vasudevan, *Biomaterials* **1982**, 3, 16.
- [49] K. Hettrich, W. Wagenknecht, B. Volkert, S. Fischer, *Macromol. Symp.* **2008**, 262, 162.
- [50] D. Klemm, T. Heinze, A. Stein, T. Liebert, *Macromol. Symp.* **1995**, 99, 129.
- [51] B. Philipp, I. Nehls, W. Wagenknecht, M. Schnabelrauch, *Carbohydr. Res.* **1987**, 164, 107.
- [52] N. Bhatt, P. K. Gupta, S. Naithani, *J. Appl. Polym. Sci.* **2008**, 108, 2895.
- [53] L. Zhu, J. M. Qin, X. Q. Yin, L. Ji, Q. Lin, Z. Y. Qin, *Polym. Adv. Technol.* **2014**, 25, 168.
- [54] K. Zhang, D. Peschel, E. Brendler, T. Groth, S. Fischer, *Macromol. Symp.* **2009**, 280, 28.
- [55] K. Zhang, E. Brendler, S. Fischer, *Cellulose* **2010**, 17, 427.
- [56] S. C. Fox, B. Li, D. Q. Xu, K. J. Edgar, *Biomacromolecules* **2011**, 12, 1956.
- [57] B. Philipp, W. Wagenknecht, I. Nehls, D. Klemm, A. Stein, T. Heinze, *Polym. News* **1996**, 21, 155.
- [58] K. Zeng, T. Groth, K. Zhang, *ChemBioChem* **2019**, 20, 737.
- [59] W. Wagenknecht, I. Nehls, B. Philipp, *Carbohydr. Res.* **1992**, 237, 211.
- [60] a) C. L. Coulter, M. L. Greaves, *Science* **1970**, 169, 1097; b) F. H. Westheimer, *Science* **1987**, 235, 1173; c) L. D. Quin, in *A Guide to Organophosphorus Chemistry*, John Wiley & Sons, New York **2000**, pp. 1–387.
- [61] a) R. B. Stockbridge, R. Wolfenden, *J. Am. Chem. Soc.* **2009**, 131, 18248; b) K. Heller, P. Ochtrup, M. F. Albers, F. B. Zauner, A. Itzen, C. Hedberg, *Angew. Chem., Int. Ed.* **2015**, 54, 10467; *Angew. Chem., Int. Ed.* **2015**, 54, 10327.
- [62] R. W. Brauer, R. L. Pessotti, *Science* **1949**, 110, 395.
- [63] a) J. Lei, L. B. Su, K. Zeng, T. Q. Chen, R. H. Qiu, Y. B. Zhou, C. T. Au, S. F. Yin, *Chem. Eng. Sci.* **2017**, 171, 404; b) J. Yang, T. Q. Chen, L. B. Han, *J. Am. Chem. Soc.* **2015**, 137, 1782.
- [64] a) N. Illy, M. Fache, R. Menard, C. Negrell, S. Caillol, G. David, *Polym. Chem.* **2015**, 6, 6257; b) K. Zeng, L. Chen, B. Q. Xiong, Y. B. Zhou, C. T. Au, S. F. Yin, *Tetrahedron Lett.* **2016**, 57, 2222.
- [65] In *Phosphorus-Based Polymers: From Synthesis to Applications*, Vol. 11 (Eds: S. Monge, G. David), Royal Society of Chemistry, Cambridge, UK **2014**, pp. 1–294.
- [66] T. Heinze, T. Liebert, A. Koschella, *Esterification of Polysaccharides*, Springer Science & Business Media, New York **2006**, pp. 1–229.
- [67] J. D. Reid, L. W. Mazzeno, *Ind. Eng. Chem.* **1949**, 41, 2828.
- [68] A. Nuessle, F. Ford, W. Hall, A. Lippert, *Text. Res. J.* **1956**, 26, 32.
- [69] N. Inagaki, S. Nakamura, H. Asai, K. Katsuura, *J. Appl. Polym. Sci.* **1976**, 20, 2829.
- [70] O. Petreus, T. Bubulac, I. Petreus, G. Cazacu, *J. Appl. Polym. Sci.* **2003**, 90, 327.
- [71] P. L. Granja, L. Pouysegue, M. Petraud, B. De Jeso, C. Baquey, M. A. Barbosa, *J. Appl. Polym. Sci.* **2001**, 82, 3341.
- [72] D. M. Suflet, G. C. Chitanu, V. I. Popa, *React. Funct. Polym.* **2006**, 66, 1240.
- [73] N. Gospodinova, A. Grelard, M. Jeannin, G. C. Chitanu, A. Carpov, V. Thiery, T. Besson, *Green Chem.* **2002**, 4, 220.
- [74] J. H. Zhang, J. Q. Zhang, L. Lin, T. M. Chen, J. Zhang, S. J. Liu, Z. J. Li, P. K. Ouyang, *Molecules* **2009**, 14, 5027.
- [75] Y. H. P. Zhang, J. B. Cui, L. R. Lynd, L. R. Kuang, *Biomacromolecules* **2006**, 7, 644.
- [76] G. A. Towle, R. L. Whistler, in *General Carbohydrate Method*, Vol. VI (Eds: R. L. Whistler, J. N. BeMiller) Academic Press, New York **1972**, pp. 408–410.
- [77] W. D. Wanrosli, R. Rohaizu, A. Ghazali, *Carbohydr. Polym.* **2011**, 84, 262.
- [78] M. Barbosa, P. Granja, C. Barrias, I. Amaral, *ITBM-RBM* **2005**, 26, 212.
- [79] P. L. Granja, B. De Jeso, R. Bareille, F. Rouais, C. Baquey, M. A. Barbosa, *React. Funct. Polym.* **2006**, 66, 728.
- [80] a) V. Dowd, R. J. Yon, *J. Chromatogr. A* **1992**, 627, 145; b) J. Sugihara, T. Imamura, T. Yanase, H. Yamada, T. Imoto, *J. Chromatogr. B: Biomed. Sci. Appl.* **1982**, 229, 193.

- [81] a) J. C. Fricain, P. L. Granja, M. A. Barbosa, B. de Jeso, N. Barthe, C. Baquey, *Biomaterials* **2002**, 23, 971; b) P. L. Granja, M. A. Barbosa, L. Pouysegue, B. De Jeso, F. Rouais, C. Baquey, *J. Mater. Sci.* **2001**, 36, 2163; c) M. Yanamandra, L. Kole, A. Giri, S. Mitra, *Anal. Biochem.* **2014**, 449, 132; d) R. D. S. Bezerra, A. I. S. Morais, J. A. Osajima, L. C. C. Nunes, E. C. Silva, *Int. J. Biol. Macromol.* **2016**, 86, 362.
- [82] B. Boursier, G. Bussiere, F. Devos, M. Hughtette, *US4497846A*, **1985**.
- [83] T. Koyama, *US4784848A*, **1988**.
- [84] N. Ninan, M. Muthiah, I. K. Park, A. Elain, S. Thomas, Y. Grohens, *Carbohydr. Polym.* **2013**, 98, 877.
- [85] T. Ito, Y. Yeo, C. B. Highley, E. Bellas, C. A. Benitez, D. S. Kohane, *Biomaterials* **2007**, 28, 975.
- [86] T. Heinze, U. Erler, I. Nehls, D. Klemm, *Angew. Makromol. Chem.* **1994**, 215, 93.
- [87] L. A. Ramos, E. Frollini, T. Heinze, *Carbohydr. Polym.* **2005**, 60, 259.
- [88] H. S. Qi, T. Liebert, F. Meister, T. Heinze, *React. Funct. Polym.* **2009**, 69, 779.
- [89] H. Qi, T. Liebert, F. Meister, L. Zhang, T. Heinze, *Macromol. Symp.* **2010**, 294, 125.
- [90] E. Jansen, *Ger332203*, **1918**.
- [91] R. Chagas, M. Gericke, R. B. Ferreira, T. Heinze, L. M. Ferreira, *Cellulose* **2020**, 27, 1965.
- [92] a) D. R. Biswal, R. P. Singh, *Carbohydr. Polym.* **2004**, 57, 379; b) A. Baar, W. M. Kulicke, K. Szablikowski, R. Kiesewetter, *Macromol. Chem. Phys.* **1994**, 195, 1483.
- [93] R. W. Eyley, E. D. Klug, F. Diephuis, *Anal. Chem.* **1947**, 19, 24.
- [94] L. Grosse, W. Klaus, *Fresenius' Z. Anal. Chem.* **1972**, 259, 195.
- [95] T. Heinze, A. Koschella, *Macromol. Symp.* **2005**, 223, 13.
- [96] D. Capitani, F. Porro, A. L. Segre, *Carbohydr. Polym.* **2000**, 42, 283.
- [97] W. Jaeger, J. Bohrisch, A. Laschewsky, *Prog. Polym. Sci.* **2010**, 35, 511.
- [98] H. J. Prado, M. C. Matulewicz, *Eur. Polym. J.* **2014**, 52, 53.
- [99] B. Vega, H. Wondraczek, C. S. P. Zarth, E. Heikkila, P. Fardim, T. Heinze, *Langmuir* **2013**, 29, 13388.
- [100] T. Mohan, K. Niengelhell, C. S. P. Zarth, R. Kargl, S. Kostler, V. Ribitsch, T. Heinze, S. Spirk, K. Stana-Kleinschek, *Biomacromolecules* **2014**, 15, 3931.
- [101] H. Wondraczek, A. Pfeifer, T. Heinze, *Cellulose* **2012**, 19, 1327.
- [102] K. Hotzel, T. Heinze, *Carbohydr. Res.* **2016**, 434, 77.
- [103] C. S. P. Zarth, A. Koschella, A. Pfeifer, S. Dorn, T. Heinze, *Cellulose* **2011**, 18, 1315.
- [104] T. Elschner, F. Scholz, P. Miethe, T. Heinze, *Macromol. Biosci.* **2014**, 14, 1539.
- [105] M. Zink, K. Hotzel, U. S. Schubert, T. Heinze, D. Fischer, *Macromol. Biosci.* **2019**, 19, 1900085.
- [106] T. Mohan, C. S. P. Zarth, A. Doliska, R. Kargl, T. Griesser, S. Spirk, T. Heinze, K. Stana-Kleinschek, *Carbohydr. Polym.* **2013**, 92, 1046.
- [107] T. Heinze, M. Siebert, P. Berlin, A. Koschella, *Macromol. Biosci.* **2016**, 16, 10.
- [108] T. Heinze, M. Nikolajski, S. Daus, T. M. D. Besong, N. Michaelis, P. Berlin, G. A. Morris, A. J. Rowe, S. E. Harding, *Angew. Chem., Int. Ed.* **2011**, 50, 8602.
- [109] P. Berlin, D. Klemm, A. Jung, H. Liebegott, R. Rieseler, J. Tiller, *Cellulose* **2003**, 10, 343.
- [110] A. Jung, B. Wolters, P. Berlin, *Thin Solid Films* **2007**, 515, 6867.
- [111] A. Jung, T. M. A. Gronewold, M. Tewes, E. Quandt, P. Berlin, *Sens. Actuators, B* **2007**, 124, 46.
- [112] T. Elschner, T. Heinze, *Macromol. Biosci.* **2015**, 15, 735.
- [113] T. Elschner, K. Ganske, T. Heinze, *Cellulose* **2013**, 20, 339.
- [114] a) A. P. Krapcho, C. S. Kuell, *Synth. Commun.* **1990**, 20, 2559; b) R. N. Zuckermann, E. J. Martin, D. C. Spellmeyer, G. B. Stauber, K. R. Shoemaker, J. M. Kerr, G. M. Figliozzi, D. A. Goff, M. A. Siani, R. J. Simon, S. C. Banville, E. G. Brown, L. Wang, L. S. Richter, W. H. Moos, *J. Med. Chem.* **1994**, 37, 2678.
- [115] D. Peschel, K. Zhang, N. Aggarwal, E. Brendler, S. Fischer, T. Groth, *Acta Biomater.* **2010**, 6, 2116.
- [116] D. Peschel, K. Zhang, S. Fischer, T. Groth, *Acta Biomater.* **2012**, 8, 183.
- [117] A. Weltrowski, M. L. D. Almeida, D. Peschel, K. Zhang, S. Fischer, T. Groth, *Macromol. Biosci.* **2012**, 12, 740.
- [118] D. Weber, S. Knaak, K. Hettrich, M. Andrusis, F. Momburg, M. Quade, M. Gelinsky, R. Schwartz-Albiez, *Biomacromolecules* **2018**, 19, 4228.
- [119] M. Lovett, K. Lee, A. Edwards, D. L. Kaplan, *Tissue Eng., Part B* **2009**, 15, 353.
- [120] G. P. Huang, R. Menezes, R. Vincent, W. Hammond, L. Rizio, G. Collins, T. L. Arinze, *Tissue Eng., Part A* **2017**, 23, 1011.
- [121] A. Arora, A. Mahajan, D. S. Katti, *Colloids Surf., B* **2017**, 159, 838.
- [122] R. Menezes, S. Hashemi, R. Vincent, G. Collins, J. Meyer, M. Foston, T. L. Arinze, *Acta Biomater.* **2019**, 90, 169.
- [123] C. Scholz, J. Kressler, in *Tailored Polymer Architectures for Pharmaceutical and Biomedical Applications*, Vol. 1135 (Eds: C. Scholz, J. Kressler), ACS Publications, Washington, DC, USA **2013**, pp. 3–8.
- [124] N. Aggarwal, N. Altgarde, S. Svedhem, K. Zhang, S. Fischer, T. Groth, *Langmuir* **2013**, 29, 13853.
- [125] Q. L. Zhang, D. Q. Lin, S. J. Yao, *Carbohydr. Polym.* **2015**, 132, 311.
- [126] J. M. Silva, R. L. Reis, J. F. Mano, *Small* **2016**, 12, 4308.
- [127] N. Aggarwal, T. Groth, *J. Biomed. Mater. Res., Part A* **2014**, 102, 4224.
- [128] N. Aggarwal, N. Altgarde, S. Svedhem, K. Zhang, S. Fischer, T. Groth, *Colloids Surf., B* **2014**, 116, 93.
- [129] J. Stratz, A. Liedmann, M. L. Trutschel, K. Mader, T. Groth, S. Fischer, *Cellulose* **2019**, 26, 7371.
- [130] H. Q. Chen, M. W. Fan, *J. Bioact. Compat. Polym.* **2007**, 22, 475.
- [131] L. Y. Jiang, Y. B. Li, C. D. Xiong, *J. Biomed. Sci.* **2009**, 16, 65.
- [132] C. Chen, H. Li, J. F. Pan, Z. Q. Yan, Z. J. Yao, W. S. Fan, C. A. Guo, *Biotechnol. Lett.* **2015**, 37, 457.
- [133] M. Matinfar, A. S. Mesgar, Z. Mohammadi, *Mater. Sci. Eng., C* **2019**, 100, 341.
- [134] B. N. Singh, N. N. Panda, R. Mund, K. Pramanik, *Carbohydr. Polym.* **2016**, 151, 335.
- [135] T. Kageyama, T. Osaki, J. Enomoto, D. Myasnikova, T. Nittami, T. Hozumi, T. Ito, J. Fukuda, *ACS Biomater. Sci. Eng.* **2016**, 2, 1059.
- [136] W. Weber, M. Rinderknecht, M. Daoud-El Baba, F.-N. de Glutz, D. Aubel, M. Fussenegger, *J. Biotechnol.* **2004**, 114, 315.
- [137] S. Schaffellner, V. Stadlbauer, P. Stiegler, O. Hauser, G. Halwachs, C. Lackner, F. Iberer, K. H. Tscheliessnigg, *Transplant. Proc.* **2005**, 37, 248.
- [138] M. Gericke, T. Liebert, T. Heinze, *Macromol. Biosci.* **2009**, 9, 343.
- [139] a) H. Ijichi, A. Taketomi, T. Yoshizumi, H. Uchiyama, Y. Yonemura, Y. Soejima, M. Shimada, Y. Maehara, *J. Hepatol.* **2006**, 45, 28; b) R. Olsson, A. Maxhuni, P. O. Carlsson, *Transplantation* **2006**, 82, 340; c) C. C. Lee, S. C. Chen, S. C. Tsai, B. W. Wang, Y. C. Liu, H. M. Lee, K. G. Shyu, *J. Biomed. Sci.* **2006**, 13, 143.
- [140] P. Stiegler, V. Matzi, E. Pierer, O. Hauser, S. Schaffellner, H. Renner, J. Greilberger, R. Aigner, A. Maier, C. Lackner, F. Iberer, F. M. Smolle-Juttner, K. Tscheliessnigg, V. Stadlbauer, *Xenotransplantation* **2010**, 17, 379.
- [141] B. Salmons, W. H. Gunzburg, *Int. J. Pharm.* **2018**, 548, 15.
- [142] T. Groth, W. Wagenknecht, *Biomaterials* **2001**, 22, 2719.
- [143] Z. M. Wang, L. Li, B. S. Zheng, N. Normakhamatov, S. Y. Guo, *Int. J. Biol. Macromol.* **2007**, 41, 376.
- [144] N. N. Droz, S. A. Kuznetsova, T. B. Kalinina, N. Y. Vasilieva, *Bull. Exp. Biol. Med.* **2016**, 160, 767.
- [145] M. Guerrini, D. Beccati, Z. Shriver, A. Naggi, K. Viswanathan, A. Bisio, I. Capila, J. C. Lansing, S. Guglieri, B. Fraser, A. Al-Hakim, N. S. Gunay, Z. Q. Zhang, L. Robinson, L. Buhse, M. Nasr,

- J. Woodcock, R. Langer, G. Venkataraman, R. J. Linhardt, B. Casu, G. Torri, R. Sasisekharan, *Nat. Biotechnol.* **2008**, 26, 669.
- [146] L. H. Fan, X. Y. Zhou, P. H. Wu, W. G. Xie, H. Zheng, W. Tan, S. H. Liu, Q. Y. Li, *Int. J. Biol. Macromol.* **2014**, 66, 245.
- [147] M. Gericke, A. Doliska, J. Stana, T. Liebert, T. Heinze, K. Stana-Kleinschek, *Macromol. Biosci.* **2011**, 11, 549.
- [148] F. Han, W. B. Yao, X. B. Yang, X. N. Liu, X. D. Gao, *Int. J. Biol. Macromol.* **2005**, 36, 201.
- [149] M. C. Giano, Z. Ibrahim, S. H. Medina, K. A. Sarhane, J. M. Christensen, Y. Yamada, G. Brandacher, J. P. Schneider, *Nat. Commun.* **2014**, 5, 4095.
- [150] S. Patra, E. Roy, P. Karfa, S. Kumar, R. Madhuri, P. K. Sharma, *ACS Appl. Mater. Interfaces* **2015**, 7, 9235.
- [151] A. Hebeish, M. Hashem, M. M. Abd El-Hady, S. Sharaf, *Carbohydr. Polym.* **2013**, 92, 407.
- [152] S. Anjum, A. Gupta, D. Sharma, D. Gautam, S. Bhan, A. Sharma, A. Kapil, B. Gupta, *Mater. Sci. Eng., C* **2016**, 64, 157.
- [153] a) F. Eshghi, S. J. Hosseinimehr, N. Rahmani, M. Khademloo, M. S. Norozi, O. Hojati, *Altern. Complement. Med.* **2010**, 16, 647; b) K. Varaprasad, Y. M. Mohan, K. Vimala, K. M. Raju, *J. Appl. Polym. Sci.* **2011**, 121, 784.
- [154] S. A. Marathe, R. Kumar, P. Ajitkumar, V. Nagaraja, D. Chakravorty, *J. Antimicrob. Chemother.* **2013**, 68, 139.
- [155] P. Zhu, Z. Y. Weng, X. Li, X. M. Liu, S. L. Wu, K. W. K. Yeung, X. B. Wang, Z. D. Cui, X. J. Yang, P. K. Chu, *Adv. Mater. Interfaces* **2016**, 3, 1500494.
- [156] a) C. C. Chen, M. Keller, M. Hess, R. Schifffmann, N. Urban, A. Wolfgardt, M. Schaefer, F. Bracher, M. Biel, C. Wahl-Schott, C. Grimm, *Nat. Commun.* **2014**, 5, 4681; b) S. H. Bhang, W. S. Jang, J. Han, J. K. Yoon, W. G. La, E. Lee, Y. S. Kim, J. Y. Shin, T. J. Lee, H. K. Baik, B. S. Kim, *Adv. Funct. Mater.* **2017**, 27, 1603497.
- [157] C. Y. Mao, Y. M. Xiang, X. M. Liu, Z. D. Cui, X. J. Yang, K. W. K. Yeung, H. B. Pan, X. B. Wang, P. K. Chu, S. L. Wu, *ACS Nano* **2017**, 11, 9010.
- [158] K. Ganske, C. Wiegand, U. C. Hipler, T. Heinze, *Macromol. Biosci.* **2016**, 16, 451.
- [159] K. Roemhild, C. Wiegand, U. C. Hipler, T. Heinze, *Macromol. Rapid Commun.* **2013**, 34, 1767.
- [160] T. Genco, L. F. Zemljic, M. Bracic, K. Stana-Kleinschek, T. Heinze, *Macromol. Chem. Phys.* **2012**, 213, 539.
- [161] X. Y. Gao, Y. Cao, X. F. Song, Z. Zhang, X. L. Zhuang, C. L. He, X. S. Chen, *Macromol. Biosci.* **2014**, 14, 565.
- [162] a) H. Namazi, R. Rakhshaei, H. Hamishehkar, H. S. Kafil, *Int. J. Biol. Macromol.* **2016**, 85, 327; b) A. Abdulkhani, M. D. Sousefi, A. Ashori, G. Ebrahimi, *Polym. Test.* **2016**, 52, 218.
- [163] Z. Zare-Akbari, H. Farhadnejad, B. Furughi-Nia, S. Abedin, M. Yadollahi, M. Khorsand-Ghayeni, *Int. J. Biol. Macromol.* **2016**, 93, 1317.
- [164] M. Rasoulzadeh, H. Namazi, *Carbohydr. Polym.* **2017**, 168, 320.
- [165] N. S. V. Capanema, A. A. P. Mansur, S. M. Carvalho, I. C. Carvalho, P. Chagas, L. C. A. de Oliveira, H. S. Mansur, *Carbohydr. Polym.* **2018**, 195, 401.
- [166] a) B. Cullen, R. Smith, E. McCulloch, D. Silcock, L. Morrison, *Wound Repair Regen.* **2002**, 10, 16; b) D. R. Yager, B. C. Nwomeh, *Wound Repair Regen.* **1999**, 7, 433.
- [167] H. Mu, Y. Q. Wang, H. Y. Wei, H. Lu, Z. L. Feng, H. M. Yu, Y. Xing, H. J. Wang, *J. Cell. Mol. Med.* **2018**, 22, 5008.
- [168] P. Berlin, D. Klemm, J. Tiller, R. Rieseler, *Macromol. Chem. Phys.* **2000**, 201, 2070.
- [169] J. C. Tiller, R. Rieseler, P. Berlin, D. Klemm, *Biomacromolecules* **2002**, 3, 1021.
- [170] T. Heinze, T. Elschner, K. Ganske, in *Cellulose Science and Technology: Chemistry, Analysis, and Applications* (Eds: T. Rosenau, A. Potthast, J. Hell), John Wiley & Sons, Hoboken, NJ, USA **2018**, pp. 1–24.
- [171] T. Elschner, A. Doliska, M. Bracic, K. Stana-Kleinschek, T. Heinze, *Carbohydr. Polym.* **2015**, 116, 111.
- [172] J. Fraczyk, B. Kolesinski, I. Relich, Z. J. Kaminski, in *Cellulose—Medical, Pharmaceutical and Electronic Applications* (Eds: T. G. M. van de Ven, L. Godbout), InTech Open, London, UK **2013**, pp. 241–278.
- [173] K. Zhang, D. Peschel, T. Klinger, K. Gebauer, T. Groth, S. Fischer, *Carbohydr. Polym.* **2010**, 82, 92.
- [174] N. A. Ramli, T. W. Wong, *Int. J. Pharm.* **2011**, 403, 73.
- [175] S. Nayak, S. C. Kundu, *J. Biomed. Mater. Res., Part A* **2014**, 102, 1928.
- [176] B. Gaihre, A. C. Jayasuriya, *Mater. Sci. Eng., C* **2016**, 69, 733.
- [177] P. Qi, S. Ohba, Y. Hara, M. Fuke, T. Ogawa, S. Ohta, T. Ito, *Carbohydr. Polym.* **2018**, 189, 322.
- [178] J. Tripathy, A. M. Raichur, *Colloids Surf., B* **2013**, 101, 487.
- [179] M. Zaman, H. N. Xiao, F. Chibante, Y. H. Ni, *Carbohydr. Polym.* **2012**, 89, 163.
- [180] T. Saito, S. Kimura, Y. Nishiyama, A. Isogai, *Biomacromolecules* **2007**, 8, 2485.
- [181] N. F. Vasconcelos, J. P. A. Feitosa, F. M. P. da Gama, J. P. S. Morais, F. K. Andrade, M. D. M. de Souza, M. D. Rosa, *Carbohydr. Polym.* **2017**, 155, 425.
- [182] a) Y. W. Chen, T. H. Tan, H. V. Lee, S. B. Abd Hamid, *Materials* **2017**, 10, 42; b) Y. Nishiyama, U. J. Kim, D. Y. Kim, K. S. Katsumata, R. P. May, P. Langan, *Biomacromolecules* **2003**, 4, 1013.
- [183] Y. Habibi, L. A. Lucia, O. J. Rojas, *Chem. Rev.* **2010**, 110, 3479.
- [184] B. G. Ranby, *Discuss. Faraday Soc.* **1951**, 11, 158.
- [185] S. Beck, J. Bouchard, *Nord. Pulp Pap. Res. J.* **2014**, 29, 6.
- [186] N. Lin, A. Dufresne, *Nanoscale* **2014**, 6, 5384.
- [187] a) X. M. Dong, J. F. Revol, D. G. Gray, *Cellulose* **1998**, 5, 19; b) S. Elazzouzi-Hafraoui, Y. Nishiyama, J. L. Putaux, L. Heux, F. Dubreuil, C. Rochas, *Biomacromolecules* **2008**, 9, 57.
- [188] a) J. Araki, M. Wada, S. Kuga, T. Okano, *Langmuir* **2000**, 16, 2413; b) Y. Habibi, *Chem. Soc. Rev.* **2014**, 43, 1519.
- [189] F. Jiang, A. R. Esker, M. Roman, *Langmuir* **2010**, 26, 17919.
- [190] E. Kloser, D. G. Gray, *Langmuir* **2010**, 26, 13450.
- [191] J. Araki, M. Wada, S. Kuga, T. Okano, *J. Wood Sci.* **1999**, 45, 258.
- [192] M. Pereda, N. El Kissi, A. Dufresne, *ACS Appl. Mater. Interfaces* **2014**, 6, 9365.
- [193] S. M. Mukherjee, H. J. Woods, *Bioch. Biophys. Acta* **1953**, 10, 499.
- [194] J. Araki, M. Wada, S. Kuga, T. Okano, *Colloids Surf., A* **1998**, 142, 75.
- [195] N. Wang, E. Y. Ding, R. S. Cheng, *Polymer* **2007**, 48, 3486.
- [196] H. Liimatainen, M. Visanko, J. Sirvio, O. Hormi, J. Niinimäki, *Cellulose* **2013**, 20, 741.
- [197] J. A. Sirvio, A. Kolehmainen, M. Visanko, H. Liimatainen, J. Niinimäki, O. E. O. Hormi, *ACS Appl. Mater. Interfaces* **2014**, 6, 14384.
- [198] A. Isogai, T. Saito, H. Fukuzumi, *Nanoscale* **2011**, 3, 71.
- [199] A. E. J. de Nooy, A. C. Besemer, H. Vanbekkum, *Carbohydr. Res.* **1995**, 269, 89.
- [200] T. Saito, A. Isogai, *Biomacromolecules* **2004**, 5, 1983.
- [201] T. Saito, M. Hirota, N. Tamura, S. Kimura, H. Fukuzumi, L. Heux, A. Isogai, *Biomacromolecules* **2009**, 10, 1992.
- [202] a) Y. X. Zhou, T. Saito, L. Bergstrom, A. Isogai, *Biomacromolecules* **2018**, 19, 633; b) T. Paakkonen, P. Spiliopoulos, Nonappa, K. S. Kontturi, P. Penttilä, M. Viljanen, K. Svedstrom, E. Kontturi, *ACS Sustainable Chem. Eng.* **2019**, 7, 14384.
- [203] A. C. W. Leung, S. Hrapovic, E. Lam, Y. L. Liu, K. B. Male, K. A. Mahmoud, J. H. T. Luong, *Small* **2011**, 7, 302.
- [204] A. A. Oun, J. W. Rhim, *Carbohydr. Polym.* **2017**, 174, 484.
- [205] K. T. Zhang, P. P. Sun, H. Liu, S. B. Shang, J. Song, D. Wang, *Carbohydr. Polym.* **2016**, 138, 237.
- [206] a) H. Yang, M. N. Alam, T. G. M. van de Ven, *Cellulose* **2013**, 20, 1865; b) J. A. Sirvio, S. Honkaniemi, M. Visanko, H. Liimatainen, *ACS Appl. Mater. Interfaces* **2015**, 7, 19691.

- [207] H. Liimatainen, M. Visanko, J. A. Sirvio, O. E. O. Hormi, J. Niinimäki, *Biomacromolecules* **2012**, *13*, 1592.
- [208] P. W. Liu, B. Pang, S. Dechert, X. C. Zhang, L. B. Andreas, S. Fischer, F. Meyer, K. Zhang, *Angew. Chem.* **2020**, *132*, 3244; *Angew. Chem., Int. Ed.* **2020**, *59*, 3218.
- [209] S. Iwamoto, T. Endo, *ACS Macro Lett.* **2015**, *4*, 80.
- [210] H. Sehaqui, K. Kulasinski, N. Pfenninger, T. Zimmermann, P. Tingaut, *Biomacromolecules* **2017**, *18*, 242.
- [211] L. H. Chen, J. Y. Zhu, C. Baez, P. Kitin, T. Elder, *Green Chem.* **2016**, *18*, 3835.
- [212] R. Koshani, T. G. M. van de Ven, A. Madadlou, *J. Agric. Food Chem.* **2018**, *66*, 7692.
- [213] M. Ghanadpour, F. Carosio, P. T. Larsson, L. Wagberg, *Biomacromolecules* **2015**, *16*, 3399.
- [214] L. L. Li, W. Ma, Y. Higaki, K. Kamitani, A. Takahara, *Langmuir* **2018**, *34*, 13361.
- [215] S. C. Espinosa, T. Kuhnt, E. J. Foster, C. Weder, *Biomacromolecules* **2013**, *14*, 1223.
- [216] T. Oshima, K. Kondo, K. Ohto, K. Inoue, Y. Baba, *React. Funct. Polym.* **2008**, *68*, 376.
- [217] Y. Noguchi, I. Homma, Y. Matsubara, *Cellulose* **2017**, *24*, 1295.
- [218] H. Rosilo, J. R. McKee, E. Kontturi, T. Koho, V. P. Hytonen, O. Ikkala, M. A. Kostianen, *Nanoscale* **2014**, *6*, 11871.
- [219] M. Hasani, E. D. Cranston, G. Westman, D. G. Gray, *Soft Matter* **2008**, *4*, 2238.
- [220] N. Lin, A. Geze, D. Wouessidjewe, J. Huang, A. Dufresne, *ACS Appl. Mater. Interfaces* **2016**, *8*, 6880.
- [221] S. Eyley, W. Thielemans, *Chem. Commun.* **2011**, *47*, 4177.
- [222] E. Feese, H. Sadeghifar, H. S. Gracz, D. S. Argyropoulos, R. A. Ghiladi, *Biomacromolecules* **2011**, *12*, 3528.
- [223] L. Jasmani, S. Eyley, R. Wallbridge, W. Thielemans, *Nanoscale* **2013**, *5*, 10207.
- [224] D. Roy, M. Semsarilar, J. T. Guthrie, S. Perrier, *Chem. Soc. Rev.* **2009**, *38*, 2046.
- [225] J. T. Tang, M. F. X. Lee, W. Zhang, B. X. Zhao, R. M. Berry, K. C. Tam, *Biomacromolecules* **2014**, *15*, 3052.
- [226] U. D. Hemraz, K. A. Campbell, J. S. Burdick, K. Kless, Y. Boluk, R. Sunasee, *Biomacromolecules* **2015**, *16*, 319.
- [227] P. Singhsa, R. Narain, H. Manuapiya, *ACS Appl. Nano Mater.* **2018**, *1*, 209.
- [228] M. Salajkova, L. A. Berglund, Q. Zhou, *J. Mater. Chem.* **2012**, *22*, 19798.
- [229] a) Y. Potzinger, M. Rabel, H. Ahrem, J. Thamm, D. Klemm, D. Fischer, *Cellulose* **2018**, *25*, 1939; b) Z. Y. Zhang, Y. Sun, Y. D. Zheng, W. He, Y. Y. Yang, Y. J. Xie, Z. X. Feng, K. Qiao, *Mater. Sci. Eng., C* **2020**, *106*, 110249.
- [230] V. Palaninathan, S. Raveendran, A. K. Rochani, N. Chauhan, Y. Sakamoto, T. Ukai, T. Maekawa, D. S. Kumar, *J. Tissue Eng. Regen. Med.* **2018**, *12*, 1634.
- [231] K. A. Mahmoud, J. A. Mena, K. B. Male, S. Hrapovic, A. Kamen, J. H. T. Luong, *ACS Appl. Mater. Interfaces* **2010**, *2*, 2924.
- [232] A. L. Menas, N. Yanamala, M. T. Farcas, M. Russo, S. Friend, P. M. Fournier, A. Star, I. Iavicoli, G. V. Shurin, U. B. Vogel, B. Fadeel, D. Beezhold, E. R. Kisin, A. A. Shvedova, *Chemosphere* **2017**, *171*, 671.
- [233] J. Li, Y. Z. Wan, L. F. Li, H. Liang, J. H. Wang, *Mater. Sci. Eng., C: Biomimetic Supramol. Syst.* **2009**, *29*, 1635.
- [234] H. Hu, X. J. Hou, X. C. Wang, J. J. Nie, Q. Cai, F. J. Xu, *Polym. Chem.* **2016**, *7*, 3107.
- [235] H. Hu, W. Yuan, F. S. Liu, G. Cheng, F. J. Xu, J. Ma, *ACS Appl. Mater. Interfaces* **2015**, *7*, 8942.
- [236] N. Li, W. Lu, J. H. Yu, Y. Xiao, S. Y. Liu, L. Gan, J. Huang, *Mater. Sci. Eng., C* **2018**, *91*, 179.
- [237] N. Li, H. Zhang, Y. Xiao, Y. S. Huang, M. D. Xu, D. L. You, W. Lu, J. H. Yu, *Biomacromolecules* **2019**, *20*, 937.
- [238] C. Ruiz-Palmero, M. L. Soriano, M. Valcarcel, *Analyst* **2015**, *140*, 3431.
- [239] G. M. A. Ndong Ntoutoume, R. Granet, J. P. Mbakidi, F. Bregier, D. Y. Leger, C. Fidanzi-Dugas, V. Lequart, N. Joly, B. Liagre, V. Chaleix, V. Sol, *Bioorg. Med. Chem. Lett.* **2016**, *26*, 941.
- [240] N. Lin, A. Dufresne, *Biomacromolecules* **2013**, *14*, 871.
- [241] H. R. Wang, J. L. He, M. Z. Zhang, K. C. Tam, P. H. Ni, *Polym. Chem.* **2015**, *6*, 4206.
- [242] V. Mohanta, G. Madras, S. Patil, *ACS Appl. Mater. Interfaces* **2014**, *6*, 20093.
- [243] R. Singla, S. Soni, P. M. Kulurkar, A. Kumari, M. S. V. Patial, Y. S. Padwad, S. K. Yadav, *Carbohydr. Polym.* **2017**, *155*, 152.
- [244] I. Sulava, U. Henniges, T. Rosenau, A. Potthast, *Biotechnol. Adv.* **2015**, *33*, 1547.
- [245] E. A. Kamoun, E. R. S. Kenawy, X. Chen, *J. Adv. Res.* **2017**, *8*, 217.
- [246] J. Wu, Y. D. Zheng, W. H. Song, J. B. Luan, X. X. Wen, Z. G. Wu, X. H. Chen, Q. Wang, S. L. Guo, *Carbohydr. Polym.* **2014**, *102*, 762.
- [247] R. Singla, S. Soni, V. Patial, P. M. Kulurkar, A. Kumari, S. Mahesh, Y. S. Padwad, S. K. Yadav, *Sci. Rep.* **2017**, *7*, 10457.
- [248] H. S. Du, W. M. Liu, M. L. Zhang, C. L. Si, X. Y. Zhang, B. Li, *Carbohydr. Polym.* **2019**, *209*, 130.
- [249] A. Basu, J. Lindh, E. Alander, M. Stromme, N. Ferraz, *Carbohydr. Polym.* **2017**, *174*, 299.
- [250] A. Basu, K. Heitz, M. Stromme, K. Welch, N. Ferraz, *Carbohydr. Polym.* **2018**, *181*, 345.
- [251] R. Liu, L. Dai, C. L. Si, Z. G. Zeng, *Carbohydr. Polym.* **2018**, *195*, 63.
- [252] W. J. Huang, Y. X. Wang, Z. Q. Huang, X. L. Wang, L. Y. Chen, Y. Zhang, L. N. Zhang, *ACS Appl. Mater. Interfaces* **2018**, *10*, 41076.
- [253] L. Dai, T. Cheng, C. Duan, W. Zhao, W. P. Zhang, X. J. Zou, J. Aspler, Y. H. Ni, *Carbohydr. Polym.* **2019**, *203*, 71.
- [254] a) J. Leppiniemi, P. Lahtinen, A. Paajanen, R. Mahlberg, S. Metsa-Kortelainen, T. Pinornaa, H. Pajari, I. Vikholm-Lundin, P. Pursula, V. P. Hytonen, *ACS Appl. Mater. Interfaces* **2017**, *9*, 21959; b) K. M. O. Hakansson, I. C. Henriksson, C. D. Vazquez, V. Kuzmenko, K. Markstedt, P. Enoksson, P. Gatenholm, *Adv. Mater. Technol.* **2016**, *1*, 1600096; c) K. Markstedt, A. Mantas, I. Tournier, H. M. Avila, D. Hagg, P. Gatenholm, *Biomacromolecules* **2015**, *16*, 1489.
- [255] A. Rees, L. C. Powell, G. Chinga-Carrasco, D. T. Gethin, K. Syverud, K. E. Hill, D. W. Thomas, *Biomed Res. Int.* **2015**, *2015*, 925757.
- [256] C. L. Xu, B. Z. Molino, X. J. Wang, F. Cheng, W. Y. Xu, P. Molino, M. Bacher, D. D. Su, T. Rosenau, S. Willfor, G. Wallace, *J. Mater. Chem. B* **2018**, *6*, 7066.
- [257] R. E. Abouzeid, R. Khiari, D. Beneventi, A. Dufresne, *Biomacromolecules* **2018**, *19*, 4442.
- [258] G. Siqueira, D. Kokkinis, R. Libanori, M. K. Hausmann, A. S. Gladman, A. Neels, P. Tingaut, T. Zimmermann, J. A. Lewis, A. R. Studart, *Adv. Funct. Mater.* **2017**, *27*, 1604619.
- [259] B. C. Wang, A. J. Benitez, F. Lossada, R. Merindol, A. Walther, *Angew. Chem., Int. Ed.* **2016**, *55*, 5966.
- [260] D. Kokkinis, M. Schaffner, A. R. Studart, *Nat. Commun.* **2015**, *6*, 8643.
- [261] A. S. Gladman, E. A. Matsumoto, R. G. Nuzzo, L. Mahadevan, J. A. Lewis, *Nat. Mater.* **2016**, *15*, 413.
- [262] J. T. Muth, D. M. Vogt, R. L. Truby, Y. Menguc, D. B. Kolesky, R. J. Wood, J. A. Lewis, *Adv. Mater.* **2014**, *26*, 6307.
- [263] J. U. Shin, J. Gwon, S. Y. Lee, H. S. Yoo, *ACS Omega* **2018**, *3*, 16150.
- [264] P. Bobber, J. Liu, K. S. Mikkonen, P. Ihalainen, M. Pesonen, C. Plumed-Ferrer, A. von Wright, T. Lindfors, C. L. Xu, R. M. Latonen, *Biomacromolecules* **2014**, *15*, 3655.
- [265] S. W. Wang, J. S. Sun, Y. X. Jia, L. Yang, N. X. Wang, Y. L. Xianyu, W. W. Chen, X. H. Li, R. T. Cha, X. Y. Jiang, *Biomacromolecules* **2016**, *17*, 2472.
- [266] S. Berndt, F. Wesarg, C. Wiegand, D. Kralisch, F. A. Muller, *Cellulose* **2013**, *20*, 771.

- [267] H. L. Nguyen, Y. K. Jo, M. Cha, Y. J. Cha, D. K. Yoon, N. D. Sanandiyaa, E. Prajatelista, D. X. Oh, D. S. Hwang, *Polymers* **2016**, *8*, 102.
- [268] R. Xiong, C. H. Lu, W. Zhang, Z. H. Zhou, X. X. Zhang, *Carbohydr. Polym.* **2013**, *95*, 214.
- [269] Z. Q. Shi, J. T. Tang, L. Chen, C. R. Yan, S. Tanvir, W. A. Anderson, R. M. Berry, K. C. Tam, *J. Mater. Chem. B* **2015**, *3*, 603.
- [270] M. S. Wang, F. Jiang, Y. L. Hsieh, N. Nitin, *J. Mater. Chem. B* **2014**, *2*, 6226.
- [271] H. Liu, J. Song, S. B. Shang, Z. Q. Song, D. Wang, *ACS Appl. Mater. Interfaces* **2012**, *4*, 2413.
- [272] N. Drogat, R. Granet, V. Sol, A. Memmi, N. Saad, C. K. Koerkamp, P. Bressollier, P. Krausz, *J. Nanopart. Res.* **2011**, *13*, 1557.
- [273] a) O. L. Galkina, K. Onneby, P. Huang, V. K. Ivanov, A. V. Agafonov, G. A. Seisenbaeva, V. G. Kessler, *J. Mater. Chem. B* **2015**, *3*, 7125; b) O. L. Galkina, V. K. Ivanov, A. V. Agafonov, G. A. Seisenbaeva, V. G. Kessler, *J. Mater. Chem. B* **2015**, *3*, 1688.
- [274] J. J. Li, R. T. Cha, K. W. Mou, X. H. Zhao, K. Y. Long, H. Z. Luo, F. S. Zhou, X. Y. Jiang, *Adv. Healthcare Mater.* **2018**, *7*, 180034.
- [275] K. W. Mou, J. J. Li, Y. Y. Wang, R. T. Cha, X. Y. Jiang, *J. Mater. Chem. B* **2017**, *5*, 7876.
- [276] a) L. Bretschneider, A. Koschella, T. Heinze, *Polym. Bull.* **2015**, *72*, 473; b) B. Vega, H. Wondraczek, L. Bretschneider, T. Nareoja, P. Fardim, T. Heinze, *Carbohydr. Polym.* **2015**, *132*, 261.
- [277] Y. Beshpalova, D. Kwon, N. Vasanthan, *J. Appl. Polym. Sci.* **2017**, *134*, 44789.
- [278] M. Li, X. H. Liu, N. Liu, Z. H. Guo, P. K. Singh, S. Y. Fu, *Colloids Surf., A* **2018**, *554*, 122.
- [279] a) J. Wu, N. Yin, S. Y. Chen, D. B. Weibel, H. P. Wang, *Cellulose* **2019**, *26*, 2513; b) S. Saska, L. N. Teixeira, P. T. de Oliveira, A. M. M. Gaspar, S. J. L. Ribeiro, Y. Messaddeq, R. Marchetto, *J. Mater. Chem.* **2012**, *22*, 22102; c) C. A. Gao, Y. Z. Wan, C. X. Yang, K. R. Dai, T. T. Tang, H. L. Luo, J. H. Wang, *J. Porous Mater.* **2011**, *18*, 139; d) A. Svensson, E. Nicklasson, T. Harnah, B. Panilaitis, D. L. Kaplan, M. Brittberg, P. Gatenholm, *Biomaterials* **2005**, *26*, 419.
- [280] M. Bhattacharya, M. M. Malinen, P. Lauren, Y. R. Lou, S. W. Kuisma, L. Kanninen, M. Lille, A. Corlu, C. GuGuen-Guillouzo, O. Ikkala, A. Laukkanen, A. Urtti, M. Yliperttula, *J. Controlled Release* **2012**, *164*, 291.
- [281] M. M. Malinen, L. K. Kanninen, A. Corlu, H. M. Isoniemi, Y. R. Lou, M. L. Yliperttula, A. O. Urtti, *Biomaterials* **2014**, *35*, 5110.
- [282] Y. R. Lou, L. Kanninen, T. Kuisma, J. Niklander, L. A. Noon, D. Burks, A. Urtti, M. Yliperttula, *Stem Cells Dev.* **2014**, *23*, 380.
- [283] N. E. Zander, H. Dong, J. Steele, J. T. Grant, *ACS Appl. Mater. Interfaces* **2014**, *6*, 18502.
- [284] J. G. Torres-Rendon, T. Femmer, L. De Laporte, T. Tigges, K. Rahimi, F. Gremse, S. Zafarnia, W. Lederle, S. Ifuku, M. Wessling, J. G. Hardy, A. Walther, *Adv. Mater.* **2015**, *27*, 2989.
- [285] M. C. Echave, R. M. A. Domingues, M. Gomez-Florit, J. L. Pedraz, R. L. Reis, G. Orive, M. E. Gomes, *ACS Appl. Mater. Interfaces* **2019**, *11*, 47771.
- [286] K. Sano, Y. Ishida, T. Aida, *Angew. Chem.* **2018**, *130*, 2558; *Angew. Chem., Int. Ed.* **2018**, *57*, 2532.
- [287] R. M. Domingues, S. Chiera, P. Gershovich, A. Motta, R. L. Reis, M. E. Gomes, *Adv. Healthcare Mater.* **2016**, *5*, 1364.
- [288] K. J. De France, K. G. Yager, K. J. W. Chan, B. Corbett, E. D. Cranston, T. Hoare, *Nano Lett.* **2017**, *17*, 6487.
- [289] C. Uth, S. Zielonka, S. Horner, N. Rasche, A. Plog, H. Orelma, O. Avrutina, K. Zhang, H. Kolmar, *Angew. Chem., Int. Ed.* **2014**, *53*, 12618.
- [290] K. A. Mahmoud, K. B. Male, S. Hrapovic, J. H. T. Luong, *ACS Appl. Mater. Interfaces* **2009**, *1*, 1383.
- [291] K. A. Mahmoud, E. Lam, S. Hrapovic, J. H. T. Luong, *ACS Appl. Mater. Interfaces* **2013**, *5*, 4978.
- [292] Y. X. Zhang, R. G. Carbonell, O. J. Rojas, *Biomacromolecules* **2013**, *14*, 4161.
- [293] M. Vuoriluoto, H. Orelma, B. L. Zhu, L. S. Johansson, O. J. Rojas, *ACS Appl. Mater. Interfaces* **2016**, *8*, 5668.
- [294] S. P. Dong, M. Roman, *J. Am. Chem. Soc.* **2007**, *129*, 13810.
- [295] a) T. Leng, Z. J. Jalcubek, M. Mazloumi, A. C. W. Leung, L. J. Johnston, *Langmuir* **2017**, *33*, 8002; b) L. Zhao, W. Li, A. Plog, Y. P. Xu, G. Buntkowsky, T. Gutmann, K. Zhang, *Phys. Chem. Chem. Phys.* **2014**, *16*, 26322.
- [296] L. Z. Zhang, Q. Li, J. P. Zhou, L. N. Zhang, *Macromol. Chem. Phys.* **2012**, *213*, 1612.
- [297] M. L. Hassan, C. M. Moorefield, H. S. Elbatal, G. R. Newkome, D. A. Modarelli, N. C. Romano, *Mater. Sci. Eng., B* **2012**, *177*, 350.
- [298] Q. A. Yang, X. J. Pan, *J. Appl. Polym. Sci.* **2010**, *117*, 3639.
- [299] L. J. Nielsen, S. Eyley, W. Thielemans, J. W. Aylott, *Chem. Commun.* **2010**, *46*, 8929.
- [300] T. Abitbol, A. Palermo, J. M. Moran-Mirabal, E. D. Cranston, *Biomacromolecules* **2013**, *14*, 3278.
- [301] a) J. L. Huang, C. J. Li, D. G. Gray, *ACS Sustainable Chem. Eng.* **2013**, *1*, 1160; b) J. R. G. Navarro, G. Conzatti, Y. Yu, A. B. Fall, R. Mathew, M. Eden, L. Bergstrom, *Biomacromolecules* **2015**, *16*, 1293; c) Y. J. Zhang, X. Z. Ma, L. Gan, T. Xia, J. Shen, J. Huang, *Cellulose* **2018**, *25*, 5831.